# PROTON MAGNETIC RESONANCE STUDIES OF BIOLOGICALLY SIGNIFICANT MOLECULES

## I. CATION-BINDING PROPERTIES OF NONACTIN

## II. SALT EFFECTS ON NUCLEOTIDE CONFORMATION

Thesis by

James Harold Prestegard

In Partial Fulfillment of the Requirements

For the Degree of

Doctor of Philosophy

California Institute of Technology

Pasadena, California

1971

(Submitted July 15, 1970)

# ACKNOWLEDGMENTS

There are many people to whom I owe thanks for their continued support and encouragement throughout the past four years. Foremost among them is my advisor, Professor Sunney I. Chan, without whose physical intuition and academic guidance much of this thesis would not yet have reached completion. I also must acknowledge the support of the other members of the Chan research group, especially that of B. W. Bangerter and J. H. Nelson whose help was so valuable during those first few years at Caltech. To my wife, Bert, I owe special thanks for her continued moral support, as well as her patience in typing this thesis. Finally, I wish to express my appreciation to the National Science Foundation and to Caltech for their financial support during the last four years.

# ABSTRACT

Part I: Cation-Binding Properties of Nonactin.

In an effort to elucidate the cation specificity of certain macrocyclic antibiotics in metabolic behavior, the nature of the binding of $K^+$, $Na^+$ and $Cs^+$ ions to the macrotetrolide nonactin and the molecular structure of the nonactin complexes have been investigated by 220 MHz proton magnetic resonance spectroscopy. Studies were made in dry acetone and in an acetone-water mixture as a function of varying perchlorate salt concentrations. Salt-induced chemical shifts were observed for all the nonactin protons, except $H_2$ and $H_{21}$, with accompanying changes in the vicinal coupling constants between the $H_2$ and $H_3$ protons and between the $H_5$ and $H_6$-$H_{6'}$ protons. Analysis of the salt-induced shifts yielded apparent formation constants for each of the ions in both solvent systems. The results indicate that all three ions bind to nonactin with equally high affinity in dry acetone, but that in wet acetone the binding constants are preferentially reduced making the potassium complex highly favored. It is shown that in wet acetone the alkali ion must be stripped of its hydration shell prior to its accomodation in the nonactin cavity, and hence we surmise that differences in hydration energies for the various ions must contribute significantly to the ion selective behavior of nonactin. Analysis of limiting chemical shifts and

coupling constants also indicates that the nonactin molecule undergoes sizable conformation changes on complex formation, but that the complexes formed, all spherical with a nonsolvated ion at their center, differ little in exterior geometry. These results are interpreted in terms of their implications on a simple model for ion transport in a biological membrane.

Part II: Salt Effects on Nucleotide Conformation.

Aqueous solutions of uracil, uridine, deoxyuridine, uridine 3'-monophosphate (3'-UMP), and uridine 5'-monophosphate (5'-UMP) have been investigated by proton magnetic resonance spectroscopy as a function of electrolyte concentration. The addition of a "solvent-structure breaking" salt such as $Mg(ClO_4)_2$ or $NaClO_4$ to solutions of the nucleosides and nucleotides was found to result in significant upfield shifts of the uracil $H_6$ resonance. In the cases of uridine and 5'-UMP, these salt-induced shifts were accompanied by a decrease in the ribose $H_1$,-$H_2$, coupling constant, and in the case of 5'-UMP, significant changes in certain intramolecular nuclear Overhauser effects were observed. These observations are interpreted in terms of a salt-induced conformation change, involving the orientation of the uracil base about the glycosidic bond and the puckering of the furanose ring. In view of apparent correlation between the salt-induced shifts of the uracil $H_6$ resonance

and the "solvent-structure breaking" properties of the salt, it is proposed that the addition of salt modifies the solvent structure of the solution, which in turn can affect the average orientation of the base about the glycosidic bond. The ribose conformation change is considered to be a secondary effect resulting from nonbonded interactions between the base and furanose moieties and occurring only to an extent commensurate with the rigidity of the ribose ring. Calculations based on current theories describing the roles of the solvent in hydrophobic bonding are given in support of these conclusions.

TABLE OF CONTENTS

# PART I

# CATION-BINDING PROPERTIES OF NONACTIN

# 1. INTRODUCTION

The mechanism of ion transport through natural membranes, especially that of $Na^+$-$K^+$ transport, is of great importance in biology. Membranes which are normally impervious to ions are here provided with complex enzymatic transport systems which provide for the selective, and even active, transport of potassium ion against established electro-chemical potentials. This process is essential to the transmission of nerve impulses, the secretion and absorption of ions by specialized cells, the maintenance of cellular volume and the regulation and coupling of a host of metabolic systems. In spite of its potential significance, the elucidation at a molecular level of this potassium transport chain has escaped researchers for many years; this basically because of its inherent complexity and intimate coupling to other membrane functions.

## 1.1. Characterization of the Ionophorous Antibiotics

There are, however, simple molecules which, when added to a natural or artificial membrane, can mimic the more complex transport systems in many respects. These molecules, designated ion transport or "ionophorous" antibiotics, impart ion permeability and selectivity to synthetic membranes and enhance ion transport in functioning natural membrane systems. They may in fact be a part of the

transport chain in the unicellular organisms from which they are isolated. These molecules can thus aid in the study of naturally occurring ion transport systems, not only by analogy, but also by their additive and repressive effects on the more complex systems found in higher organisms.[1,2]

Most of the ionophores were discovered in connection with the antimicrobial activity of certain strains of the streptomyces family of fungi;[3,4] hence their classification as antibiotics. The active agents in these streptomyces fermentations were isolated and from these a number of ionophores characterized.[5,6]

Although they display similar physiological effects, these molecules are chemically quite diverse. The diversity is apparent from the examples given in Figure 1. The molecules range from cyclic polypeptides, such as gramicidin S[7] and alimethicin,[1] to macrotetrolides, such as nonactin and dinactin.[8] Cyclic depsipeptides like valinomycin and the enniatins[8] are included along with the less well characterized carbohydrate molecules monensin[1] and nigericin.[9] Recently Pedersen of duPont has also succeeded in making synthetic analogues of the natural ionophores, namely the cyclic polyethers exemplified by the dibenzo-18-crown-6 depicted in Figure 1.[10,11]

Pressman has suggested the division of the ionophores into two classes on the basis of a difference in their

FIGURE 1

Ionophorous antibiotics:

(a) nonactin

(b) dibenzo-18-crown-6

(c) gramicidin S

(d) valinomycin

(e) monensin.

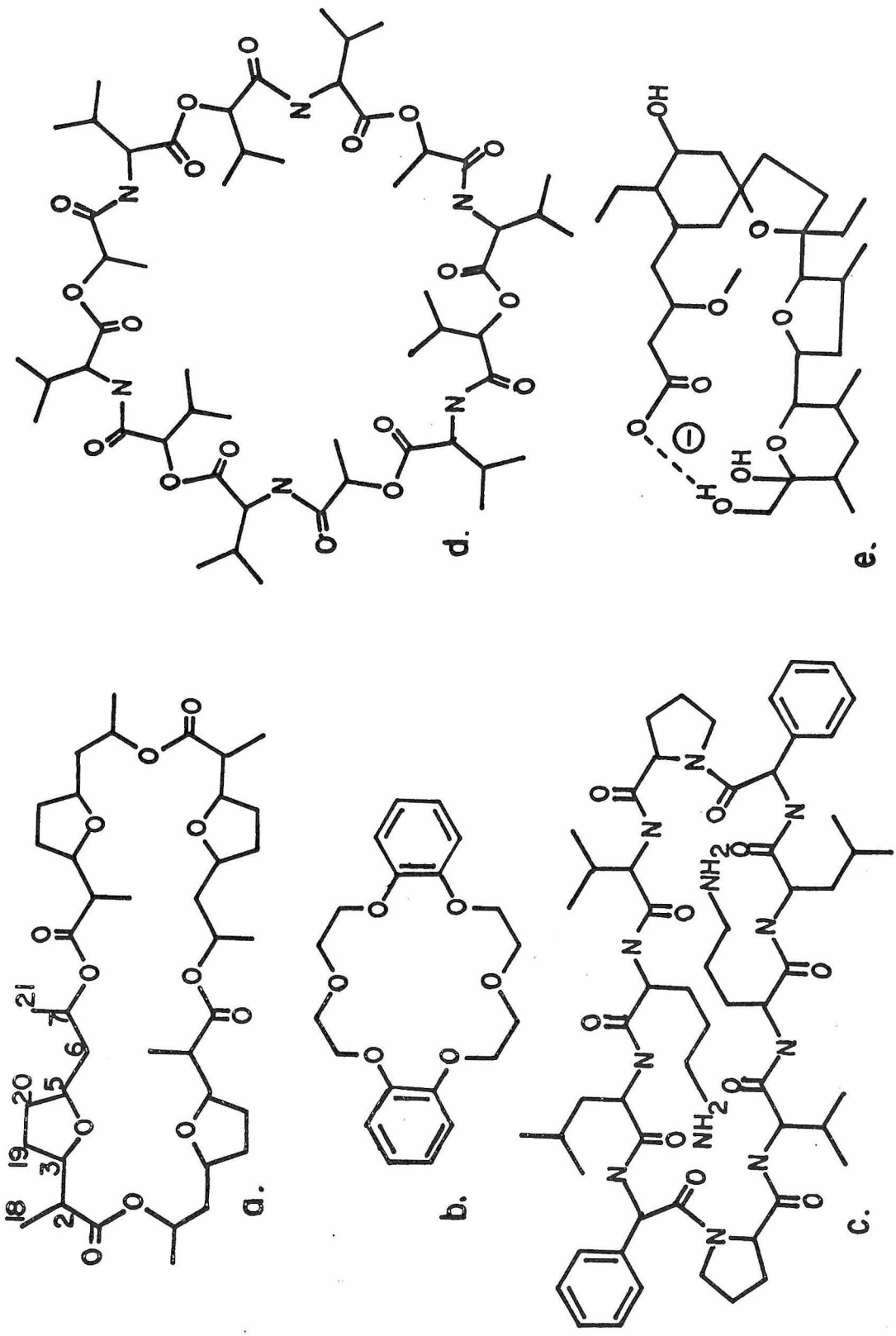
a.
b.
c.
d.
e.

action on respiring mitochondria.[1,12] These are the valinomycin class which stimulates the active accumulation of $K^+$ in mitochondria and the nigericin class which, although also stimulating transport, does so in such a way as to dissipate the energy-supported $K^+$ gradient normally present.

The members of each class, although still chemically diverse, have a great many properties in common. For instance, the members of the valinomycin class are all neutral, cyclic molecules, having a basically hydrophobic exterior and an ionophilic core. They are small molecules of molecular weight 500 to a few thousand and they have a curious alternation of d and l isomers about their rings. In addition to valinomycin itself, this class includes: nonactin, gramicidin S, and the enniatins a and b.[12] The members of the nigericin class tend to be linear, at least with respect to their primary structure, with an ionizable carbonylic acid group as a salient feature. Cyclic secondary structures for these molecules have, however, been proposed.[1] They, like the valinomycin-type molecules, have large, hydrophobic areas and exhibit an affinity for certain alkali cations. The nigericin class includes, in addition to nigericin, molecules such as monensin and dianemycin.[12] In this thesis we wish to direct our attention to the macrotetrolide nonactin, a valinomycin-type antibiotic.

The earliest and most extensive physiochemical

studies employing nonactin and other valinomycin class antibiotics concern their effects on the metabolic processes of mitochondria, bacterial chromatophores and other subcellular structures. Mitochondria have as their principal function the production of energy-storing ATP through the oxidative phosphorylation cycle. The membrane structure of mitochondria provides for the organization of enzyme systems and the maintenance of the ion gradients which seem essential to the production process. The addition of a valinomycin-type antibiotic to this structure disrupts the normal flow of synthesis, presumably by changing the permeability characteristics of the membrane. The principal results of this disruption are: a stimulation of respiration,[13-15] an increase in ATPase activity,[5,15] an uncoupling of the normal oxidation to phosphorylation ratio,[5,15] a swelling of the mitochondrial structure[7,13,14,16] and an uptake of $K^+$ from the surrounding medium.[7,13,17]

In bacterial chromatophores photosynthesis replaces oxidation as the primary energy source. As a result, uncoupling of photophosphorylation, rather than oxidative phosphorylation, is a frequent consequence of the addition of an ionophore. In addition, light dependent $H^+$ uptake, membrane swelling, and the inhibition of ATP formation is observed in the presence of the antibiotics.[18-20]

Present concepts of the mechanism of the antibiotic action arose slowly from these and subsequent studies. The

observation that all of the effects depended on the simultaneous presence of an alkali cation, preferentially $K^+$, first led to the belief that valinomycin action was mediated through the $K^+$ transport system.[17] The relation of ion transport to the other processes of oxidation, phosphorylation, and membrane swelling is a complex one. The two most common theories involve coupling via a common high energy intermediate,[21] or via an electrochemical potential, established by unidirectional movement of hydrogen ions during the oxidation process.[22] According to the first theory the valinomycin class antibiotic would act by facilitating transport of the ion to the initiation site for the active transport chain putting an additional drain on the common high energy intermediate.[12,15] According to the second theory, which seems more applicable in the case of the nigericin-type antibiotic, the potential driving ATP synthesis would be somewhat reduced, either by the neutralization of charge through the promoted efflux of $K^+$ or by a more direct effect due to the transport of $H^+$ in the neutralized form of the antibiotic.[14,23] Regardless of the mechanism which proves to be correct, both rely on the ability of the ionophore to increase to some extent membrane permeability. That the antibiotics have this ability was subsequently established by $K^+$ tracer studies on natural membrane systems[24] and conductance measurements on a number of synthetic analogues.

Foremost among the conductance studies are measurements on lipid bilayers. Here Meuller and Rudin measured directly the bilayer conductance and biionic potentials in the presence and absence of valinomycin, the gramicidins, the enniatins, nonactin, and dinactin. Valinomycin reduced membrane conductance by as much as a factor of $10^8$ and selective permeability ratios for $K^+$ over $Na^+$ as high as 400 were observed.(8) Štefanac and Simon have demonstrated similar behavior using antibiotic -$CCl_4$ saturated sintered glass discs as a model membrane. For nonactin saturated membranes, EMF measurements indicated selectivity constants for $K^+$ over $Na^+$ of 500 or more.(25) These induced conductance changes make plausible the anticipated permeability increase in natural membranes as well as the preferential requirement for potassium.

The conductance studies have also given rise to a number of more direct studies involving the interaction of antibiotics with ions. In organic solvents, notably methanol, several antibiotics have been found to form stable, 1 to 1 complexes with the ions. In a few cases binding constants have been measured and, although they show a qualitative preference for $K^+$, they do not in general show selectivity of the magnitude observed in conductance experiments.(26,27) These studies, nevertheless, give some insight into the interaction of the antibiotic with the ion. Infrared observations of the enniatins, nonactin, and valinomycin have

established that the central carbonyl groups of many of these compounds interact with the bound ion, and have led to the picture of the ion being bound in a polar core, while the quite hydrophobic exterior allows the complex to be lipid soluble.[26,28,29] In fact, this picture has been recently confirmed, at least in crystal form, for $K^+$ complexes of valinomycin and nonactin by X-ray studies.[30,31]

Experiments, such as the conductance measurements and ion binding studies, have provided sufficient information about the properties of these antibiotics to lead to several proposed mechanisms for ion transport. One of the earlier proposals postulates the antibiotics to be surface active forming an ionophilic pore in the normally impervious membrane through which the ion could pass.[14] This was later extended to a channel model which necessitates the alignment of a series of the toroidal antibiotics in the form of a continuous ionophilic channel through the membrane. Here the ion is rapidly passed from one stationary ionophore to another during the transport process. Both models derive their ion selectivity from steric limitations of the macrocycle pore, invoking a correlation between either ionic radius or hydrated ionic radius and pore size to determine the selected ion.[8] A more recent and inherently simpler theory relies on the ability of the ionophore to act as a lipid soluble ion carrier. The antibiotic complexes with the ion at or near the surface and then diffuses as an

entity through the lipid phase to the opposite interface where the ion is released.[12,32] In general, this may involve the participation of several ionophores, the ion being passed from one to another during the course of diffusion.[33] Eisenman et al. have treated the model in detail for a somewhat simplified case in which the process is diffusion limited and have met with limited success in explaining conductance data.[34] Here the complex is formed rapidly and reversibly at the surface and then diffuses slowly through the membrane. Under these circumstances Eisenman feels that selectivity is determined largely by a difference in aqueous solution complex formation constants. There are, however, differences of opinion over this point. It has also been proposed that for this model selectivity can arise from a difference in complex mobilities.[32] In the lipid phase these differences would come largely from variations in the exterior complex geometry. Such variations could be indirectly the result of size variations of bound non-hydrated or hydrated ions.

As is apparent from the diversity in these proposed models for ionophore facilitated transport and ion selectivity, there remain a number of important points which must be considered if the various mechanisms are to be distinguished. The first is the question of precise complex stoichiometry. Existing X-ray and spectrophotometric studies have provided only evidence of 1:1 complex

stoichiometry,[26,30] but under appropriate conditions the antibiotic must have some tendency for aggregation if the channel mechanism is to be at all feasible. An experiment capable of detecting such aggregation would be of value in testing the plausibility of the channel mechanism. Providing a distinction between carrier and channel mechanisms is made, one is faced with a second question of the origin of ion selectivity. An important consideration here is that of complex geometry. In the pore model it was proposed that selectivity arises from rigid steric limitations imposed by the ring, and in the carrier model differences in exterior geometry were cited as giving rise to selectivity through their effect on complex mobilities. Recently a few structural studies of gramicidin S, valinomycin, and monensin have appeared,[35-37] and earlier X-ray work on nonactin has provided some information about the conformation of its $K^+$ complex in crystal form,[30] but without further data on complexes with other ions no comparison of structural properties can be made. In Eisenman's model selectivity arises from simple thermodynamic properties of the ion,[34] so here a determination of equilibrium complex formation constants becomes important. For the study of ion-binding the choice of an appropriate medium is particularly important and especially the role of water and an ion hydration sphere should be investigated. A third question for study is one involving the kinetics of

the transport process. An ion carrier model such as Eisenman's depends heavily on the validity of certain assumed kinetic limits.[34] Only when complex formation rates in the aqueous phase are extremely fast can thermodynamic binding constants influence directly selectivity in ion transport, and only when dissociation rates in the lipid phase are very slow is a single carrier involved in the transport process. Therefore an independent measure of the rate of any one step in the transport process would be of considerable value.

As an attempt to clarify some of these points we have undertaken a detailed proton magnetic resonance (pmr) study of the solution properties of the ionophorous antibiotic nonactin. Complex stoichiometry, especially any tendency for aggregation, will be noted. The characterization of the solution conformation of a number of alkali ion-nonactin complexes will be attempted. The thermodynamic binding constants for the various ions will be determined, specifically in the presence and absence of ion hydration spheres, and kinetic limits for the complex formation process will be estimated. The successful completion of this study should add substantially to our insight into the action of at least this one ionophorous antibiotic.

## 1.2. Selection of Pmr as a Method of Study

Although the properties of nonactin could have been studied in part by the use of a number of experimental techniques, the selection of proton magnetic resonance was not entirely by chance. Pmr as an experimental technique offers many advantages. First, a wealth of data is attainable from most biological molecules, since pmr requires only the presence of a proton, as opposed to a more complex molecular chromophore. Second, the data obtained can be interpreted in structural terms in a relatively straightforward manner. Third, for processes which occur at a rate of 10 to $10^4$ times per second kinetic, as well as structural, data are available. And fourth, these data can be obtained in a solution environment which at least approximates the natural one. Therefore for a molecule of the size and complexity of a typical ionophore, having as an important feature the structure of its hydrocarbon exterior and involving kinetics occurring at the rate of $K^+$ transport, proton magnetic resonance (pmr) spectroscopy is perhaps one of the more useful methods.

In the conventional magnetic resonance experiment there are three parameters which can yield useful information: the chemical shift, the spin-spin coupling constant, and the inherent resonance line width. The chemical shift is a measure of the relative extent of shielding of the

proton from an externally applied field. For C-H bonds the major effect is that of diamagnetic shielding arising from the electronic structure of the bond involving the proton in question. This, however, is modified by space contributions of functional groups having large magnetic anisotropies which directly alter the shielding of the proton from the externally applied magnetic field or of functional groups whose electric polarizations can distort the electron distribution about the proton in such a way as to indirectly change the extent of local shielding. Effects of both local electric fields and magnetic fields depend strongly on the spacial relationship of the source and the proton in question making the chemical shift sensitive to both molecular conformation changes and molecular associations.[38] Now, with respect to the problem at hand, changes in chemical shift can be interpreted in terms of the molecular structure of a free or complexed antibiotic and, under fast exchange conditions, alterations in chemical shifts arising from the association of ion and ionophore may be used to monitor as a function of solution stoichiometry the extent of complex formation. In this way ion association constants, as well as structural information, can be determined.

Coupling constants can also be useful in the investigation of molecular conformation by pmr. Scalar proton coupling is transferred from one proton to another via nuclear polarization of the intervening electrons. The

magnitude of the coupling constant is then determined by the electron density at the two coupled nuclei, as well as the extent of electron exchange along the bonding chain of atoms. The electron density is largely independent of molecular conformation, but the exchange term, at least for vicinal coupling along C-C double bonds, depends on the dihedral angle between $^{H}\diagdown$C-C fragments. Karplus has expressed this relationship in equation form and this equation will be used to give insight into nonactin conformation in free and complexed states.(39)

Line widths, although giving little conformational information, imply much in relation to the kinetic processes involved. For systems in which the magnetic environment of a proton differs either through a conformational or associative change, line widths can be chemical exchange broadened. For changes which occur at a rate that is fast compared to the difference in resonance frequencies of protons in the two states (usually faster than $10^4$ times/sec), a single set of sharp resonances is observed, whose resonance positions are characterized by an average magnetic environment. For systems which exchange slower than this difference (usually slower than 10 times/sec) two sets of sharp resonances are observed, one for each of the distinct species. Between these limits lines are exchange broadened and the widths can be used to infer kinetic information.(40) Or more significantly, they can be used to set limits on the rates

of various processes involved in ion transport.

In spite of the possibilities for application of magnetic resonance to the problem of ionophore-facilitated ion transport, there are some severe limitations. First nmr is a relatively insensitive technique, it being difficult to work below concentrations of $10^{-3}$ M with presently available instrumentation. This is a very real concern for a system such as this where the molecules are physiologically active at concentrations of $10^{-5}$ to $10^{-7}$ M. Secondly, it is not always possible to resolve individual resonances for such detailed interpretation. Protons of large molecules, those of the size that are so often important in biological processes, frequently have spin lattice relaxation times which give rise to significant life time broadening of the resonances. Also, molecules such as these which have large numbers of nearly chemical shift equivalent protons give rise to a multitude of closely spaced resonances. Both of these effects make it difficult to resolve and identify individual resonances. These problems have been somewhat alleviated by the development of a 220 MHz spectrometer which has more than doubled the dispersion of chemical shifts over the previous 100 MHz instruments, while at the same time more than doubling the inherent sensitivity. In addition to the study to be presented here,[41,42] evidence of these instrumental improvements has been demonstrated in the recent application of magnetic resonance to

conformational analysis of valinomycin, gramicidin, and a number of related cyclic polypeptides.[43-47]

## 1.3. Selection of Nonactin as a Subject of Investigation

Just as the selection of pmr as a spectroscopic tool is not without justification, so the choice of nonactin as an ionophore appropriate for this study is well founded. A selection among the various antibiotics had to take into account not only the goals of this work, but also the advantages and limitations of the pmr method.

The macrotetrolide nonactin seems ideal in many respects for a study such as this. It is a relatively simple molecule of the valinomycin class, being composed of four similar nonactic acid residues which have little functionality other than the ester and tetrahydrofuran oxygens and which appear to be involved in coordination to a centrally bound ion. There are several protons in close proximity to these functional groups whose resonances would be expected to be extremely sensitive to conformational changes and ion-binding. In addition, several vicinal proton-proton couplings occur along the nonactin backbone. These too should provide information as to conformational differences among complexes. In the crystal structure (Figure 2), the molecule is nearly in the form of the seam on a tennis ball approaching $S_4$ symmetry.[30] Thus, despite the alternation of two optical isomers in the four nonactic

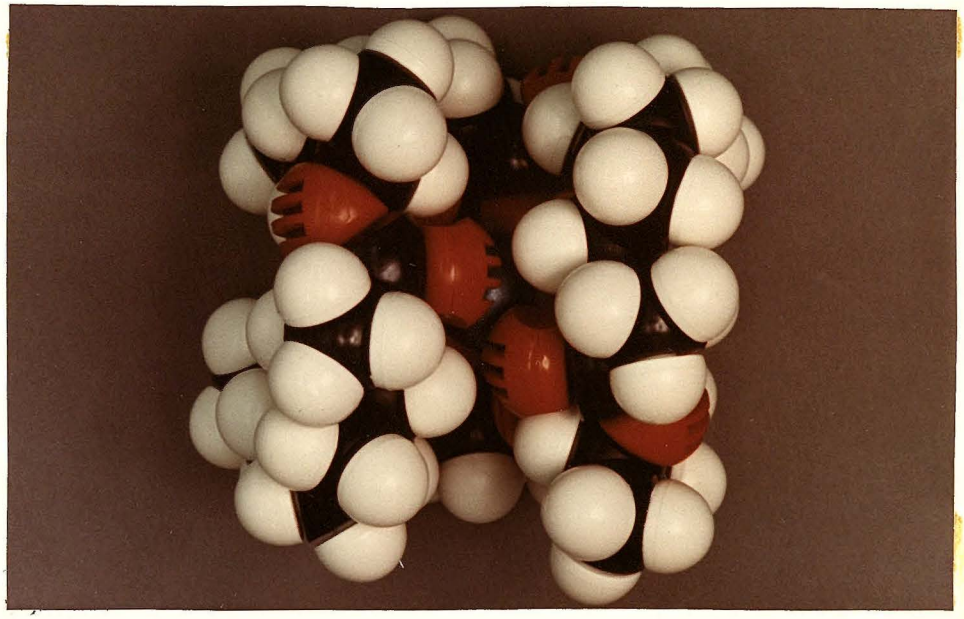

FIGURE 2

CPK model depicting $K^+$-nonactin crystal structure.

acid residues of which the ring is composed, analogous protons in the four subunits remain magnetically equivalent giving a fourfold enhancement to each resonance in the pmr spectrum. All of these properties add to nonactin's suitability for this pmr study.

Our preference for a given solvent system in which to conduct this study would normally be governed by an attempt to mimic the environment where the antibiotic affects ion transport. In this sense it would obviously be desirable to study nonactin complex formation in an aqueous phase. Unfortunately, nonactin is soluble only to the extent of $10^{-5}$ molal in water and a compromise solvent had to be selected where nonactin concentration could be raised to a concentration accessible to a pmr experiment ($10^{-3}$ M or more). Also in order to study the binding process the free ion must exist independently in solution. This requirement eliminates a large class of possible organic solvents from consideration. The choice we eventually reached for the study of ion-binding is the $d_6$-acetone, $d_6$-acetone-$D_2O$ system. It will eventually become apparent that this system is sufficiently close to an aqueous system to make some generalizations about binding selectivity in the more natural medium. For the study of nonactin in a more lipid-like phase a solvent with a low dielectric constant was chosen, namely $CDCl_3$. Studies of the cation-binding properties of nonactin as determined in these two systems are described in

the following sections and will be interpreted in terms of their implications on ionophore-facilitated ion transport in a simple membrane system.

## 2. EXPERIMENTAL SECTION

### 2.1. Materials and Methods

For the study of nonactin ion complexation properties in a quasi-aqueous environment, dry acetone and wet acetone solutions of the antibiotic in the presence of varying amounts of alkali salts were employed. The nonactin used in this study was generously provided by Dr. B. Stearns of the Squibb Institute for Medical Research, New Brunswick, N.J. The $KClO_4$, $NaClO_4$, and $CsClO_4$ were supplied by the Mallinckrodt Chemical Works, St. Louis, Mo., by the G. Frederick Smith Chemical Company, Columbus, Ohio, and by Research Inorganic Chemicals, Sun Valley, Calif., respectively. The $K^+$ and $Na^+$ salts were reagent grade chemicals, while the $Cs^+$ salt was 99.9% pure. All were used without further purification. Solutions were prepared by the simple addition of the salts and nonactin to acetone-$d_6$ or $D_2O$-acetone-$d_6$ mixtures. The deuterated solvents were used to minimize interference from solvent protons in the spectra. The acetone-$d_6$ was obtained from Chemi Standards, Inc., New Castle, Delaware, or from Dia Prep Inc., Atlanta, Ga. The $D_2O$ was supplied by Columbia Organic Chemicals, Columbia,

S.C.

For the studies in anhydrous solutions, special precautions were taken to exclude water from the system: the salts were dried under high vacuum at elevated temperatures, and the acetone-$d_6$ was distilled from anhydrous $CaSO_4$ and sealed under vacuum.[48] Subsequently, solutions were prepared by weight in a water-free atmosphere. After preparation, residual water as detected by pmr spectroscopy was found to be less than $3 \times 10^{-3}$ mole fraction. For the studies in wet acetone solutions, sufficient $D_2O$ (Columbia Organic Chemicals, Columbia, S.C.) was added to make up solutions 0.39 to 0.55 mole fraction in water. To facilitate the determination of binding constants, nonactin was added to the extent of 0.005 M in these solutions while the salt concentration was varied.

For the study of nonactin and its complexes in a more lipid-like phase, $CDCl_3$ solutions were employed. The $CDCl_3$ was a Chemi Standards Inc. reagent and the $Na^+$ and $K^+$ perchlorate salts were those described in the acetone experiments. However, presumably because of the kinetic limitations imposed by the extreme insolubility of these salts in chloroform, solutions could not be prepared in the straightforward manner employed in the preceding experiments. Instead, a method analogous to that used by Haynes et al. in the preparation of the valinomycin-$K^+$ complex was followed.[45] The complex was prepared in methanol, the

methanol was removed under vacuum and then the complex was redissolved in $CDCl_3$. Attempts were made to prepare a $Cs^+$ complex in a similar manner using both perchlorate and thiocyanate salts. However, both efforts were unsuccessful, probably due to a thermodynamically unfavorable situation.

## 2.2. Instrumentation

The pmr spectra of these samples were recorded at 17°C on a Varian HR-220 nmr spectrometer, operating at a magnetic field of 51.7 kilogauss. This magnetic field was produced by a superconducting solenoid immersed in liquid helium. The advantages of the greater dispersion of chemical shifts possible at the higher magnetic fields as well as the high-grade performance of the spectrometer both in sensitivity (90:1) and in resolution (2 parts in $10^9$) were clearly evident in this work. TMS was used as an internal standard and chemical shifts were measured relative to this standard by sideband modulation techniques. Where additional signal-to-noise was necessary, a Varian C-1024 time-averaging computer was employed.

# 3. RESULTS

## 3.1. Spectral Assignment

Although the nonactin macrotetrolide consists of four nonactic acid subunits, two optical isomers of the

residue are involved and these are arranged alternately about the nonactin ring. There are, therefore, in actuality only two identical sets of carbon atoms and they are usually numbered accordingly. But despite this geometrical non-equivalence, there is no a priori reason to expect magnetic nonequivalence of the protons attached to analogous carbon atoms of the two optically related subunits. In fact, if the backbone of the macrocycle assumes an overall configuration which possesses an $S_4$ symmetry axis, as it nearly does in the $K^+$-nonactin crystalline complex,[30] the magnetic environments of the protons in the two types of subunit would be identical. We observe this magnetic equivalence in all of our pmr spectra, and hence in Figure 1 and the following discussion we have used the numbering system for the protons in the first subunit to refer simultaneously to the remaining three.

The 220 MHz pmr spectrum of nonactin is shown in Fiqure 3. The assignment of this spectrum is based on the correlation of intensities, chemical shifts, and coupling constants with the chemical environment of each proton. It was later confirmed by double irradiation experiments. The $H_{18}$ and $H_{21}$ methyl resonances are readily identified by their intensities, their positions at high field, and their coupling to a single proton. The three groups of resonances at low field are expected to arise from the $H_7$, $H_3$, and $H_5$ protons, these protons being adjacent to ether oxygens.[49]

FIGURE 3

220 MHz pmr spectrum of nonactin in $CCl_4$.
Nonactin concentration: 0.026 m;
temperature: 17°.

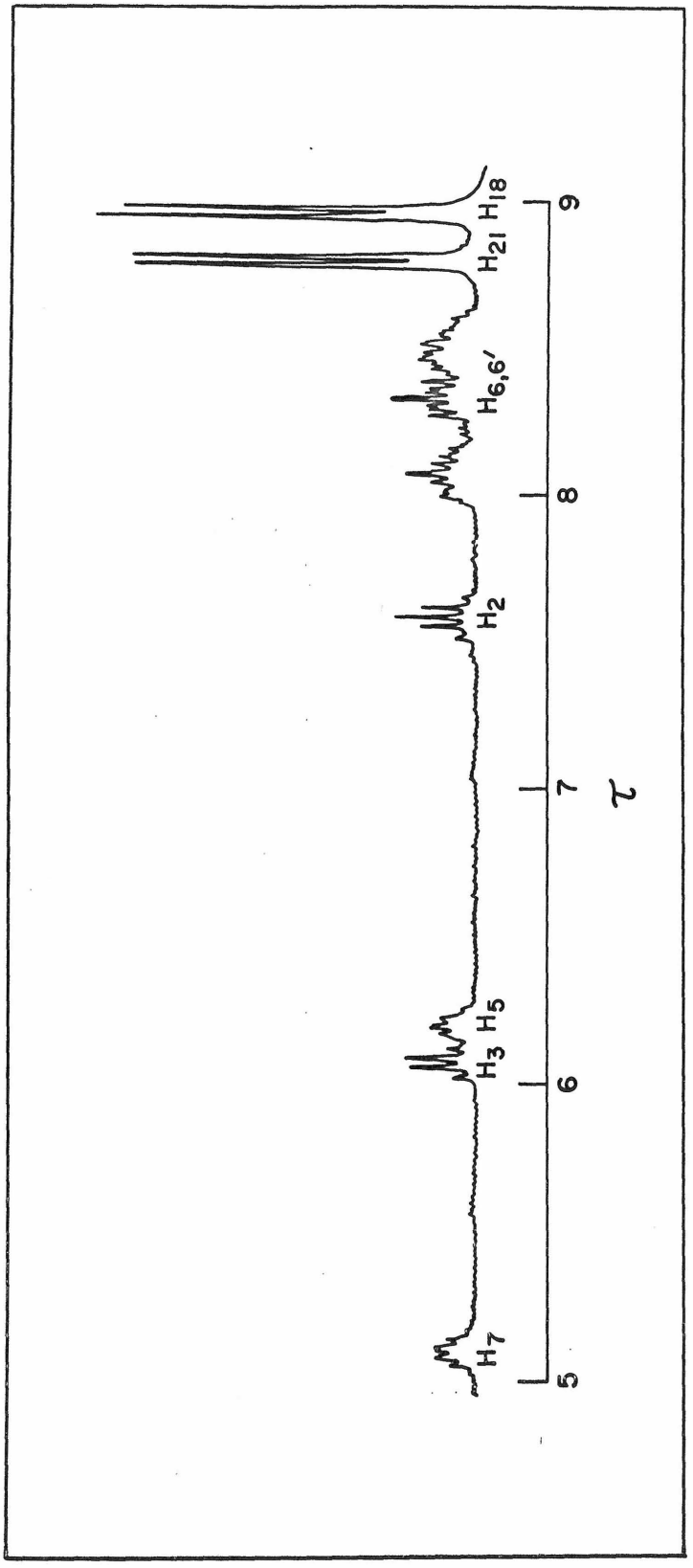
H18
H21
H6,6'
H2
H3 H5
H7
9
8
7
6
5
τ

Irradiation of the spin multiplet furthest downfield was found to collapse the downfield methyl doublet to a singlet. These resonances must therefore be assigned to $H_7$ and $H_{21}$, since neither $H_3$ nor $H_5$ is expected to be coupled to a methyl proton. Irradiation of the remaining methyl doublet ($H_{18}$) was shown to collapse the quintet at 7.58 $\tau$ to a doublet, thus assigning the $H_2$ multiplet. Similarly, irradiation of the $H_2$ spin multiplet collapses the quartet at 6.08 $\tau$ to a triplet, identifying the $H_3$ multiplet, since the $H_2$ and $H_3$ protons are expected to be coupled. By the process of elimination, we therefore assign the multiplet centered at 6.20 $\tau$ to $H_5$ and the remaining resonances in the spectral region between 8.64 $\tau$ and 7.96 $\tau$ to the various methylene hydrogens. On the basis of similar double-irradiation experiments, the methylene multiplet centered at 8.33 $\tau$ can be assigned to the $H_6$, $H_6$, protons with reasonable certainty. This tentative assignment was later verified by computer simulation of the methylene $H_6$, $H_6$, spin multiplet.

The chemical shifts of the various protons and the coupling constants deduced from analysis of the various spin multiplets are summarized in Table I. These results do not include data for the methylene protons of the tetrahydrofuran rings, since the spin multiplets corresponding to these protons were not analyzed in detail. The chemical shifts for the protons in various solvents and at various

TABLE I: Observed Proton Chemical Shifts and Coupling Constants of Nonactin in Acetone-$d_6$.

| Chemical Shifts[a] ($\tau$) | | Coupling Constants[b] (Hz) |
|---|---|---|
| $H_7$ | 5.039 | $J_{H_7-H_{21}} = 6.4\pm0.2$ |
| $H_3$ | 6.013 | $\frac{1}{2}(J_{H_7-H_6} + J_{H_7-H_{6'}}) = 6.4\pm0.4$ |
| $H_5$ | 6.129 | $J_{H_3-H_2} = 7.6\pm0.4$ |
| $H_2$ | 7.513 | $\frac{1}{2}(J_{H_3-H_{19}} + J_{H_3-H_{19'}}) = 7.0\pm0.4$ |
| $H_{21}$ | 8.785 | $J_{H_2-H_{18}} = 7.1\pm0.2$ |
| $H_{18}$ | 8.946 | $\frac{1}{2}(J_{H_5-H_6} + J_{H_5-H_{6'}}) = 6.2\pm0.4$ |
| $H_6$-$H_{6'}$ | 8.260 | $\frac{1}{2}(J_{H_5-H_{20}} + J_{H_5-H_{20'}}) = 6.8\pm0.4$ |
| | | $J_{H_6-H_{6'}} = 12.0\pm0.4$ |

[a] ± 0.005. [b] Absolute values.

concentrations are included for comparison in Table II. One notes that neither solvent nor concentration affects the chemical shifts to a great extent. The same can be said of any coupling constant involved.

## 3.2. Cation-Induced Changes with Acetone as a Solvent

When $NaClO_4$, $KClO_4$ or $CsClO_4$ is added to an acetone solution of nonactin, a number of these resonances are shifted gradually downfield as the concentration of the alkali cation is increased. Several of the coupling constants are also modified. The fact that during the course of these spectral changes the lines remain a sharp single set of proton resonances indicates the redistribution of nonactin between rapidly interconverting complexed and uncomplexed states. Under these circumstances, the high salt limiting values of the chemical shifts and coupling constants in themselves give insight into the structural changes which have occurred upon the incorporation of the ion. A detailed study of the chemical shift changes as a function of salt concentration and solvent system also provides a convenient method for following the relative affinities of the nonactin aperture for various ions under a variety of experimental conditions.

The induced chemical shifts observed upon the addition of these $Na^+$, $K^+$ and $Cs^+$ salts are more quantitatively presented in Figures 4, 5 and 6. The results for dry

TABLE II: Chemical Shifts of Nonactin Protons in Various Solvents at Various Concentrations.

| Solvent | Conc[a] | $H_7$ | $H_3$ | $H_5$ | $H_{18}$ | $H_{21}$ | $H_2$ | (Hz) |
|---|---|---|---|---|---|---|---|---|
| $CDCl_3$ | 0.02 | 1092 | 882 | 846 | 238 | 270 | 550 | |
| $CDCl_3$ | 0.11 | 1093 | 882 | 847 | 236 | 267 | 552 | |
| $CD_3COCD_3$ | 0.005 | 1092 | 877 | 852 | 232 | 267 | 547 | |
| $CD_3COCD_3$ | 0.02 | 1090 | 876 | 851 | 231 | 267 | 547 | |

[a]Concentration in molal units.

FIGURE 4

Salt-induced shifts of the nonactin $H_7$, $H_3$, $H_5$, $H_2$, $H_{18}$, and $H_{21}$ protons as a function of $KClO_4$ concentration observed in (a) dry acetone-$d_6$ containing minimal water ($<7 \times 10^{-3}$ mole fraction), and (b) wet acetone-$d_6$ containing 0.34 mole fraction $D_2O$. Nonactin concentration: $3.0 \times 10^{-4}$ mole fraction; temperature: 17°.

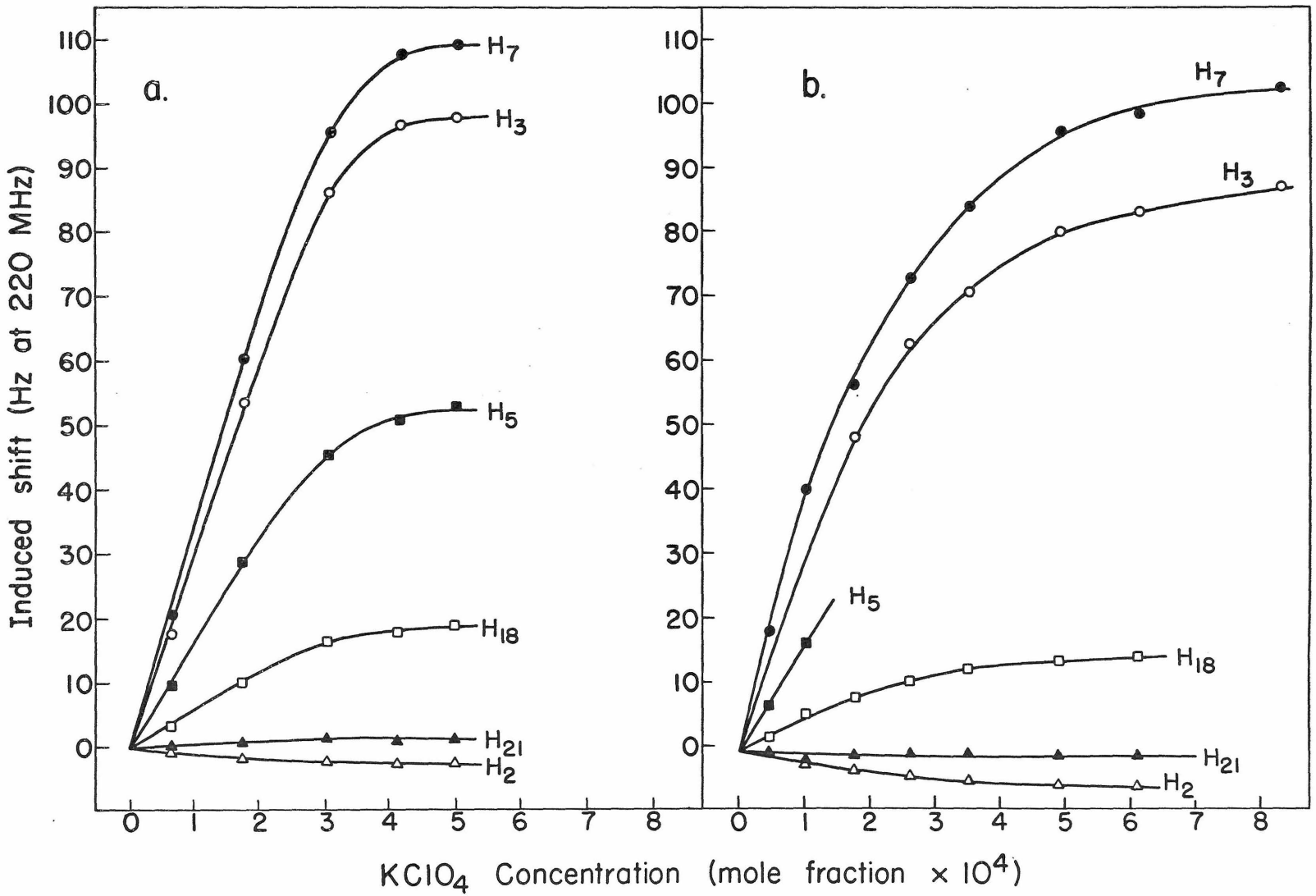
a.
b.
$H_7$
$H_3$
$H_5$
$H_{18}$
$H_{21}$
$H_2$
Induced shift (Hz at 220 MHz)
$KClO_4$ Concentration (mole fraction $\times 10^4$)
0
10
20
30
40
50
60
70
80
90
100
110
0 1 2 3 4 5 6 7 8

FIGURE 5

Salt-induced shifts of the nonactin $H_7$, $H_3$, $H_5$, $H_2$, $H_{18}$, and $H_{21}$ protons as a function of $NaClO_4$ concentration observed in (a) dry acetone-$d_6$ containing minimal water ($1 \times 10^{-3}$ mole fraction), and (b) wet acetone-$d_6$ containing 0.39 mole fraction $D_2O$. Nonactin concentration: $3.1 \times 10^{-4}$ mole fraction; temperature: $17^{\circ}$.

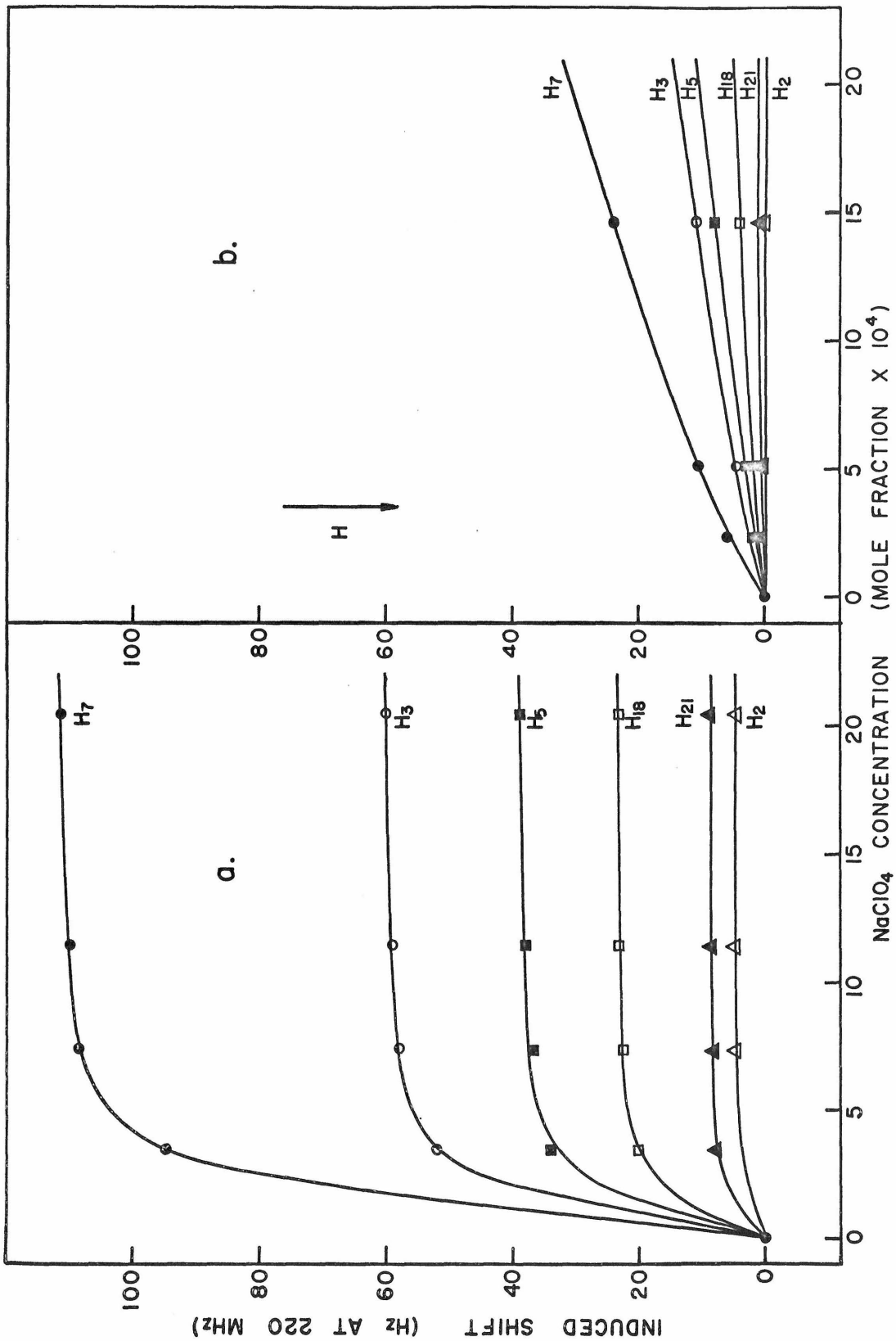
a.
b.
H
H7
H3
H5
H18
H21
H2
INDUCED SHIFT (Hz AT 220 MHz)
NaClO4 CONCENTRATION (MOLE FRACTION X 10^4)
0
20
40
60
80
100
5
10
15
20

FIGURE 6

Salt-induced shifts of the nonactin $H_7$, $H_3$, $H_5$, $H_2$, $H_{18}$, and $H_{21}$ protons as a function of $CsClO_4$ concentration observed in (a) dry acetone-$d_6$ containing minimal water ($3 \times 10^{-3}$ mole fraction), and (b) wet acetone-$d_6$ containing 0.55 mole fraction $D_2O$. Nonactin concentration: $3.7 \times 10^{-4}$ mole fraction; temperature: 17°.

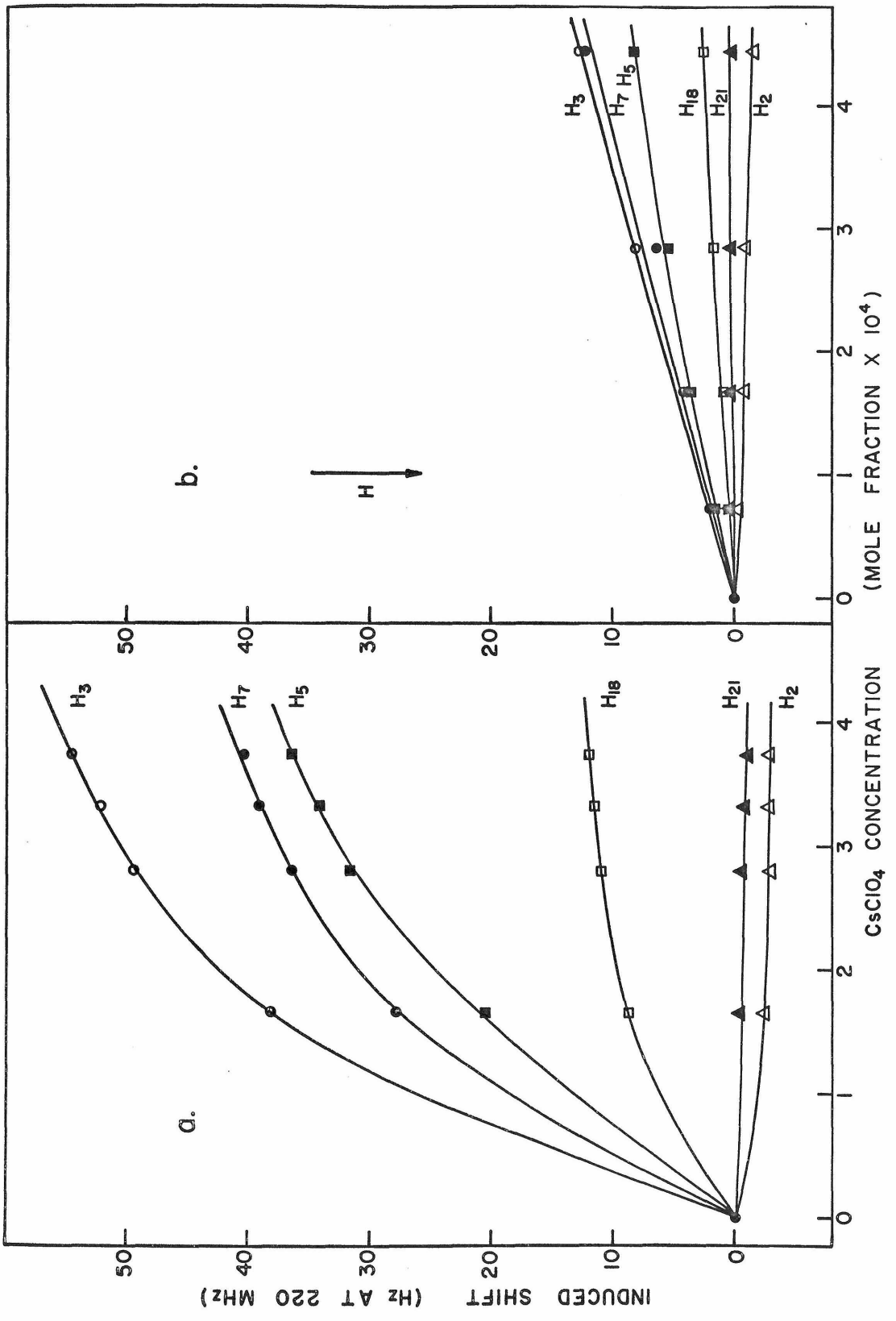
INDUCED SHIFT (Hz AT 220 MHz)
CsClO4 CONCENTRATION (MOLE FRACTION X 10^4)
a.
b.
H
H3
H7
H5
H18
H21
H2

acetone are shown in Figures 4a, 5a and 6a, and those for wet acetone in Figures 4b, 5b and 6b. The largest shifts in all cases are observed for $H_7$, $H_3$ and $H_5$. From an examination of the crystal structure of the potassium complex, these are the protons which are expected to be in close proximity to either one of the coordinating keto oxygens or to one of the coordinating ether oxygens of the tetrahydrofuran rings.

In dry acetone, Figures 4a, 5a and 6a, the induced shifts are quite abrupt being essentially complete at a salt concentration of $5 \times 10^{-4}$ mole fraction for the $Na^+$ and $K^+$ studies. In these cases the limiting shifts can be measured directly and should be highly accurate. In the $Cs^+$ study, the shift as a function of salt is again reasonably abrupt, but, because of solubility problems, a limiting shift could not be reached experimentally and the value had to be determined by least squares fit to a theoretical chemical shift equation to be presented later. As a result these shifts are more susceptible to error. The limiting shifts determined for the $H_3$, $H_5$, $H_7$, $H_{21}$ and $H_{18}$ protons are presented in Table III. The induced shifts of the remaining methylene resonances were not followed because of the complexity of this region and interference from resonances of residual protons in the $d_6$-acetone. However, shifts in this region are not expected to exceed 50 Hz.

Meaningful trends in the data for the three complexes

TABLE III: Chemical Shifts of the Nonactin Protons in the $Na^+$, $K^+$ and $Cs^+$ Complexes.[a]

| | $H_7$ | $H_3$ | $H_5$ | $H_{18}$ | $H_{21}$ | $H_2$ (Hz) |
|---|---|---|---|---|---|---|
| $Na^+$ | -113±5 | -62±3 | -39± 2 | -23±1 | -8.8±1 | -4.4±1 |
| $K^+$(dry) | -115±5 | -103±4 | -56± 2 | -20±1 | -1.9±1 | 2.2±1 |
| $K^+$(wet) | -113±5 | -97±4 | | -17±1 | 1 ±1 | 5 ±1 |
| $Cs^+$ | -67±13 | -90±18 | -60±12 | -20±4 | 1.8±1 | 4.8±1 |

[a]Relative to their corresponding values in free nonactin.

are difficult to detect because of the interplay of a number of effects on the chemical shifts. However, if one considers the ratios of the $H_3$ to $H_7$ shifts or the $H_5$ to $H_7$ shifts rather than their absolute magnitudes, there appears to be a notable increase in these ratios as one increases the size of the central ion (Table IV). For $H_3$ the ratios are 0.55, 0.89 and 1.34 for $Na^+$, $K^+$ and $Cs^+$, respectively, and for $H_5$ they are 0.35, 0.49 and 0.90. The salt-induced shifts of the other protons are too small to interpret with any degree of confidence.

In wet acetone, Figures 4b, 5b and 6b, induced shifts are not nearly so abrupt. For the $K^+$ complex formed in an acetone solution containing 0.34 mole fraction $D_2O$, the salt-induced shifts reach their limiting values only when a salt concentration of $8 \times 10^{-4}$ mole fraction is attained, nearly twice that required in dry acetone. However, the limiting shifts could still be directly measured, with the exception of $H_5$ where it was necessary to extrapolate on the basis of other data due to interference by the HDO resonance at higher salt concentrations. The limiting shift values for this $K^+$ case are also presented in Table III. It is apparent for each proton that they agree within limits of error with values obtained in dry acetone solution. For $Na^+$ and $Cs^+$ complexes in solutions containing similar proportions of $D_2O$, the salt-induced shifts are much more gradual, being small and nearly linear with salt concentration throughout

TABLE IV: Ratios of the Salt-Induced Shifts for the Various Nonactin Complexes in Dry and Wet Acetone Solutions.

| | | $Na^+$ | $K^+$ | $Cs^+$ |
|---|---|---|---|---|
| $H_3/H_7$ | dry | 0.55 | 0.89 | 1.34 |
| | wet | 0.47[a] | 0.85 | 1.16[a] |
| $H_5/H_7$ | dry | 0.35 | 0.49 | 0.90 |
| | wet | 0.33[a] | 0.44 | 0.75[a] |

[a]Experimental error: ± 10%; otherwise ± 5%.

the range studied. As a result, limiting shifts in these cases could not be reached experimentally. The relative shifts of the various protons, however, could be measured and it is apparent that they are similar for a given complex whether formed in wet or dry acetone (Table IV). For example, in the acetone-water mixture, the ratios of the $H_3$ and $H_5$ shifts to the $H_7$ shift for $Cs^+$ are 1.2 and 0.8, respectively, and the corresponding ratios for $Na^+$ are 0.5 and 0.3. These can be compared to the ratios obtained in dry acetone solutions: 1.3 and 0.9 for the $H_3$ and $H_5$ protons in the case of $Cs^+$, and 0.6 and 0.4 in the case of $Na^+$. Thus ratios of chemical shifts can change dramatically with the size of the central ion, but are essentially constant for the complexes formed in dry and wet acetone. Since at any point in the equilibrium, the ratios of the shifts for any two protons must be equal to the ratios of their limiting shifts, it seems reasonable to conclude that the limiting shifts for complexes with $Cs^+$ and $Na^+$ salts are also very similar in dry and wet solvent systems.

In addition to inducing changes in the chemical shifts of certain protons, the addition of $Na^+$, $K^+$ and $Cs^+$ salts to either solvent system modifies several vicinal proton-proton coupling constants. With the exception of $H_{18}$ and $H_{21}$, all the spin multiplets involve spin coupling of the proton in question to at least two vicinal protons and with the exception of these two methyl multiplets all undergo some degree

of change on ion complexation. Such changes are apparent in the variations of the $H_5$ and $H_7$ multiplets presented in Figures 7 and 8.

The $H_2$ multiplet results from coupling of the $H_2$ proton to $H_3$ and $H_{18}$. The effects of the $H_2$-$H_{18}$ coupling can be ascertained by measuring this coupling constant directly from the $H_{18}$ methyl resonance; the residual $H_2$-$H_3$ coupling can then be readily determined, albeit with some uncertainty. For all three ions, complexation increases the value of $J_{H_2-H_3}$ substantially (from 7.6 to 9.3 for potassium), however, the solvent system again has little effect on the limiting value in each case. Values for the $J_{H_2-H_3}$ in the uncomplexed nonactin molecule, as well as the $Na^+$, $K^+$ and $Cs^+$ complexes, are given in Table V. The size of the bound ion, however, seems to have little effect on this coupling constant.

The $H_7$ proton is coupled to the $H_{21}$ methyl protons, as well as the two nearly chemical shift equivalent methylene $H_6$-$H_{6'}$ protons. The $H_7$ multiplet essentially constitutes the X spectrum of an $ABP_3X$ system,[50] where A, B refer to the nearly chemical shift equivalent $H_6$-$H_{6'}$ protons, and P denotes the three magnetically equivalent $H_{21}$ methyl protons. Its overall width is expected to be given by $3|J_{H_7-H_{21}}| + |J_{H_7-H_6} + J_{H_7-H_{6'}}|$. Since $|J_{H_7-H_{21}}|$ can be measured directly from the $H_{21}$ resonance, the value of $|J_{H_7-H_6} + J_{H_7-H_{6'}}|$ can in theory be determined from the overall width of the multiplet. Because of second order

FIGURE 7

Comparison of the observed and calculated spectral changes in the $H_7$ multiplet of nonactin upon ion complexation. ( ---- computer simulated.)

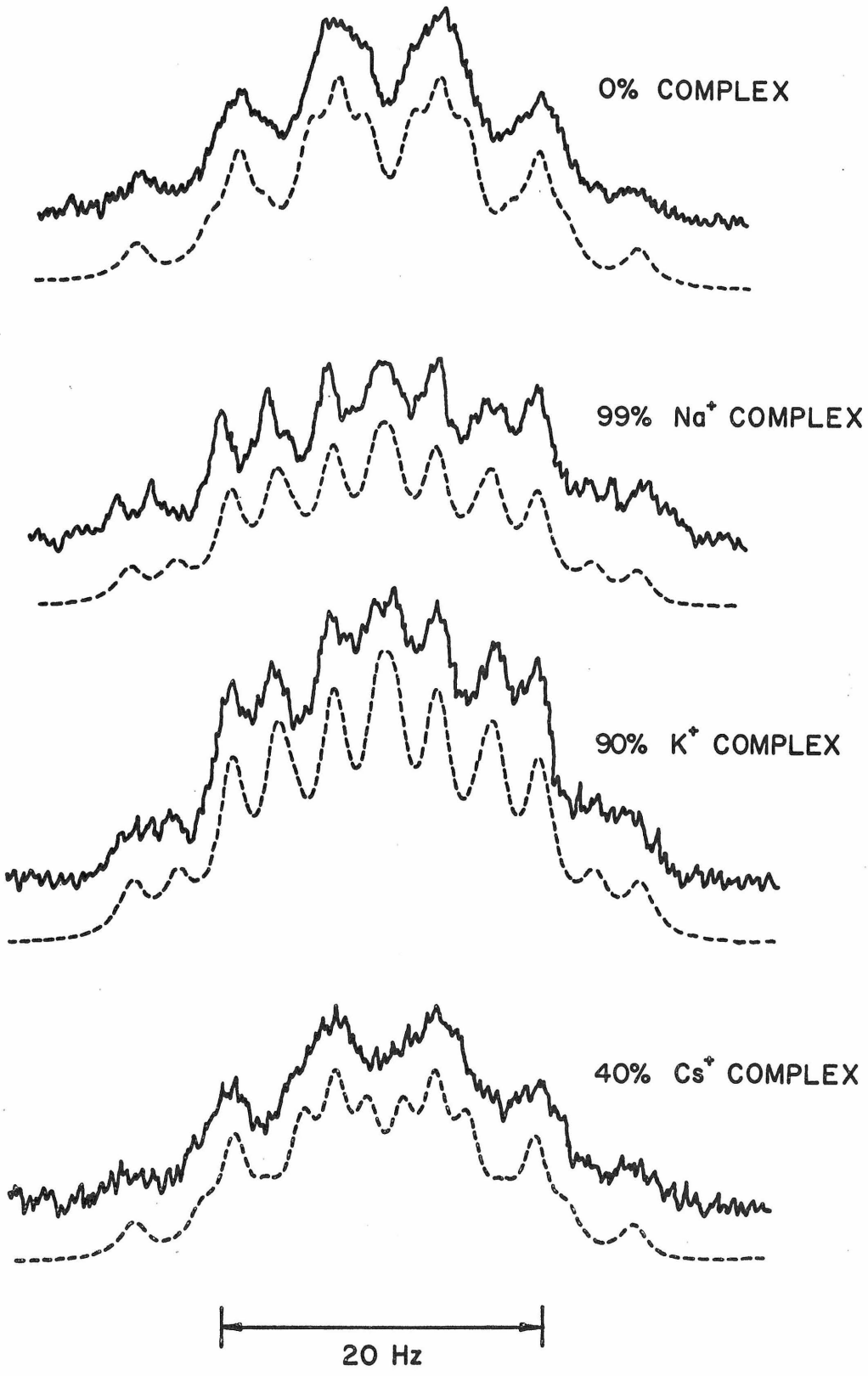
0% COMPLEX
99% Na+ COMPLEX
90% K+ COMPLEX
40% Cs+ COMPLEX
20 Hz

FIGURE 8

Comparison of the observed and calculated spectral changes in the $H_5$ multiplet of nonactin upon ion compexation. ( ---- computer simulated.)

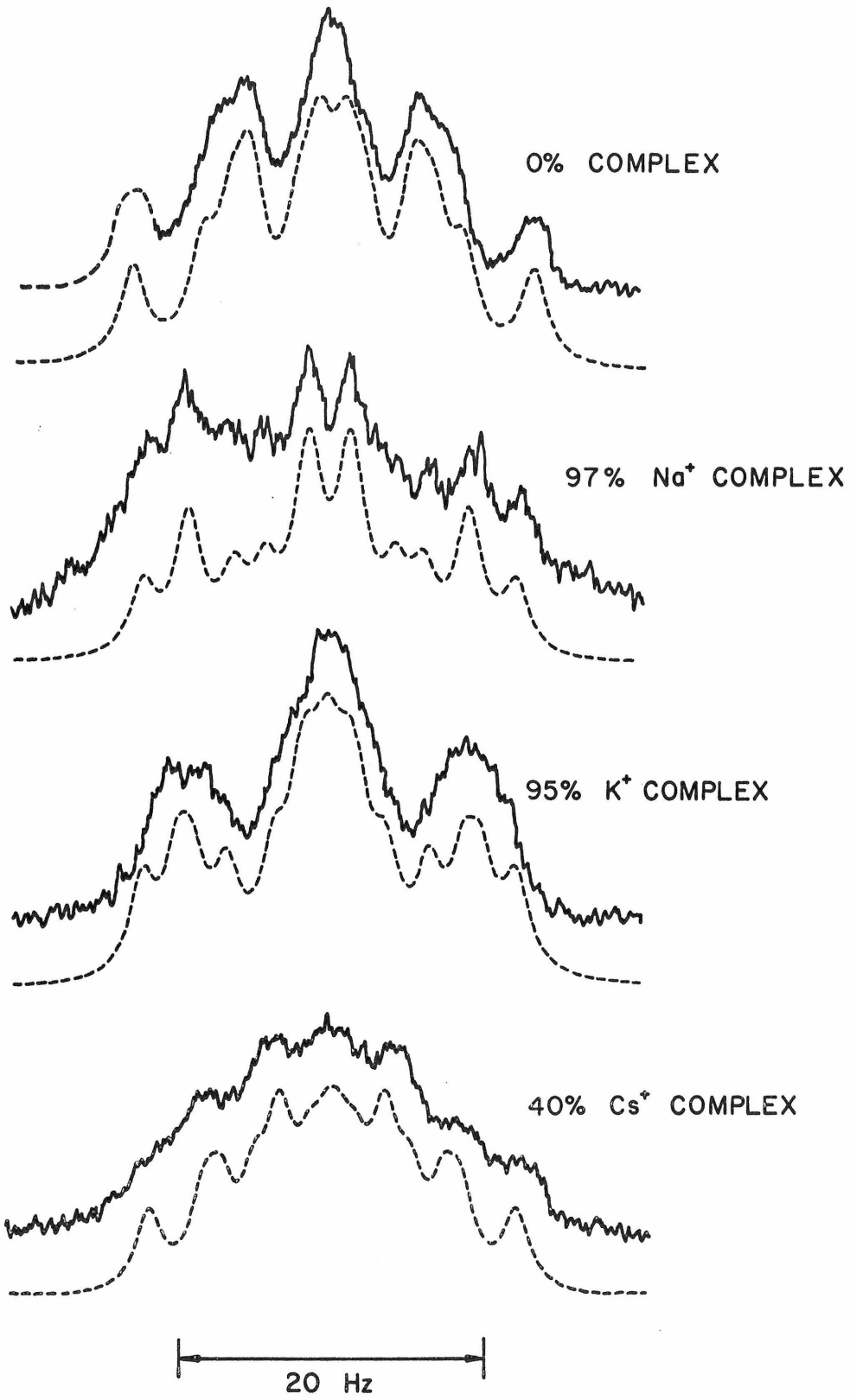
0% COMPLEX
97% Na+ COMPLEX
95% K+ COMPLEX
40% Cs+ COMPLEX
20 Hz

TABLE V: Vicinal Proton-Proton Coupling Constants Observed for Nonactin and its Complexes.

| (Hz) | $\lvert J_{H_2-H_3}\rvert$ | $\lvert J_{H_5-H_6} + J_{H_5-H_6'}\rvert$ | $\lvert J_{H_7-H_6} + J_{H_7-H_6'}\rvert$ |
|---|---|---|---|
| Nonactin | 7.6±0.4 | 12.4±0.4 | 13.0±0.4 |
| $Na^+$ Complex | 10.0±0.4 | 10.9±0.4 | 13.2±0.4 |
| $K^+$ Complex | 9.4±0.4 | 11.0±0.4 | 13.0±0.4 |
| $Cs^+$Complex | 9.7±0.8 | 9.3±0.8 | 13.0±0.8 |

effects, the positions of other lines in the $H_7$ multiplet depend upon the quantities

$$D_{\pm} = \tfrac{1}{2}\left\{\left[\delta_{AB} \pm \tfrac{1}{2}(J_{AX} - J_{BX})\right]^2 + J_{AB}^2\right\}^{\frac{1}{2}}, \qquad (1)$$

specifically $|D_+ - D_-|$, where $\delta_{AB}$ is the chemical shift difference between the methylene $H_6$-$H_{6'}$ protons in Hz. These parameters can also in theory be determined directly from the multiplet structure. In practice, however, the lines of the multiplet are not well resolved. We therefore have resorted to a computer simulation technique to determine more accurately $|J_{H_7-H_6} + J_{H_7-H_{6'}}|$ and $|D_+ - D_-|$. The technique simply involves plotting the sum of Lorentzian lines of appropriate position, intensity and width in an iterative manner until the multiplet pattern is reproduced. The results of this procedure are shown along with experimental spectra for the $H_7$ multiplet in Figure 7. The line position so determined was used to determine the spectral parameters given in Table V. The results show that in all cases complexation does not vary the total width of the $H_7$ multiplet from that observed in the uncomplexed molecule. This implies that since $J_{H_7-H_{21}}$ is known not to change, $|J_{H_7-H_6} + J_{H_7-H_{6'}}|$ must remain constant. The observed change in the multiplet structure must then be the result of a change in $|D_+ - D_-|$. As the geminal spin-spin coupling constant $|J_{H_6-H_{6'}}|$ is not expected to be altered by the formation of the complex, the observed spectral changes in

the $H_7$ multiplet must be due to changes in ($J_{H_7-H_6}$ - $J_{H_7-H_6'}$) and/or $\delta_{AB}$. In view of the constancy of ($J_{H_7-H_6}$ + $J_{H_7-H_6'}$), changes in the magnetic nonequivalence between the $H_6-H_6'$ protons appear to be more likely. This magnetic nonequivalence must vary slightly from complex to complex, while ($J_{H_7-H_6}$ + $J_{H_7-H_6'}$) remains fixed. Again, the solvent system did not affect any of these parameters greatly.

The analysis of the $H_5$ multiplet proceeded along similar lines. The $H_5$ multiplet is best characterized as the X spectrum of an ABPQX system, arising from coupling of the $H_5$ proton to the $H_6-H_6'$ methylene protons (A,B) and to the $H_{20}-H_{20}'$ tetrahydrofuran ring protons (P,Q). Theoretically the overall width of the $H_5$ multiplet should be given by $|J_{H_5-H_6} + J_{H_5-H_6'}|$ + $|J_{H_5-H_{19}} + J_{H_5-H_{19}'}|$, and the observed changes in line width of this multiplet could be due to modifications in either coupling. In our computer simulation it was not possible to distinguish between changes in $|J_{H_5-H_6} + J_{H_5-H_6'}|$ and $|J_{H_5-H_{19}} + J_{H_5-H_{19}'}|$ by simple curve fitting. However, the tetrahydrofuran ring is expected to be relatively rigid and little change in $|J_{H_5-H_{19}} + J_{H_5-H_{19}'}|$ is likely. Therefore, the value of $|J_{H_5-H_6} + J_{H_5-H_6'}|$ was determined holding $|J_{H_5-H_{19}} + J_{H_5-H_{19}'}|$ constant at its uncomplexed value of 13.6 Hz for all cases. Since second order effects are involved in both $H_{19}$ and $H_6$ terms, values of $|D_+ - D_-|$ were determined for both, but they are not necessarily unique. The experimental

spectra for the $H_5$ multiplet in the various complexes are reproduced in Figure 8 along with computed curves. The limiting values determined for the various coupling constants sensitive to backbone conformation changes are reported in Table V for $Na^+$, $K^+$ and $Cs^+$ complexes along with values for the free nonactin molecule. The value of $|J_{H_5\text{-}H_6} + J_{H_5\text{-}H_{6'}}|$ seems to be quite sensitive both to the presence of an ion and a variation in ion size.

For the uncomplexed molecule the $H_6\text{-}H_5$ and $H_6\text{-}H_7$ coupling parameters determined in the above manner were used in conjunction with the LAOCN3 program to calculate the $H_6\text{-}H_{6'}$ region of the spectrum.[52] Unfortunately, because of the interference of HDO and $CHD_2\text{-}CO\text{-}CD_3$ resonances, a spectrum suitable for comparison could not be obtained in acetone solutions at 0.005 M nonactin concentration. However, in Figure 9 a comparison with a spectrum taken in $CCl_4$ is made and it is apparent that reasonable agreement is obtained with $\delta_{AB}$ = 22 Hz and $J_{H_6\text{-}H_{6'}}$ = 12.2 Hz.

## 3.3. Cation-Induced Changes with Chloroform as a Solvent

In sharp contrast to the coupling constants and chemical shifts observed in acetone solution, where these parameters represent an average of complexed and uncomplexed environments, two sets of resonances are apparent simultaneously in $CDCl_3$ solution: one set characteristic of $K^+$ and $Na^+$ complexes, and a second independent set characteristic

FIGURE 9

Comparison of the observed and calculated $H_6$-$H_6$, multiplet. ( ---- computer simulated.)

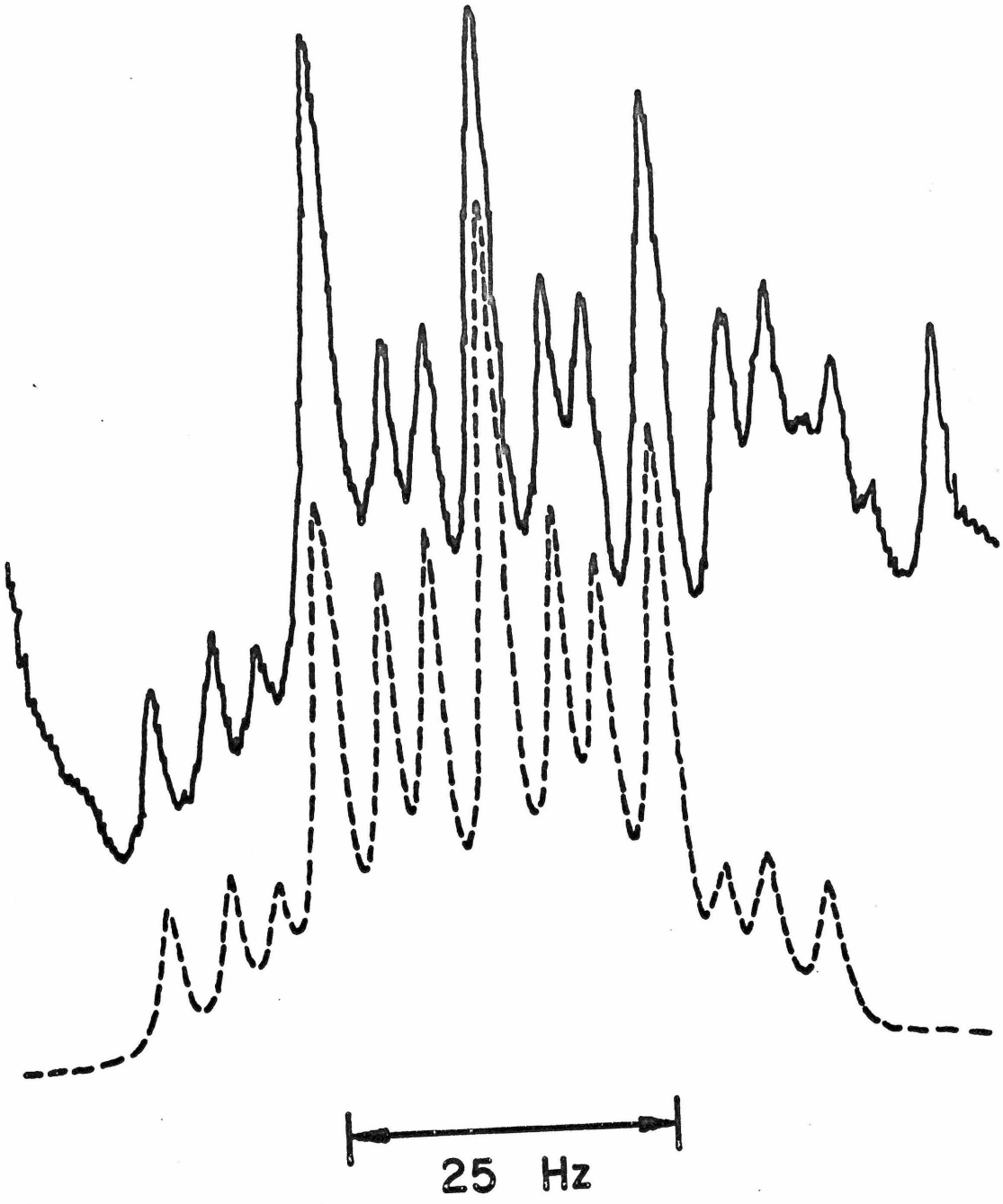
25 Hz

of the free nonactin molecule (see Figure 10). This is indicative of a slow exchange situation where the lifetimes of the complexed and free nonactin are long compared to the chemical shift difference in reciprocal seconds. In this case, relative intensities of the resonances for each state, rather than the extent of induced shift, indicate the proportionate populations of each, and the chemical shifts and coupling constants observed for the various complexes measure directly the properties of the nonactin molecule in that particular configuration.

Coupling constants were measured from the various multiplets using procedures outlined for the acetone experiments. In both $K^+$ and $Na^+$ complexes, $J_{H_2-H_3}$, $J_{H_2-H_{18}}$ and $J_{H_7-H_{21}}$ were found to be identical within experimental error to limiting values measured for the corresponding complexes in acetone solution. The $H_7$ multiplet was again fitted by computer simulation and was found to be identical to the extrapolated $H_7$ multiplet in acetone. The same appears to be true of the $H_5$ multiplet for the $K^+$ case. For the $Na^+$ case, however, the $H_5$ multiplet of the complex in $CDCl_3$ appears slightly different. Nevertheless, computer simulation shows $|J_{H_5-H_6} + J_{H_5-H_6'}|$ to be invariant to solvent changes and, in fact, the entire multiplet can be reproduced with a slight decrease (about 0.5 Hz) in the value of $|D_+ - D_-|$ for the $H_{19}, H_{19'}$ - $H_5$ coupled set of protons. This probably indicates the difference to originate

FIGURE 10

Slow exchange spectrum of $K^+$-nonactin-nonactin solution in $CDCl_3$. Nonactin concentration: 0.01 M; temperature: 17°.

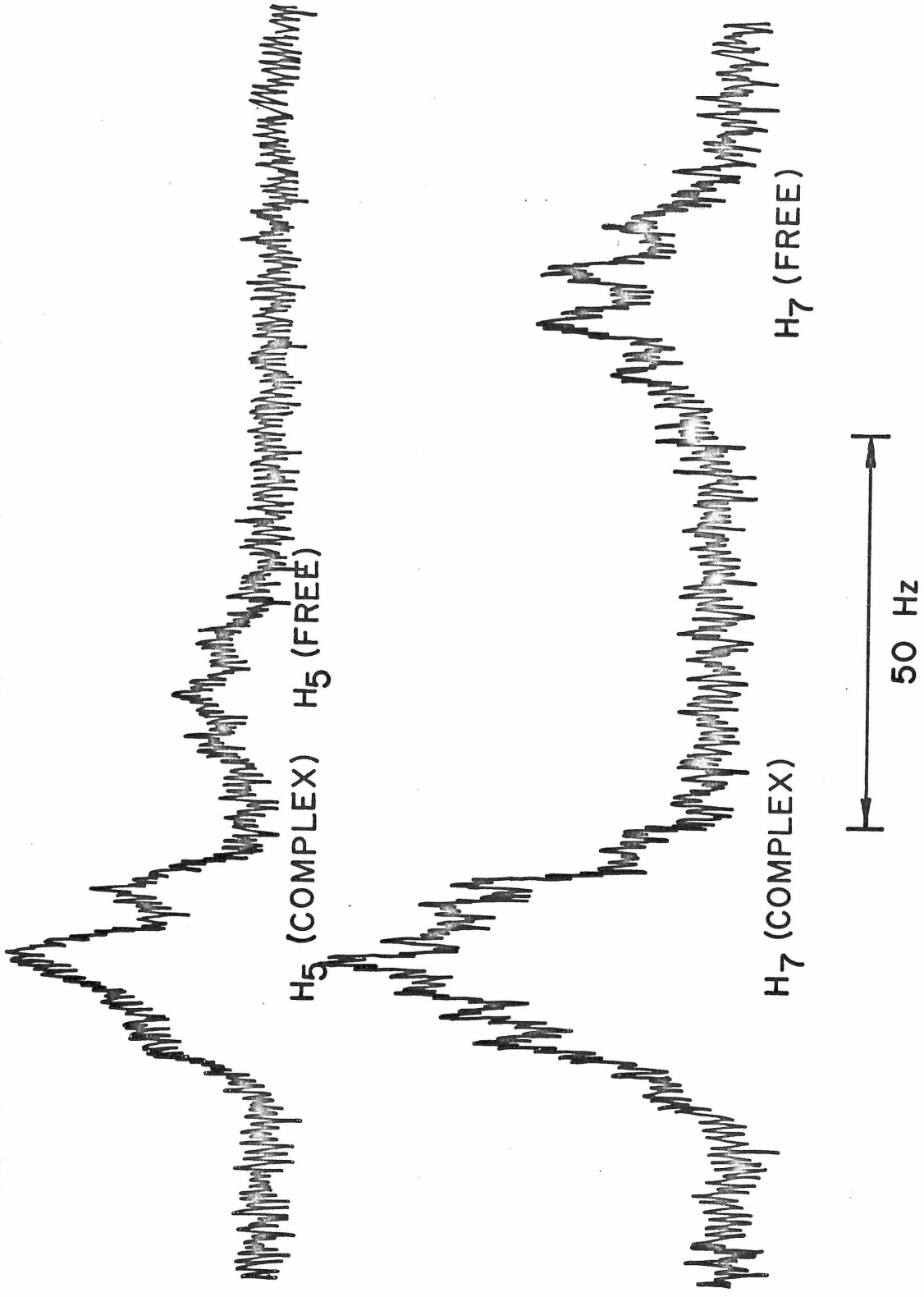
H5 (COMPLEX)
H5 (FREE)
H7 (COMPLEX)
H7 (FREE)
50 Hz

in a change in the chemical shift nonequivalence of the $H_{19}$ and $H_{19'}$ protons.

Such a variation in $H_{19}$-$H_{19'}$ chemical shift nonequivalence between complexes formed in acetone and $CDCl_3$ seems more reasonable in light of discrepancies observed for other proton resonances. The chemical shifts of the free and complexed forms, both $Na^+$ and $K^+$, are summarized in Table VI. A comparison of the induced shifts in $CDCl_3$, with induced shifts measured in acetone, is also made. From the table it is apparent that the induced shifts observed in $CDCl_3$ suffer from an additional upfield contribution of 10 to 30 Hz in the complexed form. Although most protons are still shifted downfield in the complexed forms, and $H_7$, $H_3$ and $H_5$ are still shifted to the largest extent, the magnitudes of the shift are less than those observed in acetone. Some protons, the $H_2$ proton for example, are even shifted slightly upfield. Although such differences in chemical shifts for complexes formed in the two solvent systems do exist, they can be shown to result from a difference in extent of ion pairing and solvent polarization in the different media, rather than any difference in the conformations of the complexes, and it is the similarities between spectra in the two solvents, rather than the differences, which should be stressed.

The sharpness of the lines observed in these $CDCl_3$ spectra is also of interest. In a slow exchange case,

TABLE VI: Comparison of Induced Chemical Shifts for Nonactin Complexes in Acetone and Chloroform.

| | $H_7$ | $H_3$ | $H_5$ | $H_{18}$ | $H_{21}$ | $H_2$ | (Hz) |
|---|---|---|---|---|---|---|---|
| $K^+$ $CDCl_3$ | -85 | -70 | -34 | -11 | ~0 | 25 | |
| $K^+$ acetone | -115 | -103 | -56 | -20 | -2 | 2 | |
| Difference | 30 | 33 | 22 | 9 | 2 | 23 | |
| $Na^+$ $CDCl_3$ | -82 | -21.8 | -14.8 | -20.5 | -11.2 | 17.7 | |
| $Na^+$ acetone | -113 | -62 | -40 | -23 | -9 | -5 | |
| Difference | 31 | 40 | 25 | 2 | -2 | 23 | |

linewidth is indicative of the lifetime of the species. Since no variation from the uncomplexed widths of 1-2 Hz is noted, exchange between complexed and uncomplexed states must indeed be very slow. In the $K^+$ case an attempt was even made to enhance intermolecular exchange of an ion between two nonactin molecules by increasing the free nonactin concentration from 0.01 to 0.11 M, making the free ionophore concentration a factor of 10 in excess over the complex concentration employed. Again, no change in line width or chemical shift could be observed. This observation has important kinetic implications on the mechanism of ion transport and will be discussed more fully in the following sections.

## 4. DISCUSSION

From the results thus far presented it is apparent that all three alkali cations considered interact strongly with the nonactin molecule, both in acetone and in chloroform solution. It is also apparent that the interaction with each is slightly different in terms of extent and in terms of interaction mode. However, to determine whether these differences are of the proper magnitude and direction to successfully explain selectivity in transport on the basis of one of the models currently under consideration, we must consider our results in more detail.

## 4.1. Complex Stoichiometry

The stoichiometry of the complexation process is easily established. In the slow exchange $CDCl_3$ spectra, two, and only two, species were observed regardless of the extent to which the ratio of free nonactin to complexed nonactin was raised above 1:1. The intensity of the free nonactin resonances simply increased, while those of the complex remained constant. In addition, the magnetic parameters corresponding to the two species were not in any way concentration dependent. Therefore, at least in this solvent, the interaction of ion and nonactin appears to be 1 to 1 with no tendency for aggregation with the excess ionophore molecules. The same is true of the dry acetone data. No changes in the nmr spectra appear to occur much beyond a 1 to 1 ratio of ion to nonactin. In view of these facts, cooperation between ionophores to form conduction channels seems unlikely and the origin of ion selective transport must be sought in the properties of the ion-nonactin complex itself.

## 4.2. Complex Conformation

Foremost among the properties which may influence selectivity is the solution conformation of nonactin. Binding selectivity could originate in the geometry of the polar core on the basis of steric limits to ion size or,

alternatively, differences in the exterior structure of the various complexes could lead to discrimination on the basis of diffusion rates within the membrane. Both of these structural factors can be investigated through a careful interpretation of the limiting chemical shift and coupling constant data obtained for the various complexes.

In a magnetic resonance experiment both chemical shifts and vicinal coupling constants are sensitive to variations in molecular conformation. It is, however, difficult to unequivocally assign the conformation of a molecule, such as nonactin, on the basis of this information alone. Therefore, it is convenient to have an alternate structure determination, such as that done for the potassium complex by Kilbourn et al.,[30] to which the magnetic parameters can be compared. In view of this, we will first discuss the consistency of our observations for the $K^+$ complex in dry acetone with the crystallographic data and interpret our observations for the free molecule and other complexes as departures from this structure.

At a somewhat superficial level, the chemical shift data obtained from the limiting behavior of the $K^+$ complex appear to be consistent with the crystal structure of Kilbourn. There is no noticeable salt-induced magnetic nonequivalence between similar protons on the four subunits, so one must conclude that at least on the nmr time scale the potassium ion is coordinated symmetrically to the four

subunits of the nonactin molecule. This is in agreement with the Kilbourn structure. Upon examination of a molecular model of the nonactin molecule constructed using CPK atomic models and the crystal structure data, we also note that the protons whose resonances are shifted to the greatest extent upon complex formation, namely $H_7$ and $H_3$, are those which are geometrically in close proximity to one of the four centrally directed carbonyl groups, each located at the corners of an approximate tetrahedron enclosing the central cavity of the nonactin ring. This observation suggests possible participation of these carbonyl oxygens in coordination of the potassium ion. The $H_5$ proton also experiences a fairly large downfield shift upon complex formation. Since this proton is not in close proximity to a carbonyl group, but is instead adjacent to the ether oxygen of its tetrahydrofuran ring, one might infer from the sizeable $H_5$ shifts some participation of the ether oxygens in the coordination as well. Approximate eight-fold cubic coordination has been indicated by the crystallographic studies of Kilbourn with the carbonyl oxygens occupying the alternate corners of a cube and the ether oxygens occupying the corners of the remaining tetrahedron.[30]

This cursory comparison, however, could be misleading and a more detailed analysis of chemical shifts would be desirable. Although valuable, such an analysis is not straightforward since the shifts are actually the result of

the interplay of several effects. The least complicated of these effects is that due to the direct electrostatic polarization of the various C-H bonds by the bound positive ion. In equation form the additional contribution to the shielding of a proton can be expressed as

$$\sigma_{elec} = -2\times10^{-12}E_z - 10^{-18}E^2 , \qquad (2)$$

where E is the electric field due to the bound positive ion and $E_z$ is the component of that field along the C-H bond axis.[53] Since the E field varies with the inverse square of the distance, the effect depends on the distance between the polarizing ion and the proton in question, as well as the relative orientation of the polarizing field and the bond axis. Thus, addition of a centrally located positive charge contributes in varying degrees to the observed limiting chemical shifts of protons, and to a certain extent they can be interpreted in terms of these distance and orientation parameters. The more difficult effects to take into consideration are those which have their origins in polar substituents or magnetically anisotropic groups within the nonactin molecule. Because of their proximity to the coordinating ligands, it is likely the $H_7$ and $H_5$ limiting shifts reflect, in part, interactions of the potassium ion with its ligands and conformational changes which alter the spatial relationships of these protons and their adjacent ligands. Some additional effects due to interactions with solvent

molecules are also expected, but at least for the protons undergoing large shifts, these should be of secondary importance.

Although the limiting shifts observed for the hydrogens on the periphery of the nonactin ring, such as those attached to $C_{18}$ or $C_{21}$, are more susceptible to solvent effects, they are relatively far removed from more serious complications such as the coordinating ligands and other polar substituents of the ring. Therefore, it is reasonable to attempt their interpretation on the basis of direct electrostatic polarization of the C-H bonds by the central ion. Calculations based on the standard formula for electric field effects and the geometry of the crystalline complex, in fact, succeed very well in predicting these values: 30 Hz for the $H_{18}$ proton and 4 Hz for the $H_{21}$ proton. The $H_5$ proton, although adjacent to one of the coordinating ligands, the ether oxygen of the tetrahydrofuran ring, is relatively fixed in orientation with respect to this group. Therefore, its shift was also quite successfully predicted on the basis of this model (70 Hz as compared to an experimental value of 55 Hz). But as might be expected, the shifts of $H_3$ and $H_7$ are far more complex. In the case of $H_7$, for example, ion-induced polarization accounts for a mere 10% of the observed limiting shift. Thus, unless the geometry of the complex assumed in these calculations is grossly in error, we are forced to conclude that

complexation of the $K^+$ ion results in some modification of the electronic distribution of the carbonyl groups and/or is accompanied by a conformational change about the ester linkages which brings the carbonyl oxygens in close proximity to these protons. We take this as positive evidence for the participation of the carbonyl groups in the coordination of nonactin to the centrally bound potassium ion. The $H_2$ resonance is complicated by similar effects. Here the calculated polarization shift is some 50 Hz downfield, whereas the observed salt-induced shift is small and upfield. Since the $H_2$ proton is adjacent to both the ether oxygen of the tetrahydrofuran ring and the carbonyl oxygen of the ester linkage, it is possible that the small shifts here reflect a compensating contribution originating from conformational changes in this part of the nonactin ring. In fact, there is other evidence for a salt-induced conformation change about the $C_2$-$C_3$ bond which could easily decrease the net deshielding effect of the ether oxygen on the $H_2$ proton. Thus, even under more detailed analysis, the chemical shift data is largely consistent with the potassium crystal structure, but one must invoke fairly large conformation changes on complexation which bring at least the ketone oxygens from a less restricted environment into close coordination with the central ion. These conformation changes will become more apparent in consideration of coupling constant data.

Coupling constants between vicinal protons along the

backbone of the nonactin ring are sensitive to rotations about the various carbon-carbon bonds. In nonactin, for example, $J_{H_6-H_7}$, $J_{H_6-H_5}$, and $J_{H_2-H_3}$ would be sensitive to such rotations. For simple aliphatic compounds a theory developed by Karplus is probably adequate to relate these coupling constants to the appropriate dihedral angles.[39] Basically it expresses the vicinal coupling constant as follows:

$$J = 8.5 \cos^2 \theta - 0.28 \quad \text{for} \quad 0^\circ \leq \theta \leq 90^\circ$$
$$\text{and } J = 9.5 \cos^2 \theta - 0.28 \quad \text{for} \quad 90^\circ \leq \theta \leq 180^\circ, \tag{3}$$

where $\theta$ is the dihedral angle between the vicinal protons. The theory has been refined somewhat for the interpretation of coupling along peptide chains, but these refinements consist merely of slight changes in the values of the constants in eq (3).[54] The theory thus retains its qualitative, and much of its quantitative, significance, even in this case. Since the present situation is complicated not only by the presence of functional groups, but also by the possibility of direct electrostatic effects when the positive ion is bound, we will here rely principally on these qualitative aspects of the theory. From the rather large changes in coupling constants on complex formation it is apparent that sizeable changes in the backbone structure do occur. The increase in $|J_{H_2-H_3}|$ from 7.6 to 9.3 Hz, for instance, indicates a change in the dihedral angle between the $C_2$-H and

$C_3$-H bonds. If one wishes to make quantitative estimates, the value of 9.3 Hz observed for the complex would correspond to a dihedral angle near 180°. This is approximately the angle predicted from the crystal structure data of Kilbourn et al.[30] A departure from 180° to a dihedral angle of 155° would account for the coupling constant of 7.6 Hz observed for the free nonactin molecule. Likewise, the apparent decrease in $|J_{H_5,H_6} + J_{H_5,H_6'}|$ from 12.4 to 11.0 Hz indicates a small increase in the $H_5$-$C_5$-$C_6$-$H_6$ dihedral angle, of perhaps 10 or 15°. Manipulation of a molecular model of the nonactin ring indicates that the above changes in dihedral angles would produce a change in the size of the central cavity without requiring further conformational changes in the remaining parts of the ring. A large conformational change, involving rotations about the $C_6$-$C_7$ single bond, seems unlikely since the sum of the vicinal coupling constants between the $H_7$ and $H_6$ protons remains unaltered upon formation of the complex. Unfortunately, on the basis of the present study, it is not possible to rule out conformational changes about the ester linkages, and hence we cannot ascertain more precisely the conformation of the uncomplexed ring. There is little question, however, that the dry acetone conformation of the potassium complex is in reasonable agreement with the crystal structure. In other words, the complex is nearly spherical, with the backbone resembling the seam of a tennis ball.[30] The ion is at the

center, thoroughly screened from the solvent, with at least the four keto oxygens participating in the coordination shell. The molecule also appears to be quite flexible, easily undergoing a reversible change to an uncomplexed structure which is quite different and probably much more open. It would thus appear that nonactin would have few steric limitations to ion size and should be able to adapt to fit a range of ionic radii.

4.2.1. Adaptability of the Ring

The suspicion that nonactin can adapt to the binding of a number of different ions is confirmed by analysis of the conformations of complexes formed with $Na^+$ and $Cs^+$ ions of ionic radii 0.98 and 1.67, respectively.

In comparison to the relatively large changes in the coupling constants observed upon complex formation the alternations which occur on changing the size of the central ion are relatively minor. In fact, $|J_{H_2-H_3}|$ and $|J_{H_7-H_6} + J_{H_7-H_6'}|$ are essentially identical for the three complexes. $|J_{H_5-H_6} + J_{H_5-H_6'}|$ is also invariant within experimental error for the $K^+$ and $Na^+$ complexes. But some changes do occur. In fact, $|J_{H_5-H_6} + J_{H_5-H_6'}|$ decreases from 11.0 to 9.3 Hz on substituting $Cs^+$ for $K^+$. The smaller $|J_{H_5-H_6} + J_{H_5-H_6'}|$ coupling constant indicates that the $C_{19}-C_5-C_6-C_7$ dihedral angle is less than its value of near 180° in the free nonactin molecule and the $Na^+$ and $K^+$

complexes. An examination of a CPK molecular model of nonactin indicates that such a decrease in dihedral angle can contribute to a slight expansion in the case of the $Cs^+$ complex. Thus, it appears that although the three complexes are quite similar as far as their geometries about the $C_2$-$C_3$ and $C_6$-$C_7$ bonds are concerned, some adaptation does occur at least in the case of the $Cs^+$ complex. It is also important to realize that, because of the limitations of the Karplus theory and the fact that we can monitor rotations about only 12 of the many ring linkages, it is not possible to characterize the conformational differences among the complexes more completely on the basis of coupling constant data alone.

Variations in the limiting chemical shifts observed for analogous protons of the three complexes provide some additional insight into the conformational differences among the complexes. The limiting shifts for the $H_5$ proton are again relatively easily interpreted on the basis of an electrostatic model. Since the orientation of the $C_5$-H bond with respect to the ether oxygen of the tetrahydrofuran ring is relatively fixed, to a first approximation, differences in the limiting shifts for this proton can be used to indicate changes in the stereochemistry of the tetrahydrofuran ring relative to the centrally bound ion. The observed trend can, for example, be accounted for by a reorientation of the tetrahydrofuran ring, which points the ether oxygen more

directly into the central cavity and tips the $C_5$-H bond to a more obtuse angle with respect to the $M^+$-$H_5$ vector in the case of the larger ion. Examination of a molecular model of nonactin indicates that this conformation change would lead to the change in the $C_{19}$-$C_5$-$C_6$-$C_7$ dihedral angle suggested earlier by the coupling constant data and the accompanying expansion of the central aperture necessary to accommodate the larger ion. This conformational change possibly brings the tetrahydrofuran oxygens into more effective coordination with the central ion, which may also contribute to the increased downfield limiting shifts as one goes from $Na^+$ to $K^+$ to the $Cs^+$ complex. The $H_7$ limiting shifts again do not readily lend themselves to this simple interpretation. Since in the complex, the $H_7$'s are in close proximity to the coordinating carbonyl groups, it is likely that the major part of the salt-induced shift observed here results from some modification of the electronic distribution of the keto groups and/or an accompanying conformational change about the ester linkages which brings the carbonyl oxygens into closer proximity with these protons. The observed differences in the $H_7$ limiting shifts for the three complexes, for example, probably reflect differences in the stereochemistry about this ester linkage. Thus the smaller $H_7$ limiting shift for the $Cs^+$ complex may indicate that the

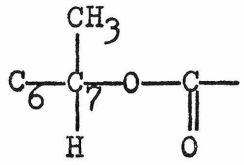

group has been rotated about the ester linkage so that the $C_7$-H bond points more directly into the central cavity and is less eclipsed with the carbonyl group. Examination of the molecular model indicates that this conformation change would also lead to a slight expansion of the nonactin aperture.

4.2.2. Uniformity of Exterior Geometry

While it is apparent from this analysis that conformational differences among complexes do exist which apparently allow the interior core to more effectively coordinate to ions both larger and smaller than $K^+$, conformational changes are not large compared to those which occur on complex formation and structural differences from the complex exterior are probably difficult to discern. We note that for protons near the exterior of the molecule, namely $H_{18}$, $H_{21}$ and $H_2$, differences in limiting shifts among the complexes are small ($\pm$ 2 for $H_{18}$, $\pm$ 5 for $H_{21}$ and $\pm$ 5 for $H_2$). Of course, because of their distance from the ion and coordinating groups the sensitivity of $H_{21}$ and $H_{18}$ to electrostatic effects is also somewhat decreased, but at least they confirm that no gross exterior differences exist. There is also some indirect evidence for the similarity of

exterior structures in $Na^+$ and $K^+$ complexes from chemical shifts in $CDCl_3$ solutions. Limiting shifts in acetone and $CDCl_3$ for the two complexes are presented for comparison in Table VI. At first glance the differences might seem to indicate a change in complex conformation as a function of solvent. However, this seems unlikely in consideration of the lack of any simultaneous change in coupling constants and the absence of any solvent-induced chemical shift or coupling constant change in the free nonactin molecule (see Table II). More likely, the differences are the result of variations in the cation-induced external associations of other constituents in the two solvents, namely anions and the solvent molecules themselves.

Of major importance is the presence of a bound anion in $CDCl_3$. While ion pair formation was minor in acetone solution (30% under the worst conditions encountered), in $CDCl_3$ the complex is expected to be nearly 100% ion paired. The effects on chemical shift of this additional surface-bound negative charge can again be treated on the basis of Buckingham's electric field effect equation.[53] Because the resonances of the four sets of analogous protons on the nonactin ring again remain magnetically equivalent, we know that in a time-average sense the bound charge is distributed over the surface with a high degree of symmetry. We have therefore calculated expectation values of $E_z$ and $E^2$ for various distributions of anions about the nonactin complex

and used these to estimate chemical shift effects. In the case that the time-average distribution of the anion was spherical, effects on chemical shifts linear in the anion electric field would, of course, average to zero and the $E^2$ effect would be in the wrong direction. However, the tightly bound ion more likely seeks some discrete point of closest approach to the center of the nonactin complex, producing a more complex field distribution within. Fields for these more discrete time-average distributions have also been calculated. But axial, tetrahedral, octahedral and cubic distributions still give results which often do not agree even qualitatively with our observations. The results for the square planar distribution do give qualitative agreement with the observed solvent-induced shifts, but in magnitude it can produce only about one-half the effect needed. The square planar distribution is nevertheless reasonable in that the ions tend to fill the indentations formed by the four loops of nonactin's "tennis ball seam" backbone configuration.

The remaining half of the "solvent" effect could be due to a second solvent-linked phenomenon which produces an effect similar in magnitude and direction to the square planar charge distribution. This involves the alignment of the highly polar acetone solvent molecules ($\mu$ = 2.88 debye) about the complex in that solution. Such alignment is less significant or entirely absent in $CDCl_3$ ($\mu$ = 1.02). In

spite of the fact that acetone molecules are largely aligned (about 80% at 17°C for a single charge dipole interaction at 7 Å), the binding is less tight than that of the anion, so a spherical distribution seems reasonable. In this model static electric field effects due to the oriented dipoles will be zero. However, this is not necessarily the case for the effects due to the anisotropic magnetic susceptibility of the C=O group. The thru-space contribution to chemical shift of the magnetic susceptibility of an oriented group, such as the acetone carbonyl, is generally expressed in tensor form. However, under conditions of rapid rotational averaging, the following formula will hold:[55]

$$\Delta\delta_{mag} = \frac{1}{3}\frac{1}{R^3}\sum_{i=1}^{3} X_i\,(3\cos^2\phi_i - 1)\,. \qquad (4)$$

Here the $X_i$ are the principal axis elements of the susceptibility tensor, the $\phi_i$ are the angles between the principal axes and the group-to-nucleus vector, and R is the magnitude of the vector. Assuming that on the average six fully-oriented C=O groups surround the nonactin complex in a spherical array at 7 to 10 Å distance, and employing accepted values for the susceptibility tensor elements,[56] an anisotropic susceptibility contribution to the chemical shifts of the internal protons of the nonactin complex is calculated to be approximately 0.1 ppm downfield. Thus, the observed upfield solvent shift in going from acetone to

$CDCl_3$ is probably the result of changes in anion and magnetic susceptibility effects. This result could lead to some minor modifications in our interpretations of salt-induced shifts, but more importantly it sheds light on the exterior conformation of the complexes. Both effects are highly dependent on the exterior size and shape of the nonactin complex and, since solvent-induced shifts are so similar for $Na^+$ and $K^+$ complexes, the exterior geometries must be similar to a commensurate extent.

Thus, it seems highly probable that differences in the geometries of anhydrous complexes cannot produce sufficient variation in complex mobilities to account for transport selectivity in membranes. It is more likely that selectivity resides in ion-binding constants, but, in view of the flexibility of the nonactin ring and the apparent adaptability of its core to the effective coordination of ions of various size, selectivity cannot be the result of simple imposition of steric limits to ion size. It is therefore necessary to more closely examine the ion-binding properties in these systems.

## 4.3. Complex Formation Constants

### 4.3.1. Determination of Constants

As a first step in a detailed analysis of the nonactin ion-binding process, we have subjected our acetone and

acetone-water salt concentration studies to a theoretical analysis designed to accurately determine binding constants and limiting spectral parameters for the various complexes formed. In acetone solution, all three ions studied exchange rapidly between the solvent and the nonactin cavity, and as a result the salt-induced shifts, summarized in Figures 4, 5 and 6, reflect the distribution of nonactin molecules between the free and complexed states. The distribution can be described more precisely in terms of the following simple equilibrium:

$$\text{Nonactin} + K^+ \rightleftharpoons \text{Complex} . \qquad (5)$$

The salt-induced shifts observed for a given proton become an average of the chemical shifts in the free and complexed environments, weighted by the respective fractions in each state.[57] Expressing these fractions in terms of an equilibrium constant and stoichiometric concentrations of the constituents, it is readily shown that:

$$\delta = \tfrac{1}{2}\delta_c \left\{ (1 + \phi + \eta) - \left[ (1 + \phi + \eta)^2 - 4\phi \right]^{\frac{1}{2}} \right\}, \qquad (6)$$

where $\delta$ is the observed salt-induced chemical shift, $\delta_c$ is the chemical shift of the proton in the complexed state relative to that in the uncomplexed environment, $\phi$ is the stoichiometric concentration ratio of ion to nonactin, and $\eta$ is the reciprocal of the product of the apparent formation constant K and the stoichiometric nonactin concentration.

Since the stoichiometric concentration of nonactin is fixed in our experiments (changes in the mole fraction of nonactin upon the addition of salt are negligible owing to the low salt concentration), and the apparent formation constant K is not expected to vary significantly over the range of salt concentration investigated, $\eta$ may be taken to be a constant in our treatment of the data. Equation (6) then suggests a graphical procedure for the determination of K. In Figure 11 we have plotted theoretical curves of $\delta/\delta_c$ versus $\phi$ for various values of $\eta$. This family of curves can be compared with the experimentally observed variations of $\delta/\delta_c$ with $\phi$, and in this manner K can be obtained. Since values of the limiting shifts can only be determined to within 10-20% visually, further refinement of the $\delta_c$'s and K's was made by least-square fitting of the data to the theoretical expression.

The salt-induced shifts observed for the nonactin $H_7$ proton on the binding of $K^+$ to nonactin in both dry acetone and the acetone-$D_2O$ mixture are plotted versus $\phi$ in Figure 11. Comparison of the data with the theoretical curves yields the apparent ion-binding constants of $(7 \pm 2) \times 10^4$ and $(1.7 \pm 0.2) \times 10^4$ (concentrations expressed in mole fractions) for dry and wet acetone, respectively. Examination of Figure 11 indicates that the binding of $K^+$ to nonactin in dry acetone is almost stoichiometrically complete, and hence the extent to which nonactin molecules are

FIGURE 11

Theoretical curves of $\delta/\delta_c$ versus $\phi$ for various values of $\eta$, and fitting of the salt-induced shifts observed for the nonactin $H_7$ proton in dry acetone (X) and wet acetone (Θ).

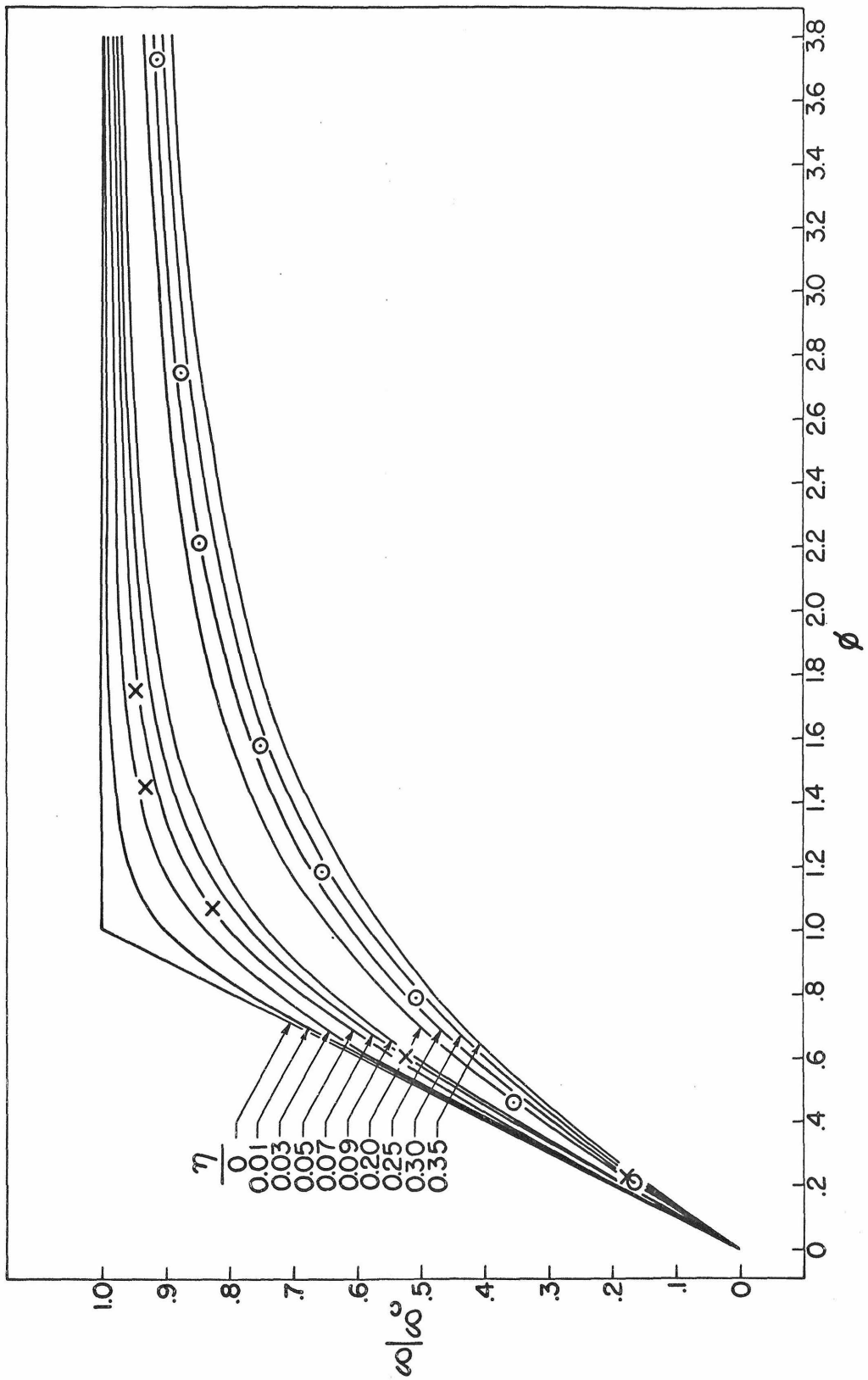
η
0
0.01
0.03
0.05
0.07
0.09
0.20
0.25
0.30
0.35
ω/ω₀
φ
0
.1
.2
.3
.4
.5
.6
.7
.8
.9
1.0
0
.2
.4
.6
.8
1.0
1.2
1.4
1.6
1.8
2.0
2.2
2.4
2.6
2.8
3.0
3.2
3.4
3.6
3.8

complexed, as expressed by $\delta/\delta_c$, is not particularly sensitive to the binding constant. In wet acetone, on the other hand, the smaller binding constant can be determined with considerably higher precision. Thus, in addition to facilitating the determination of K, the method of data treatment outlined above provides some visual assessment of the accuracy of the binding constant determined.

Binding constants and limiting shifts for $Na^+$ and $Cs^+$ complexes in dry acetone were determined in a similar manner and are presented along with those for $K^+$ in Table VII. Binding constants for $Na^+$ and $Cs^+$ in wet acetone are also presented. However, because of their extremely low values it was necessary to assume limiting chemical shifts, based on values determined in the dry acetone case, prior to making the binding constant determination.

In all cases the data fit the theoretical expressions within reasonable limits, indicating that the complex formed is indeed 1 to 1 and that there are few complications due to variations in the activities of any of the components during the course of the experiment. This is perhaps not surprising for a system such as the nonactin-alkali salt system in acetone. Since the equilibrium involves the interaction of a univalent cation with a neutral species to form a charged complex, interionic effects on the activities of the charged species are expected to largely cancel in the equilibrium expression, except at high ionic strengths. We have also

TABLE VII: Formation Constants of the Various Alkali Ion-Nonactin Complexes in Dry and Wet Acetone Solutions at 17°C.

| Salt | $D_2O$ (mole fraction) | K (mole fraction units) |
|---|---|---|
| $NaClO_4$ | $1 \times 10^{-3}$ | $7 \pm 2 \times 10^4$ |
| $NaClO_4$ | 0.39 | $210 \pm 10$ |
| $KClO_4$ | $7 \times 10^{-3}$ | $7 \pm 2 \times 10^4$ |
| $KClO_4$ | 0.34 | $1.7 \pm 0.2 \times 10^4$ |
| $CsClO_4$ | $3 \times 10^{-3}$ | $15 \pm 12 \times 10^3$ |
| $CsClO_4$ | 0.55 | $400 \pm 80$ |

considered the effect of ion-pairing. However, on the basis of reasonable ion-pairing constants in acetone, the salts can be shown to be largely dissociated under the conditions of our experiments.[58] Furthermore, ion-pairing constants do not vary dramatically within the series, so that any residual effects will tend to cancel when comparing binding constants within the series of ions. Therefore, the constants determined should represent fairly accurately the relative affinity of the nonactin cavity for the cation in question in a particular solvent system.

If, on the other hand, one wishes to compare binding constants determined in different solvents, one must define more precisely the initial and final state involved in the reaction. This is especially true since some factors which change the activity of an ion, antibiotic, or complex are independent of ion concentration and generally included as part of an apparent equilibrium constant $K_a = \frac{\gamma_M \ \gamma_N}{\gamma_C} K$. Ion solvation is predominant among these factors. It may influence the activity of the ion through a direct interference of the bound solvent molecule with the nonactin complexation process or through a more subtle change in the free energy of either the initial or final state of the ion in the binding equilibrium. The extent to which ion activity effects of this type might vary from experiments conducted in dry acetone to experiments conducted in wet acetone can be ascertained through an examination of ion

hydration constants for the acetone solvent system. In acetone a monomeric water molecule binds to sodium ion with a binding constant of about 40 (in mole fraction units).[59] Thus in the dry acetone solutions considered here, with less than $3 \times 10^{-3}$ mole fraction water present, no more than 10% of the sodium ions would be associated with a water molecule, even at their maximum concentration, and the measured apparent K of $7 \times 10^{4}$ should very nearly represent the binding constant of an acetone-solvated sodium ion to a nonactin molecule. In the case of $K^{+}$ or $Cs^{+}$ hydration constants are expected to be lower and solvation should be entirely by acetone. In wet acetone (0.5 mole fraction water) employing the same hydration constant, nearly all sodium ions (95% or more) should be hydrated to some extent and the binding constant determined in this solvent system would thus represent the binding of a hydrated sodium ion. A similar statement can be made for the other alkali ions. The extent of solvation in each case should be independent of ion concentration simply because the predominant solvating species is in great excess at all times. Thus, the effects of solvation on ion activity will appear as variations in the apparent binding constants.

Variations in the activities of the free nonactin molecule, or the complexed nonactin molecule, among different solvent systems are also possible. For example, the increased solvation of nonactin's coordinating ligands by

water could equally well interfere with the ion complexation process, producing a decrease in the apparent K for the process in a more aqueous environment. Or, increased solvation of the complex itself by water may significantly lower or raise the free energy of this state with a concomitant increase or decrease in binding constant being the result. External solvation may significantly stabilize the complex or, if the hydrated rather than the unhydrated ion is bound, direct distortion of the nonactin ring may lower the apparent binding constant.

That these possible solvent effects are important is apparent when binding constants determined in wet and dry acetone are compared. In dry acetone nonactin seems to have a high affinity for all three acetone-solvated cations, but little selectivity among them. Within limits of error there is no difference in binding constants for $Na^+$ and $K^+$. The binding constant for the larger $Cs^+$ ion is somewhat reduced which may indicate the approach of a steric limit to ion size. However, the departure from the potassium binding constant, still only a factor of 5, is not nearly large enough to account for transport selectivity. The picture in wet acetone is quite different. First the affinity of nonactin for a hydrated ion is much less. In fact, the binding constant for a hydrated sodium ion is a factor of 300 lower than that for the acetone-solvated case. But more importantly, the reduction in affinity is far greater

for $Na^+$ and $Cs^+$ than it is for $K^+$ making the binding of $K^+$ favored over $Na^+$ by a factor of 100 and over $Cs^+$ by a factor of 50. Thus in the hydrated system nonactin exhibits binding behavior which could qualitatively explain its behavior in membrane transport.(8)

4.3.2. Discussion of Ion Selectivity

The origin of the difference in binding constants for hydrated ions we believe to arise from a decrease in the activity of the ion itself, rather than from any change in the ion specific properties of the nonactin ring. We note that the apparent reduction in binding constant in itself is not sufficient evidence for this hypothesis since water may indirectly affect the properties of free nonactin or the complex. The possibility that water affects complexation through solvation or the resulting distortion of the free nonactin ring can easily be eliminated since we have already noted that the magnetic environments of the protons in the free nonactin molecule are not affected by the presence of water, either in terms of coupling constant or chemical shift (Table II). As demonstrated in the previous section, chemical shifts and coupling constants are extremely sensitive to conformational change or association of highly polar groups. Thus, changes in geometry induced by water solvation or an extensive change in solvation itself would be apparent in these parameters.

Variations in the conformational state of the three complexes in water-acetone as compared to dry acetone solution can also be investigated through observations of these parameters. Changes in geometry induced by the addition of water through the accommodation of the larger hydrated ion in the complex should result in differences in the limiting chemical shifts observed in the nonhydrated and hydrated systems. In the case of the potassium ion where the limiting shifts for complexes formed in both wet and dry acetone could be measured directly, differences in limiting shifts between the two solvent systems for all the protons were found to be no more than 10%. The limiting coupling constants, $|J_{H_2-H_3}|$, $|J_{H_5-H_6} + J_{H_5-H_6'}|$ and $|J_{H_7-H_6} + J_{H_7-H_6'}|$, are also similar for the limiting complexes formed in the two solvent systems.

In the case of $Cs^+$ and $Na^+$, where the effect of hydration is more pronounced, the limiting shifts of $H_7$, $H_3$ and $H_5$ could not be reached experimentally. However, the relative shifts of $H_7$, $H_3$ and $H_5$ here are equally indicative of changes in the properties of the complex formed, as evidenced by the changes in the ratios of these shifts as the central ion is changed. We have summarized these ratios in Table IV. The ratio of the $H_3$ to $H_7$ shifts, for example, changes from 0.55 to 1.34 on substituting $Cs^+$ for $Na^+$. In comparison to this gross dependence on ion size, the small changes in the ratios observed between complexes formed in

anhydrous and wet acetone solutions (see Table IV) are insignificant. Since it is inconceivable that the central aperture of the nonactin ring could accommodate the large hydrated ions without grossly distorting the ring conformation from that observed for the complex containing only the unhydrated ion and without modifying in the process the aforementioned vicinal coupling constants, chemical shifts or chemical shift ratios, we conclude that only the unhydrated ions are bound in the central aperture of the nonactin ring and that the same complexes are formed in the two solvent systems regardless of the state of hydration before formation. The apparent reduction in the complex formation constant when water is added to the system is then the result of a simple reduction in ion activity.

Therefore, on the basis of our knowledge of the limited adaptability of the nonactin ring and the necessary removal of a hydration shell from the complexed ion, a complete picture of the origin of ion-binding selectivity and the variation of this selectivity from solvent to solvent can be formulated. Since our model proposes the replacing of an ion solvation shell with the coordinating groups of nonactin and we know that the interaction of free nonactin or complex with the solvent does not vary greatly from wet to dry acetone, it is largely the differences in the free energy of the ion in the solvated and complexed states that we must consider. In dry acetone the similarity of binding

constants for $Na^+$, $K^+$ and $Cs^+$ would suggest a rather similar dependence of the free energy of ion-coordination on ion size for both nonactin and the acetone solvent, at least over the range of ionic radii investigated. This result is perhaps not surprising if the nonactin ring is reasonably flexible, since the keto groups of the acetone molecules could mimic rather well the coordinating carbonyl oxygens of the macrocycle. A first approximation to the exact manner in which free energy of solvation or complexation depends on ionic radius and on the properties of the solvent can be obtained by considering the energy of interaction of a polarized solvent of dielectric constant D and an ion of charge Ze and radius r.[60] The results are summarized in the following equation:

$$\Delta G_{sol} = - \frac{NZ^2e^2}{2r} \left(1 - \frac{1}{D}\right) \qquad (7)$$

In view of this result it is also not surprising that water solvates the ion more strongly than does acetone, since D increases from 20 to 80 in going from a water to an acetone solvent. It is at first surprising, however, that the difference between various solvation curves does not vary monotonically with ion size, since the same expression predicts a $\frac{1}{r}$ variation of free energy with ionic radius in all cases. But we believe the result to arise merely from the subtle deviations from ideal behavior which occur especially for the smaller ions with discrete first solvation shells.

In fact, more sophisticated theories of ion solvation attempt to take these deviations into account by considering first shell contributions separately.[61,62] To illustrate the subtle differences which may exist we have depicted schematically in Figure 12 possible dependences of the standard free energies of ion complexation and ion solvation for nonactin and the two solvent systems under consideration. Here, the standard free energies of hydration of the alkali ions relative to the free gaseous ions have been used to provide a meaningful scale to the free-energy diagram, and the standard solvation free energies of the ions in our water-acetone mixtures were assumed to be the same as in bulk water.[63] The curves for dry acetone and nonactin were included on the basis of the binding constant data reported in this paper. The similarity of the curves for acetone and nonactin simply reflects the constant free energy difference between them as dictated by the radius invariant binding constants ($RT \ln K = -\Delta G$). Similarly, the different shapes of water and nonactin curves are the source of ion selective behavior. The differences in the water and acetone solvation curves can be interpreted in terms of ion activity coefficients relative to a standard state in acetone. ($\Delta G' = -RT \ln \gamma$) The activities calculated from these differences for $Na^+$, $K^+$ and $Cs^+$, 0.003, 0.25 and 0.03, respectively, bear a qualitative correspondence to the transport activities in membranes.[8] An

FIGURE 12

Plot of free energy versus reciprocal ionic radius for ion solvation and complexation.

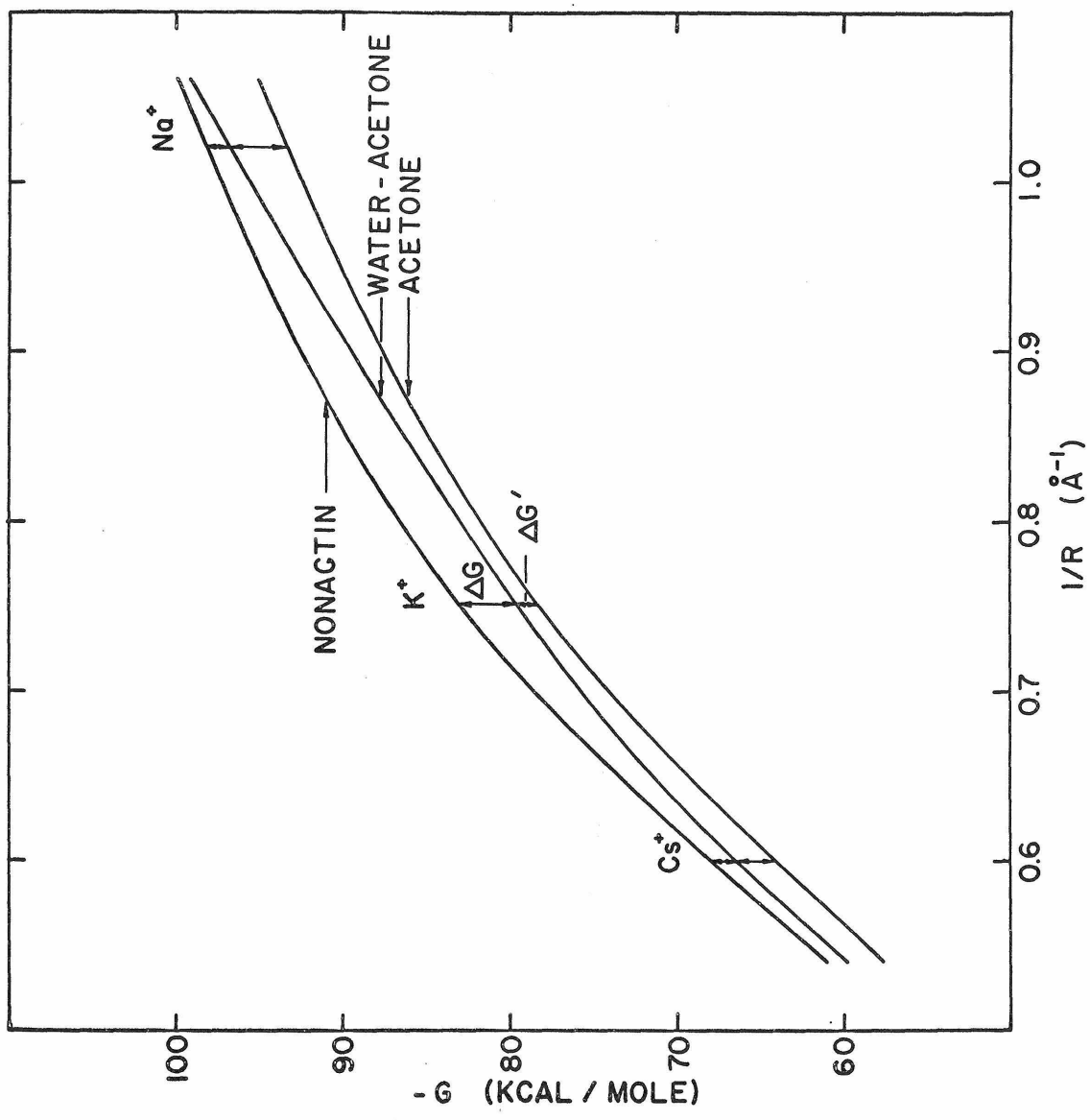
Na+
WATER - ACETONE
ACETONE
NONACTIN
K+
ΔG
ΔG'
Cs+
100
90
80
70
60
- G (KCAL / MOLE)
0.6
0.7
0.8
0.9
1.0
1/R (Å-1)

important point to notice in Figure 12 is that the variations between the solvation free energy curves in the two solvents, water and acetone, are actually small compared to the total free energy involved. It is then perhaps not so surprising that subtle variations in the radius dependence of the free energy curves for ion complexation and ion solvation (hydration) are difficult to predict on the basis of theories which describe the more general aspects of total solvation energy. Nevertheless, it is these differences in free energy which lead to the differential reduction in ion activity for the various ions and thus the observed ion selectivity when water is added to the acetone solution.

This interpretation of the origin of selective binding constants in acetone and acetone-water systems also gives some justification for extending our conclusions to systems more representative of membrane systems. First, the deviations from $\frac{1}{r}$ radius dependence which seem to result in ion selective behavior originate in the first few solvation shells. Since in the acetone-water systems the preferential binding of water to the ion makes water the predominant species in the first shell, selectivity measured in this system is probably a good approximation to a pure aqueous environment. Also for the complex in a more lipid-like environment, nonactin ligands occupy these first shells, and beyond this the solvent behaves as a pure dielectric making solvation energy proportional to $(1 - \frac{1}{D})$. Since the

dielectric constant of chloroform in retrospect is not that different from a pure hydrocarbon, extrapolation of $CDCl_3$ results to the lipid phase seems more reasonable.

## 4.4. Complex Formation Kinetics

But even with binding constant data extrapolated to an appropriate system, their implications on selectivity in ion transport can only be seen through the choice of an appropriate transport model. From the discussion thus far, the ion carrier model seems most appropriate. The lack of change in spectral parameters as a function of nonactin concentration indicates that the molecules do not tend to associate in either aqueous or non-aqueous systems. Also, the complex conformation, which is believed to present a spherically symmetric hydrophobic exterior, leaves little possibility for exchange of ions between molecules. Thus neither channel, pore, nor shuttle mechanisms seems likely. But in addition to this negative evidence for other models, some additional support for the detailed steps in the carrier mechanism can be gleaned from the kinetic limits imposed by these pmr experiments.

### 4.4.1. Estimation of Rates

In an nmr experiment, the line widths are indicative of the rates at which certain molecular processes are occurring. If a proton exchanges between two or more magnetic

environments at a rate fast compared to the frequency separation of these environments, a single sharp resonance is observed, whose parameters are representative of the average environment of the sites. If the exchange rate is much slower than this frequency separation, two individual resonances are observed, each characteristic of one of the sites. In the intermediate range the lines broaden in a complex manner, one state changing continuously into the other, but near either limit a simple analytical expression for the exchange broadening can be obtained.

In the acetone experiments, a single, fast exchange set of resonances was observed under all conditions. In this limit, any residual broadening due to the two site exchange process can be expressed as:[64]

$$\frac{1}{T_{2'}} = P_A^2 P_B^2 (\omega_A - \omega_B)^2 (\tau_A + \tau_B) \qquad (8)$$

where $P_A$ and $P_B$ are the populations of the two sites, $\tau_A$ and $\tau_B$ are the life times and $(\omega_A - \omega_B)$ is the chemical shift difference between the sites. For some protons, $H_7$ for example, $\omega_A - \omega_B$ reaches as much as 700 $sec^{-1}$ and an increased line width of 3 or 4 $sec^{-1}$ could easily be detected. Therefore, in the absence of any noticeable broadening, the life times of the complexed and uncomplexed states in a quasi-aqueous medium must be much less than $10^{-4}$ sec. Measurements by Eigen have, in fact, indicated that they reach as little as $10^{-7}$ sec.[65]

In the more lipid-like medium, in this case chloroform, exchange was found to occur at a much slower rate. Here two sets of sharp resonances were observed, one for free nonactin and one for complexed nonactin. In the slow exchange limit, contributions to the line width take the form $\frac{1}{T_{2'}} = \frac{1}{\tau_A}$, where $\tau_A$ is again the lifetime of the species, to which the resonance corresponds.(64) Here no line broadening could be detected even at 0.1 M excess of free nonactin in a solution 0.01 M in potassium complex. In other words, the lifetime of the species must have exceeded 0.25 sec.

4.4.2. Application to a Transport Model

The relation of these rates to the process of ion transport by a lipid soluble ion carrier, such as nonactin, can be most easily seen on the basis of a simple carrier model. In its most elementary form, a membrane having transport properties can be considered to be an ion impermeable organic phase separating to aqueous phases. The ion carrier is distributed between these phases, but is largely in the organic phase due to its high partition coefficient (of the order of $10^6$ for nonactin). This system is depicted schematically in Figure 13. Transport across this membrane can be broken into a number of intermediate steps. In phase I, near or at the membrane surface an antibiotic-cation complex is formed; this complex enters the organic phase;

FIGURE 13

Model for nonactin-facilitated transport across a lipid bilayer.

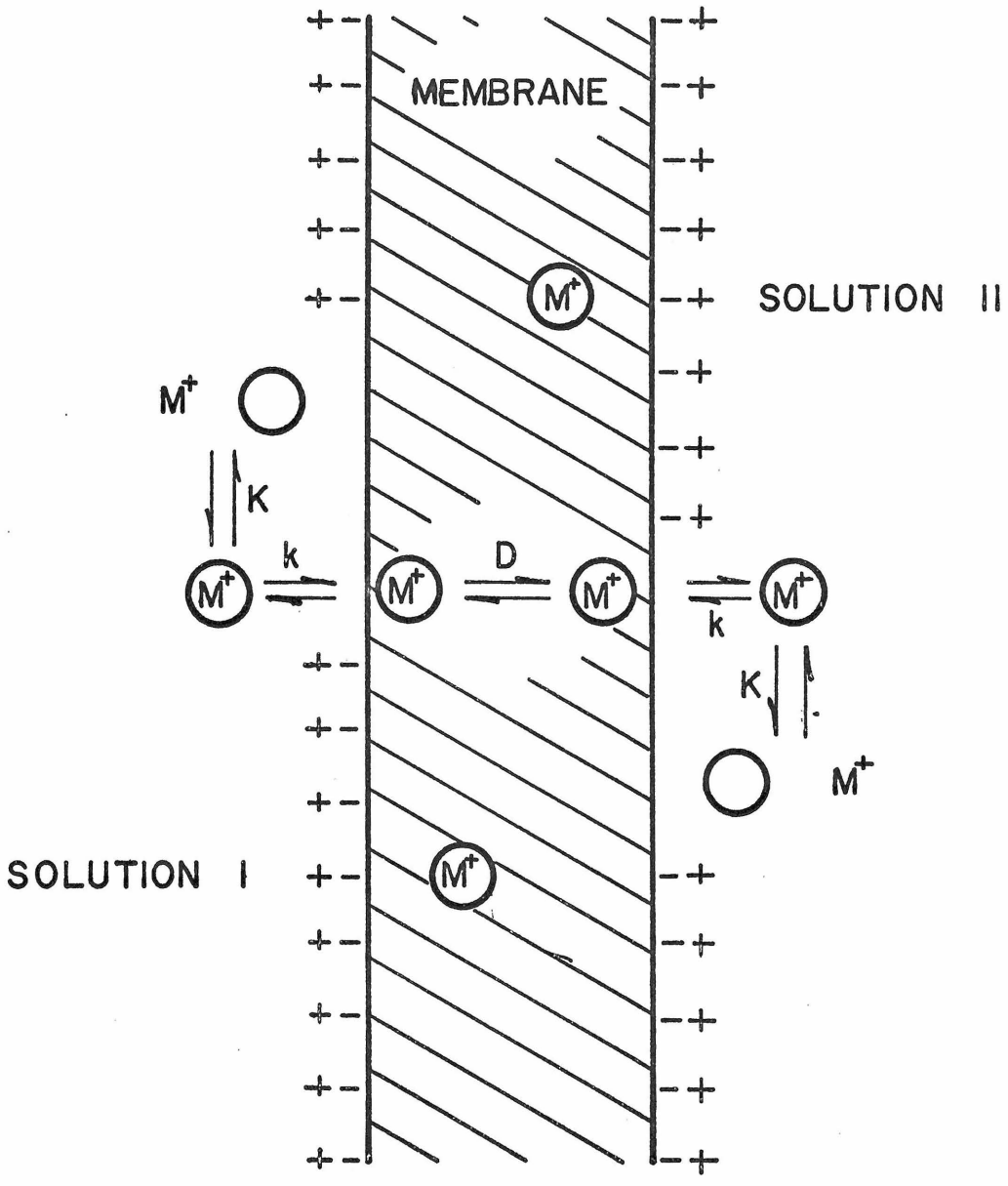
MEMBRANE
SOLUTION II
SOLUTION I
M+
K
k
D

whereupon it diffuses across the membrane; and on reaching the opposite interface the complex undergoes these steps in reverse order. Any one of the steps could be the rate limiting one for ion transport. The rate most easily estimated is that of diffusion of the complex across the organic layer. It is well known that the interior of a lipid bilayer is a semi-fluid hydrocarbon layer of about 70 Å thickness. Thus, a simple hexadecane phase of appropriate thickness will probably give a good lower limit for a diffusion time. (Palmitic acid, a common residue found in phospholipids, has a 16 carbon chain.) Using the viscosity of hexadecane and appropriate assumptions about the size and geometry of nonactin, a lower limit of about $10^{-6}$ sec for the crossing of the membrane is predicted. Estimates of the rates for the other processes can be obtained from nmr and other data. The rate of complex formation is known to be faster than $10^{-4}$ sec by the acetone experiments and is of the order of $10^{-7}$ sec according to Eigen's work.[65] Therefore, it seems reasonable to assume that this process is fast enough compared with diffusion, so that the concentration of the complex near the interface is maintained by reversible complex formation in accordance with the aqueous solution equilibrium constant K. The rate of entrance into the organic phase cannot be estimated directly from our data. The rate, however, is more likely determined by the energy necessary to remove the complex solvation shell. But

because of the envelopment of the cation in the complex, the solvent interactions which might have imposed a high activation energy to an ion entering the organic layer should be small and non-discriminant as far as the alkali cations are concerned. Therefore, we also expect this step to be fast enough to allow equilibrium between phases in accordance with a partition function, k, and electrostatic potential, $\psi$ before diffusion takes place. Once in the organic phase, we know that the ion will not shuttle between carriers since the lifetime estimated on the basis of pmr data, 0.25 sec, is long compared to any reasonable diffusion time. Exchange between carriers has, in some cases, been observed in isotope labeling experiments, but only under conditions of high carrier concentration, 0.01 M, and extremely thick membranes, 2.25 mm.[33] Thus, a model such as the one proposed, where transport is governed by an equilibrium distribution of species except at a rate limiting step of diffusion through the organic layer, seems extremely reasonable.

Eisenman has made some detailed calculations of the conductance properties of a membrane on the basis of this model and has found good agreement with experiments for nonactin-like molecules.[34] Among other things the theory predicts that conductivity be described by

$$\frac{F^2}{d} \cdot C \frac{\mu k K a_i}{1 + K a_i}, \qquad (9)$$

where C is the total concentration of the macrocyclic antibiotic, $\mu$ is the complex mobility, K is the aqueous binding constant, and $a_i$ is the activity of the ion. The selectivity is given by:

$$\frac{\mu_j k_i K_i}{\mu_j k_j K_j} , \qquad (10)$$

where the subscripts designate the different ions. The expression (10) can be simplified somewhat on the basis of our experiments. Differences in $\mu$, the complex mobility, are largely determined by the exterior geometry of the nonactin molecule for the various complexes. Since this geometry was found to be very similar for all alkali cation complexes, the subscripts can be dropped from the $\mu$'s and they can then be eliminated from the expression. The same is true of k. It is largely determined by the solvation interactions in the two phases. Beyond the first few solvation shells this can be described simply in terms of solvent dielectric, complex size and ionic charge. In the nonactin complex the first few hydration shells have been replaced with the nonactin ligands, so that from the complex exterior all ions appear to be of the same size and same charge. Thus, k is also a constant, independent of ion and can be eliminated from the selectivity expression. This leaves $\frac{K_i}{K_j}$, the ratio of the aqueous binding constants, as the only factor determining selectivity in transport. Thus, our discussion of the origin of ion binding selectivity can

be extended to the interpretation of selectivity in ion transport at least for antibiotics of the nonactin type.

Of course the model, although being in excellent agreement with some experiments, is grossly oversimplified. For example, it cannot in its present form explain the unusual depression of $K^+$ conductivity through lipid bilayers in the presence of $Ca^{++}$.[32] But even here the model becomes amenable with minor modification. In the original calculation Eisenman considered the effect of an electrostatic potential within the membrane, but only the part established by the steady state density of the complex itself. In actuality phospholipid bilayers and other membranes have an additional potential arising from membrane bound charges. For a lipid bilayer this potential might be approximated by an electrical double layer in place of the surface phosphatidyl choline groups as depicted in Figure 13. This double layer would normally increase the concentration of the positively charged complex in the hydrocarbon phase. However, in the presence of salts which form insoluble complexes with phosphates ($Ca^{++}$ for example) the normal potential may be depressed to a point where the concentration of complex in the lipid phase is decreased and with it the $K^+$ conductance. Thus, it may well be that the apparent competition of $Ca^{++}$ with $K^+$ is the result of a subtle effect on one of the other transport steps, rather than an effect on the binding selectivity itself. Other modifications of the

model might also have to be made before it can be applied to more natural systems, for example effects on the activity of the various species in the region where the complex is formed. Both of these points no doubt merit further study, but they should not affect our general interpretation of the origin of selectivity in transport.

# 5. CONCLUSION

Therefore, in summary, an antibiotic such as nonactin acts basically as a lipid-soluble ion carrier. The selectivity in transport arises through a difference in aqueous solution binding constants for various ions which originates in subtle variations in the differences between the free energy of solvation and the free energy of coordination by the antibiotic.

One must remain cognizant of the fact, however, that there are a number of criteria which the antibiotic must fulfill before the description of selective ion transport can be simplified to this extent. First, the ionophore must be flexible so that complex formation can be rapid compared to the diffusion rate for the complex. Second, the antibiotic must envelope the ion, so that the solvation energy of the complex is small and non-discriminatory in its effect on the partition of the complex between solution and membrane phases. And third, the exterior geometry of the complex must be independent of ion so that differences in diffusion rates are inconsequential. On the basis of our pmr data we know that nonactin in most respects meets these criteria, but other antibiotics may not. For example, in cases such as the more rigid, open, cyclic polyethers one must apply caution in making any analogous interpretation of the transport phenomenon.

REFERENCES


1. B. C. Pressman, Fed. Proc., 27, 1283 (1968).
2. H. A. Lardy, D. Johnson, W. C. McMurray, Arch. Biochem. Biophys., 78, 587 (1958).
3. R. Corbaz, L. Ettlinger, E. Gäumann, W. Keller-Schierlein, F. Kradolfer, L. Neipp, V. Prelog, H. Zähner, Hel. Chim. Acta, 38, 1445 (1955).
4. H. Brockmann, H. Geeren, Ann. Chem., 603, 216 (1957).
5. S. N. Graven, H. A. Lardy, D. Johnson, A. Rutter, Biochemistry, 5, 1729 (1966).
6. H. Gerlach, V. Prelog, Ann. Chem., 669, 121 (1963).
7. B. C. Pressman, Proc. Natl. Acad. Sci., U.S., 53, 1076 (1965).
8. P. Mueller, D. O. Rudin, Biochem. Biophys. Res. Commun., 26, 398 (1967).
9. S. N. Graven, S. Estrado-O, H. A. Lardy, Proc. Natl. Acad. Sci., U.S., 56, 654 (1966).
10. C. J. Pedersen, Fed. Proc., 27, 1305 (1968).
11. C. J. Pedersen, J. Am. Chem. Soc., 89, 7017 (1967).
12. B. C. Pressman, E. J. Harris, W. S. Jagger, J. H. Johnson, Proc. Natl. Acad. Sci., U. S., 58, 1949 (1967).
13. S. N. Graven, H. A. Lardy, S. Estrada-O, Biochemistry, 6, 365 (1967).

14. J. B. Chappell, A. R. Crofts, Biochem. J., 95, 393 (1965).

15. E. J. Harris, M. P. Höfer, B. C. Pressman, Biochemistry, 6, 1349 (1967).

16. S. N. Graven, H. A. Lardy, A. Rutter, Biochemistry, 5, 1735 (1966).

17. C. Moore, B. C. Pressman, Biochem. Biophys. Res. Commun., 15, 562 (1964).

18. N. Shavit, R. A. Dilley, A. San Pietro, Biochemistry, 7, 2356 (1968).

19. A. Thore, D. L. Keister, N. Shavit, A. San Pietro, Biochemistry, 7, 3499 (1968).

20. M. Nishimura, B. C. Pressman, Biochemistry, 8, 1361 (1969).

21. A. L. Lehninger, in "The Mitochondrion," W. A. Benjamin, Inc., New York, 1965, pp. 157-178.

22. P. Mitchell, Nature, 191, 144 (1961).

23. S. Estrada-O, E. Calderón, Biochemistry, 9, 2092 (1970).

24. E. J. Harris, G. Caltin, B. C. Pressman, Biochemistry, 6, 1360 (1967).

25. Z. Štefanac, W. Simon, Microchem. J., 12, 125 (1967).

26. H.-K. Wipf, L. A. R. Pioda, Z. Štefanac, W. Simon, Helv. Chim. Acta, 51, 377 (1968).

27. K. H. Wong, G. Konizer, J. Smid, J. Am. Chem. Soc., 92, 666 (1970).

28. M. M. Shemyakin, Y. A. Ovchinnikov, V. T. Ivanov, V. K. Antonov, A. M. Shkrob, I. I. Mikhaleva, A. V. Evstratov, G. G. Malenkov, Biochem. Biophys. Res. Commun., 29, 834 (1967).

29. V. T. Ivanov, I. A. Laine, N. D. Abdulaev, L. B. Senyavina, E. M. Popov, Y. A. Ovchinnikov, M. M. Shemyakin, Biochem. Biophys. Res. Commun., 34, 803 (1969).

30. B. T. Kilbourn, J. D. Dunitz, L. A. R. Pioda, W. Simon, J. Mol. Biol., 30, 559 (1967).

31. M. Pinkerton, L. K. Steinrauf, P. Dawkins, Biochem. Biophys. Res. Commun., 35, 512 (1969).

32. D. C. Tosteson, Fed. Proc., 27, 1269 (1968).

33. H.-K. Wipf, W. Pache, P. Jordan, H. Zähner, W. Keller-Schierlein, W. Simon, Biochem. Biophys. Res. Commun., 36, 387 (1969).

34. G. Eisenman, S. M. Ciani, G. Szabo, Fed. Proc., 27, 1289 (1968).

35. Y. A. Ovchinnikov, Biochem. Biophys. Res. Commun., 39, 217 (1970).

36. M. Pinkerton, L. K. Steinrauf, J. Mol. Biol., 49, 533 (1970).

37. M. Ohnishi, D. W. Urry, Science, 168, 1091 (1970).

38. R. F. Zürcher, in "Progress in N.M.R. Spectroscopy," Vol. 2, J. W. Emsley, J. Feeney, L. H. Sutcliffe, eds., Pergamon Press, Oxford, 1967, p. 212.

39. M. Karplus, J. Chem. Phys., 30, 11 (1959).

40. J. A. Pople, W. G. Schneider, H. J. Bernstein, in "High-Resolution Nuclear Magnetic Resonance," McGraw-Hill, New York, 1959, pp. 218-222.

41. J. H. Prestegard, S. I. Chan, Biochemistry, 8, 3921 (1969).

42. J. H. Prestegard, S. I. Chan, J. Am. Chem. Soc., 92, 0000 (1970).

43. A. Stern, W. A. Gibbons, L. C. Craig, Proc. Natl. Acad. Sci., U.S., 61, 734 (1968).

44. M. Ohnishi, D. W. Urry, Biochem. Biophys. Res. Commun., 36, 194 (1969).

45. D. H. Haynes, A. Kowalsky, B. C. Pressman, J. Biol. Chem., 244, 502 (1969).

46. K. D. Kopple, M. Ohnishi, A. Go, J. Am. Chem. Soc., 91, 4264 (1969).

47. K. D. Kopple, M. Ohnishi, A. Go, Biochemistry, 8, 4087 (1969).

48. A. Weissberger, in "Technique of Organic Chemistry," 2nd ed., Vol. 7, Interscience, New York, 1955, p. 382.

49. J. A. Pople, W. G. Schneider, H. J. Bernstein, in "High-Resolution Nuclear Magnetic Resonance," McGraw-Hill, New York, 1959, p.272.

50. This notation is explained in J. W. Emsley, J. Feeney, L. H. Sutcliffe, "High-Resolution Nuclear Magnetic Resonance Spectroscopy," Vol. I, Pergamon Press,

Oxford, 1965, p. 283.

51. Ibid., p. 359.

52. This program was written by A. A. Bothner-By, S. M. Castellano, Mellon Institute, Pittsburgh, Pa.

53. A. D. Buckingham, Can. J. Chem., 38, 300 (1960).

54. V. F. Bystrov, S. L. Portnova, V. I. Tsetlin, V. T. Ivanov, Y. A. Ovchinnikov, Tetrahedron, 25, 493 (1969).

55. R. F. Zürcher, in "Progress in N.M.R. Spectroscopy," Vol. 2, J. W. Emsley, J. Feeney, L. H. Sutcliffe, eds., Pergamon Press, Oxford, 1967, p. 215.

56. Ibid., p. 234.

57. J. A. Pople, W. G. Schneider, H. J. Bernstein, in "High Resolution Nuclear Magnetic Resonance," McGraw-Hill, New York, 1959, p. 218.

58. C. W. Davies, in "Ion Association," Butterworths, Washington, 1962, p. 98.

59. R. T. Iwamasa, Ph.D. Thesis, California Institute of Technology, 1969, p. 37.

60. K. B. Harvey, G. B. Porter, in "Introduction to Physical Inorganic Chemistry," Addison-Wesley, Reading, Mass., 1963, p. 332.

61. J. D. Bernal, R. H. Fowler, J. Chem. Phys., 1, 515 (1933).

62. D. D. Eley, M. G. Evans, Trans. Faraday Soc., 34, 1093 (1938).

63. R. M. Noyes, J. Am. Chem. Soc., 84, 513 (1962).

64. J. A. Pople, W. G. Schneider, H. J. Bernstein, in "High-Resolution Nuclear Magnetic Resonance," McGraw-Hill, New York, 1959, p. 221.

65. H. Diebler, M. Eigen, G. Ilgenfritz, G. Maass, R. Winkler, Pure Appl. Chem., 20, 93 (1969).

# PART II

# SALT EFFECTS ON NUCLEOTIDE CONFORMATION

# 1. INTRODUCTION

## 1.1. General Aspects of Nucleotide Conformation

During the past few years a great deal of research has been devoted to the investigation of the forces which determine the preferred conformations of DNA, RNA and their shorter oligonucleotide derivatives. Base-stacking interactions have been foremost among the forces investigated and they appear to be influential in maintaining the parallel and stacked configurations of the planar purine and pyrimidine bases found in these molecules.[1-8] Relative base orientation, however, is not the sole significant feature of nucleotide conformation. Other degrees of freedom exist within each nucleotide unit, both with respect to changes in orientation of the base about its glycosidic bond ($C_1'$-$N_1$) and with respect to conformational alterations in each contiguous ribose moiety.

The importance of these additional degrees of conformational freedom in nucleotides is suggested by the frequent observation of structurally and functionally distinct base-stacked conformers of chemically identical dinucleotides or polynucleotides. In the dinucleotide ApA, for example, the anti-anti base-stacked conformation, where the adenosine bases are rotated so that the six-membered portion of their purine rings is away from the ribose moiety, is predominant over the syn-syn and syn-anti

base-stacked conformations.[6] But appreciable populations of the minor rotomers are nevertheless known to exist,[9] and in some nucleotides, the guanosine nucleotides for example, they may even represent a major fraction.[10] It has been proposed that the differences exist not as the result of base-stacking, but as the result of variations in non-bonding interactions between base and ribose moieties,[6] making base orientation, along with base-stacking tendency, a determining characteristic of nucleoside or nucleotide conformation.

Along with possible variations in base orientation and base-stacking tendencies, concomitant variations in ribose conformation have been noted. In ApA, ApC, and CpA, for example, ribose conformation seems to change on destacking the bases,[7,11] and in polynucleotides variations in ribose conformation exist even among thermally stable conformations. The DNA double helix, for example, can exist in at least two forms: the A form where base planes are tilted with respect to the helix axis, and the more common B form where bases are perpendicular to the axis.[12] RNA can also exist in several different double helical forms, most of which are similar to the less common DNA A form.[12] These various forms, to the extent to which they have been characterized, would seem to differ very little in their base-stacking interactions; the number of bases per pitch is nearly the same (± 1) and base pairs seem effectively

overlapped in all cases. Differences in the conformation of the ribose-phosphate backbone in these helices are then of major significance. In fact, a change from 3'-endo to 2'-endo ribose conformation has been cited as a characteristic difference between A and B forms of the DNA double helix.(13)

The possible biological significance of such variations in nucleotide structure is intriguing. It has been suggested that the two forms of DNA can differentiate transcription and replication cycles in living systems.(13) At various stages of cell development DNA must either replicate itself or transcribe its code through the template synthesis of either a complementary DNA or a complementary messenger RNA chain. It is perhaps significant that only one form of DNA, the A form, seems compatible with the RNA helical structure. Also, flexibility within the nucleotide unit, either with respect to the glycosidic bond or with respect to the ribose moiety, is one of the major tenets of the "wobble hypothesis" which attempts to explain the degeneracy of the genetic code.(14) For example, the codons GCC and GCU are degenerate, both pairing with the anticodon for alanine, CGI. Crick postulates that a flexibility or "wobble" in the C base of the codon is a major factor in allowing the abnormal I-C pair to form. Thus ribose and glycosidic bond conformations, although often reported as insignificant aspects of nucleotide conformation, may in

themselves have important biological implications. Despite this potential significance, conformational differences among nucleotide units have not been well characterized and a more detailed study, even of mononucleotide segments, poses a subject worthy of further investigation.

## 1.2. General Forces Influencing Nucleotide Conformation

The forces which influence ribose or glycosidic bond conformation are likewise of much interest and merit further study. A few theories attempting to explain factors which determine or alter nucleotide conformation have been advanced, but in general they leave many experimental observations unexplained. One explanation for the preferred anti conformation of many nucleosides and nucleotides recently expounded by several authors on the basis of crystal structure data relies on the effect of steric interactions between base and ribose atoms about the glycosidic bond.[15-17] These interactions are no doubt important and they do point to the fact that rotation about the glycosidic bond and changes in ribose conformation may be closely correlated. Such interactions, however, cannot explain the apparent sensitivity of glycosidic and ribose conformation to changes in the nucleotide's external environment. For example, dehydration or the addition of a high concentration of salt to a DNA solution can cause a transition from the B to the A form, and the addition of salt or a viral protein

coat to RNA can produce similar changes in the secondary structure of this molecule,[12] some of which presumably involves a change in ribose-phosphate conformation. Even in the case of simpler mono and dinucleotides, the addition of a non-polar solvent has induced changes in the CD spectra, which have been interpreted as variations in the angle about the glycosidic bond.[18]

A second factor, deemed by some to be crucial in the maintenance of secondary structure of ribonucleotides, is the proposed hydrogen bond between the 2'-hydroxyl of the ribose ring and either a proton acceptor on the nucleoside base,[8,19] or an adjacent phosphate group on the backbone chain.[1,20] In the case of the polynucleotides this could be the principal source of difference between the RNA helix and the DNA helix, which lacks such a 2'-OH group. And in lower nucleotides, its effect on conformation would be more sensitive to external environment than mere steric interactions. However, despite the intuitively appealing nature of this suggestion, there is an increasing store of evidence which indicates that this too cannot be the only significant factor in determining nucleotide ribose-phosphate conformation. For example, mononucleotides, with and without a 2'-OH group, have been observed to display similar glycosidic bond conformations.[21,22] Many crystal structures indicate that nucleotides exist in conformations in which such hydrogen bonds are not geometrically possible,

and studies of polymer derivatives lacking a 2'-OH group show these compounds to behave in a manner more analogous to a ribose compound, than a deoxy compound.[23-25] All of the above studies indicate that the contribution of the 2'-OH hydrogen bond to ribonucleotide conformational stability is a relatively minor one.

A third proposal directed at an explanation of the effect of ionic strength on the structure and stability of double helices has been based on electrostatic arguments. In the case of at least divalent cations, binding to the negatively charged phosphates should reduce the chain-chain repulsions normally present in a double helix, thus increasing the stability of the double stranded structure.[26] An analogous argument might be set forth to explain transitions between various helical forms. But this explanation cannot be extended to the dramatic effect of some non-binding anions or the destabilizing effects of salt concentrations in excess of 1 M which do not follow predictions based on ionic strength effects.[27,28] Also, non-ionic perturbants have produced changes in non-helical, non-base-stacked nucleotide fragments, which certainly cannot be explained on a purely electrostatic basis.[18]

Therefore, there are a great many unanswered questions about the precise conformational changes which can occur in a nucleotide unit and about the forces which drive these changes that merit further study. To a large extent

changes in nucleotide conformation, although often observed, have not been characterized in terms of detailed changes in angle about the glycosidic bond and/or changes in population of various ribose conformations. And to a large extent the factors which influence conformational changes of this type have not been investigated in a systematic way in a system free of other secondary structure-perturbing factors, such as base-stacking interactions. It is these investigations that we plan to pursue and it is these conformational changes which we wish to characterize.

## 1.3. A Proposal for Further Study

### 1.3.1. Uracil Nucleosides and Nucleotides as a Subject of Study

To resolve these questions we have undertaken a detailed study of the aqueous solution conformation of single nucleosides and nucleotides under various systematic perturbations of the solvent system. In a single nucleotide unit we need not consider interference from changes in intramolecular base-stacking interactions, but, since intermolecular base-stacking can still occur, it is clear that it would be desirable to examine a simple case in which there is little base-stacking or where base-stacking does not alter the conformation of the nucleotide or nucleoside unit. Of course, in the latter case, the property monitoring the

conformation must also be insensitive to what base-stacking may exist. Uridine, deoxyuridine, uridine-5'-monophosphate (5'-UMP), and uridine-3'-monophosphate (3'-UMP) satisfy these requirements. These molecules self-associate only slightly at low concentrations (less than 0.02 M) and, as far as we can tell, any self-association which does exist, does not alter the molecular conformation or affect any of the properties which we shall use in this work to monitor the conformation of the molecule. Thus the effect of added perturbant can be interpreted directly in terms of its effect on ribose and glycosidic bond conformation for these molecules.

In order to put the evaluation of these conformational changes on a more quantitative basis we shall adopt a terminology developed in connection with X-ray and theoretical studies of nucleotide structure.[16,29] Here, conformational changes about the glycosidic bond, as well as rotatable single bonds in the ribose moiety, have been described in terms of the various torsional angles indicated for 5'-UMP in Figure 1. Donohue and Trueblood defined the torsional angle about the glycosidic bond, ($\phi_{CN}$), as being the dihedral angle between the plane of the base and the plane formed by the $C_{1'}$-$O_{1'}$ bond of the furanose ring and the $C_{1'}$-$N_1$ glycosidic bond.[29] The torsion angle, $\phi_{CN}$, is 0° when $C_6$ of the pyrimidine base is eclipsed with the ether oxygen ($O_{1'}$) of the furanose ring, and positive angles are

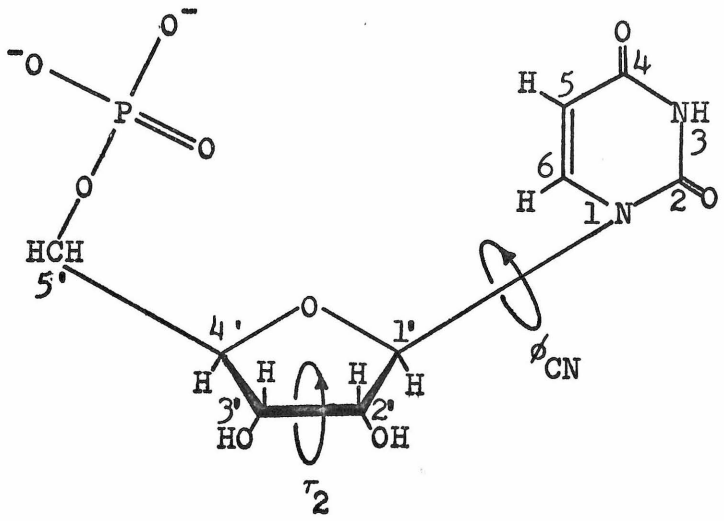


FIGURE 1. 5'-UMP.

measured when the base is rotated in the clockwise direction when viewing from $N_1$, to $C_1$,. The anti conformation expected for the pyrimidine nucleosides and nucleotides describes a range of torsion angles centered at $\phi_{CN} \sim -30^{\circ}$, and X-ray crystallographic studies have shown that this range can extend from $-5^{\circ}$ to $-65^{\circ}$.[15] In solution base orientation about the glycosidic bond is not fixed and is likely to be represented by a distribution among rotomers with torsional angles largely within this range. We shall use the torsional angle, $\phi_{CN}$, to gauge changes in the average of this angular distribution.

The conformation of the ribose ring can be described in terms of the angles, $\tau_0$, $\tau_1$, $\tau_2$, $\tau_3$, and $\tau_4$, which correspond to dihedral angles about the $O_1$,-$C_1$,, $C_2$,-$C_3$,, $C_3$,-$C_4$,, and $C_4$,-$O_0$, bonds, respectively.[16] Positive angles are measured as clockwise rotations about the bonds, as viewed from the low number carbon atom, and zero values are obtained when all bonds of the ring are planar and cis with respect to one another. The ribose conformation corresponding to all torsional angles equal to zero is inherently unstable and normally one carbon atom is displaced from the plane. Structures with an atom (n') displaced toward the side of the base and phosphate group are described as n'-endo, or alternatively, those with n' to the opposite side of the plane are described as n'-exo. Usually either $C_2$, or $C_3$, is displaced, leaving four

possible ribose conformers: $C_2$,-endo, $C_2$,-exo, $C_3$,-endo, and $C_3$,-exo. But in the present study, due to the limited data accessible with our experimental technique, we have considered the ribose conformation to be represented by a equilibrium between the two most common forms shown in Figure 2: the 2'-endo and 3'-endo conformers.[11] More recently studies have appeared which consider the existence of all four conformers. These results, however, are not inconsistent with the 2'-endo, 3'-endo interpretation adopted here.[30,31]

1.3.2. Pmr as a Method of Study

As a method for monitoring changes in the conformational equilibria for uridine, deoxyuridine, 5'-UMP, and 3'-UMP, resulting from perturbations to the solvent system, we propose to employ a proton magnetic resonance (pmr) technique. The application of pmr to problems of biological interest has been well illustrated in work on other nucleotides[6-9] and in the work on nonactin described in Part I of this thesis. Pmr should therefore be of equal value here. As in the case of nonactin, the chemical shift, being a function of local magnetic environment, is sensitive to conformational changes which alter the spacial relationships of protons and various functional groups. Thus an analysis of induced chemical shifts as a function of solvent perturbation will aid in our interpretation of conformation

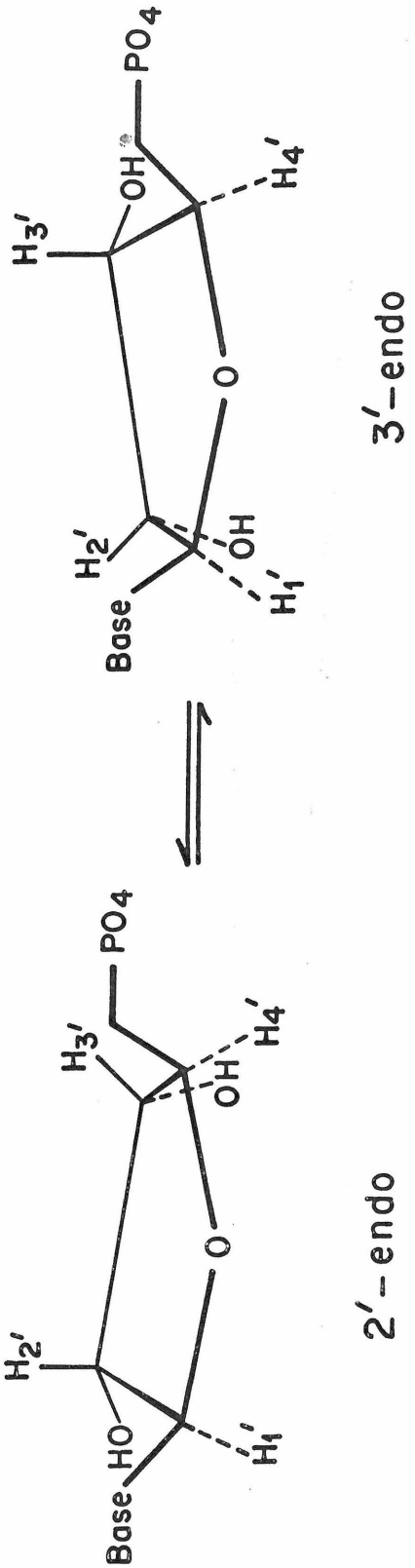


FIGURE 2. 2'-endo and 3'-endo ribose conformation.

changes, especially those involving changes in orientation of the base about the glycosidic bond. And, as in the case of nonactin, vicinal spin-spin coupling constants will be used to monitor rotations about carbon-carbon single bonds. In this work, the coupling constant between the $H_1$, and $H_2$, ribose protons is particularly suitable for monitoring $\tau_1$ and, indirectly, the equilibrium between conformers of the ribose ring.[32,33] But, in addition to the two pmr parameters monitored in the nonactin work (chemical shift and coupling constant), we have here been able to reinforce our conformational deductions with the results of nuclear-nuclear Overhauser experiments. The nuclear Overhauser effect (NOE) stems from the fact that in the case of highly proximate nuclei, the transitions between spin states of one nucleus are coupled to the transitions of the other by direct spin-coupling. Thus in a double irradiation experiment, when the distribution between spin states of one nucleus is altered, the intensity of the resonance arising from the coupled spin is simultaneously changed. The extent of this intensity change can in certain cases be related to the degree of direct coupling and so to the geometrical relationship of the two protons. The technique has been applied successfully in conformational comparison of nucleotides of fixed geometry and so promises to be of use here.[9,34] Unfortunately, the technique requires rather high sensitivity and as a result could only be

attempted at rather high nucleotide concentration. Even at this, the results are at the limit of statistical validity. Therefore, we must rely on a combined study of the chemical shift, spin-spin coupling constant, and nuclear-nuclear Overhauser effects as a function of a systematic perturbation to the solvent system to yield information about the conformation of these nucleosides and nucleotides and to lead to the elucidation of the nature of the forces which can alter the equilibrium distribution between the various stable conformers.

### 1.3.3. Electrolytes as Solvent Perturbants

The choice of appropriate perturbants for our solvent system must be made on the basis of their potential to elucidate the nature of the forces which influence nucleotide conformation, as well as on the basis of their having some biological significance. Since steric, electrostatic, and hydrogen-bonding forces have met with only limited success in the explanation of changes in nucleotide conformation, it seems most profitable to select a perturbant which will also probe the possible role of hydrophobic bonding. Numerous agents exist which are capable of acting as hydrophobic denaturants. Among the more common ones are alcohols of various chain length, tetra-alkyl ammonium ions, guanidinium chloride, and urea.[35-39] But we have chosen to employ here a group of ionic salts which are more

commonly used to adjust ionic strength, than to denature macromolecules. These are $Mg(ClO_4)_2$, $NaClO_4$, NaCl, NaOAc, $(CH_3)_4NCl$, and $\left[CH_3(CH_2)_3\right]_4NCl$. The salts, however, have been used in some cases to perturb a solvent system; specifically, they have been employed in investigations of conformational stability of macromolecules such as ribonuclease and DNA.[27,35] Their influence on the stability of these macromolecules has been well characterized and their action has been attributed to a "structure-breaking" and "structure-making" effect on the solvent.[40]

Although the non-ionic perturbants offer an advantage in not having their effects on hydrophobic forces complicated by alternative mechanisms for inducing conformation changes, such as those of electrostatic nature described previously, the ionic perturbants are particularly suitable in a study such as that proposed here for a number of reasons. The salts themselves are widely used in biologically oriented studies for the regulation of ionic strength and pH, with little regard for their structure perturbing properties. Therefore, in addition to their implication as to the forces which determine nucleoside conformation, an illustration of their possible conformation perturbing properties should be of value. There are, in fact, a number of discrepancies in the literature regarding the conformation of nucleotides which may have arisen from just such a disregard of the possible conformational effect of

salts used to maintain ionic strength.[1,2,41] This study should aid in resolving some of this conflict. In addition to the potential significance of the results obtained with these salts, they offer a purely experimental advantage in that most of them add no spurious resonances to our pmr spectra. The addition of these salts to our nucleoside and nucleotide solutions should therefore provide both a convenient and significant way of systematically perturbing the aqueous solvent system in an investigation of the possible role of hydrophobic forces in maintaining nucleotide conformation.

# 2. EXPERIMENTAL

## 2.1. Conventional Pmr Experiments

Uridine and uridine-5'-monophosphate (disodium salt) were obtained from Calbiochem, Los Angeles, Calif., as the A grade materials. Uracil and uridine-3'-monophosphate (dilithium salt) were purchased from P. L. Biochemicals, Inc., Milwaukee, Wis. Deoxyuridine was obtained from Sigma Chemical Co., St. Louis, Mo. These compounds were dried over $P_2O_5$ under vacuum at room temperature and were used without further purification. Solutions were prepared in 99.7% $D_2O$ supplied by Columbia Organic Chemicals, Columbia, S. C.

The salts, $NaClO_4$, $Mg(ClO_4)_2$, and NaOAc, were of reagent grade. Before use, they were dried under high vacuum at temperatures in excess of 100°C. Tetraethylammonium chloride (TMACl) was obtained from Matheson Coleman and Bell. It was dried under high vacuum at 35°C. Tetrabutylammonium chloride (TBACl) was prepared from the iodide salt (Eastman Organic Chemicals) by ion exchange. The salt was recrystallized from a $CCl_4$-hexane mixture and dried under high vacuum at 55°C. Reagent grade NaCl was used without further treatment.

For the investigation of chemical shifts and coupling constants, the nucleotide or nucleoside

concentration was 0.01 M in $D_2O$. The pD of each solution was measured with a Leeds and Northrup 7401 pH meter, equipped with miniature electrodes, and was taken to be the observed pH meter reading plus 0.4 (the standard correction).[42] The pD of all the nucleotide solutions was maintained at a constant value of 8.3 ± 0.3. Where adjustments were necessary, small amounts of 1 M DCl or 1 M NaOD were added. The salt concentrations quoted in this paper do not include the small amounts of sodium ion or lithium ion existing as the counter ion to the uridylic acids and the minute quantities of sodium or chloride ion introduced in the pD adjustments.

Measurement of salt-induced chemical shifts and coupling constant changes of the 0.01 M solutions proceeded in a routine manner. All spectra were run on a Varian HA-100 high-resolution NMR spectrometer, operated in the frequency sweep mode. A C-1024 time-average computer was used to enhance the signal-to-noise ratio where necessary. A TMS capillary provided the field/frequency lock signal and also served as an external standard. Chemical shifts were measured relative to the lock signal to ± 0.001 ppm by electronic counting of the difference between the lock and sweep modulation frequencies. However, in order to correct for changes in the bulk susceptibility of the solutions, all the electrolyte shifts reported are referred to an internal standard of either tetramethylammonium chloride or neopentyl

alcohol.

## 2.2. Nuclear Overhauser Experiments

For the nuclear Overhauser experiments only 5'-UMP in the presence and absence of 2 M $NaClO_4$ was studied in detail. The chemicals employed were those described above; however, because of the necessity of detecting rather small changes in the intensity of the resonances, the samples were prepared in a slightly different manner. First, the solutions employed were brought to a rather high nucleotide concentration, 0.10 and 0.30 molar in the two sets of experiments conducted. Second, the 5'-UMP was exchanged once and lyophilized from $D_2O$ to eliminate the contribution of exchangable protons to the intensity of the HOD resonance which frequently interferes with the detection and irradiation of the proper resonance in the ribose region of the spectrum. And third, after preparation of the sample and adjustment of the pH, dissolved paramagnetic oxygen was removed to minimize variations in the natural relaxation mechanisms among samples and to maximize the nuclear Overhauser effects. This removal was accomplished by three consecutive freeze-pump-thaw cycles, after which the samples were sealed under vacuum.

The NOE measurements were made on these samples employing the same basic instrumentation as that used above. The HA-100 spectrometer was used along with a Hewlett-

Packard model 120 B audio oscillator to supply the saturating modulation frequency. A modulation of 300 ± 100 mv amplitude was applied at the spectral position of an appropriate ribose proton ($H_2$, or $H_5$,) while the intensity of a uracil base proton resonance ($H_6$) was observed. Intensities were measured employing the integration circuit of the HA-100, and the percentage nuclear Overhauser enhancements were calculated by comparison of these intensities to the average intensity found with the saturating frequency moved 100 Hz to either side of the ribose resonance in question. The experiments were conducted with varying amplitudes of the saturating frequency (0-600 mv). A near maximum nuclear Overhauser effect was obtained at any amplitude over 200 mv, but 300 mv was most frequently employed because of the improved signal-to-noise ratio at the lower irradiating amplitudes. Even under these optimum conditions the reproducibility of integrals was none too good. But rather than attempt the use of a time-average device with this inherently unstable system, the experiments were repeated in the sequence described a sufficient number of times to make the results somewhat statistically valid. It is the average of these results which we report in the following section.

# 3. RESULTS

## 3.1. Initial Spectral Parameters

The proton magnetic resonance spectrum of a typical uracil nucleotide or nucleoside is presented in Figure 3. The uracil $H_6$, $H_5$, and ribose $H_1$, protons give rise to distinct resonances which are easily monitored, even at 0.01 m concentration. The assignment of these resonances is based on the work of Jardetzky et al.[43] The $H_6$ and $H_5$ resonances of the uracil base appear as doublets due to spin-spin coupling between these protons. In the ribose nucleoside and nucleotides, the $H_1$, resonance often overlaps the $H_5$ resonance and is also a doublet due to spin-spin coupling with the $H_2$, proton of the ribose ring. In the case of deoxyuridine, however, the $H_1$, resonance is a triplet due to coupling to both the ribose $H_2$, and $H_2$,, protons. Since the chemical shift difference between $H_2$, and $H_2$,, protons is small compared to the $H_2$,-$H_2$,, geminal coupling constant, only the average $H_1$,-$H_2$,($H_2$,,) coupling constant, $\frac{1}{2}\left|J_{H_1,-H_2,} + J_{H_1,-H_2,,}\right|$, can be measured.[44] The chemical shifts of these resonances and the various coupling constants in the molecules investigated are summarized in Table I.

The resonances of the other ribose protons, although easily discernible in the spectrum of Figure 3, are not so easily perceived at 0.01 m, both because of decreased

FIGURE 3

100 MHz pmr spectrum for a 0.11 m solution of 5'-UMP in $D_2O$ at pD 8.3, 30°.

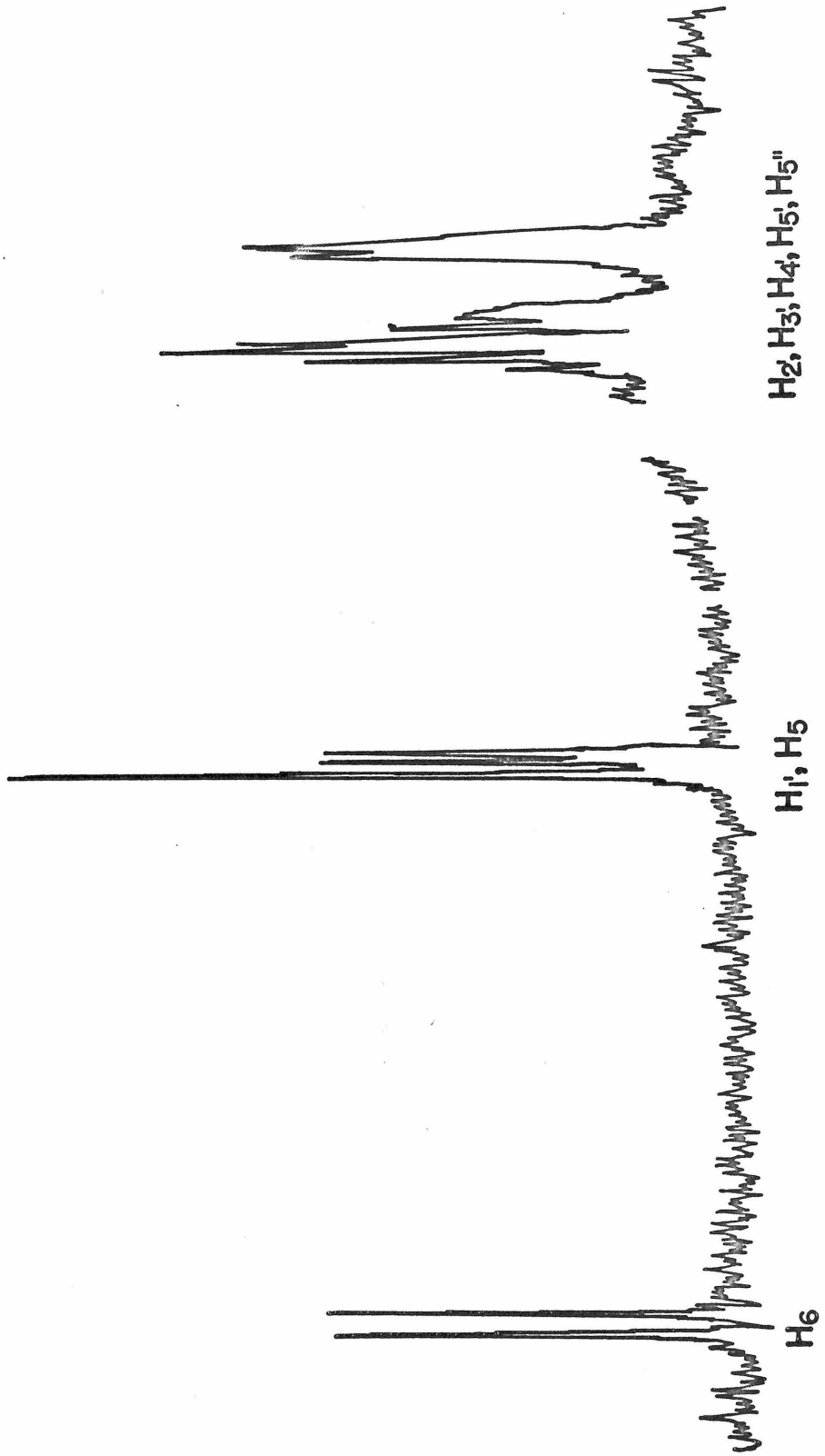
H2; H3; H4; H5'; H5"
H1'; H5
H6

TABLE I: A Summary of the Chemical Shifts and Coupling Constants Observed for Uracil and Related Nucleosides and Nucleotides.[a]

| | pD | $H_6$ ppm | $H_5$ ppm | $\lvert J_{H_6-H_5} \rvert$ cps | $H_{1'}$ ppm | $\lvert J_{H_{1'}-H_{2'}} \rvert$ cps |
|---|---|---|---|---|---|---|
| 0.02 m uracil | 7.2 | -7.955 | -6.227 | 7.7 | | |
| 0.01 m uridine | 8.3 | -8.294 | -6.338 | 8.1 | -6.353 | 4.5 |
| 0.01 m deoxyuridine | 7.5 | -8.279 | -6.337 | 8.2 | -6.730 | 6.7[b] |
| 0.01 m 5'-UMP | 8.4 | -8.554 | -6.442 | 8.1 | -6.437 | 4.8 |
| 0.01 m 3'-UMP | 8.1 | -8.332 | -6.351 | 8.1 | -6.383 | 4.3 |

[a] Shifts are measured relative to a TMS capillary.

[b] $\frac{1}{2} \left| J_{H_{1'}-H_{2'}} + J_{H_{1'}-H_{2''}} \right|$.

sensitivity and the interference of the strong HDO resonance. Thus, for the chemical shift and coupling constant studies, no attempt was made to monitor these signals. However, for the higher concentrations used in the nuclear Overhauser experiments, the $H_2$, and $H_5$, could be assigned on the basis of their multiplet patterns and spin-spin coupling to the $H_1$, proton.

Since the initiation of this work more detailed studies of the ribose protons have appeared which assign and analyze the entire ribose region of the spectrum. These works are, in general, consistent with that presented here.[30,31,33]

The hydroxyl and N-H proton resonances were not observed because of exchange with the solvent.

## 3.2. Salt-Induced Chemical Shifts

Although chemical shift data for $H_6$, $H_5$, and $H_1$, protons have been collected, the principal changes on the addition of electrolytes are observed in the position of the $H_6$ resonance. These changes for the various nucleosides and nucleotides in the presence of the several electrolytes studied will be considered first.

Uridine. The chemical shifts observed for the uracil $H_6$ resonance of uridine upon the addition of various salts to a 0.01 m uridine solution in $D_2O$ at pD = 8.3 are depicted in Figure 4. $Mg(ClO_4)_2$ produces the greatest effect,

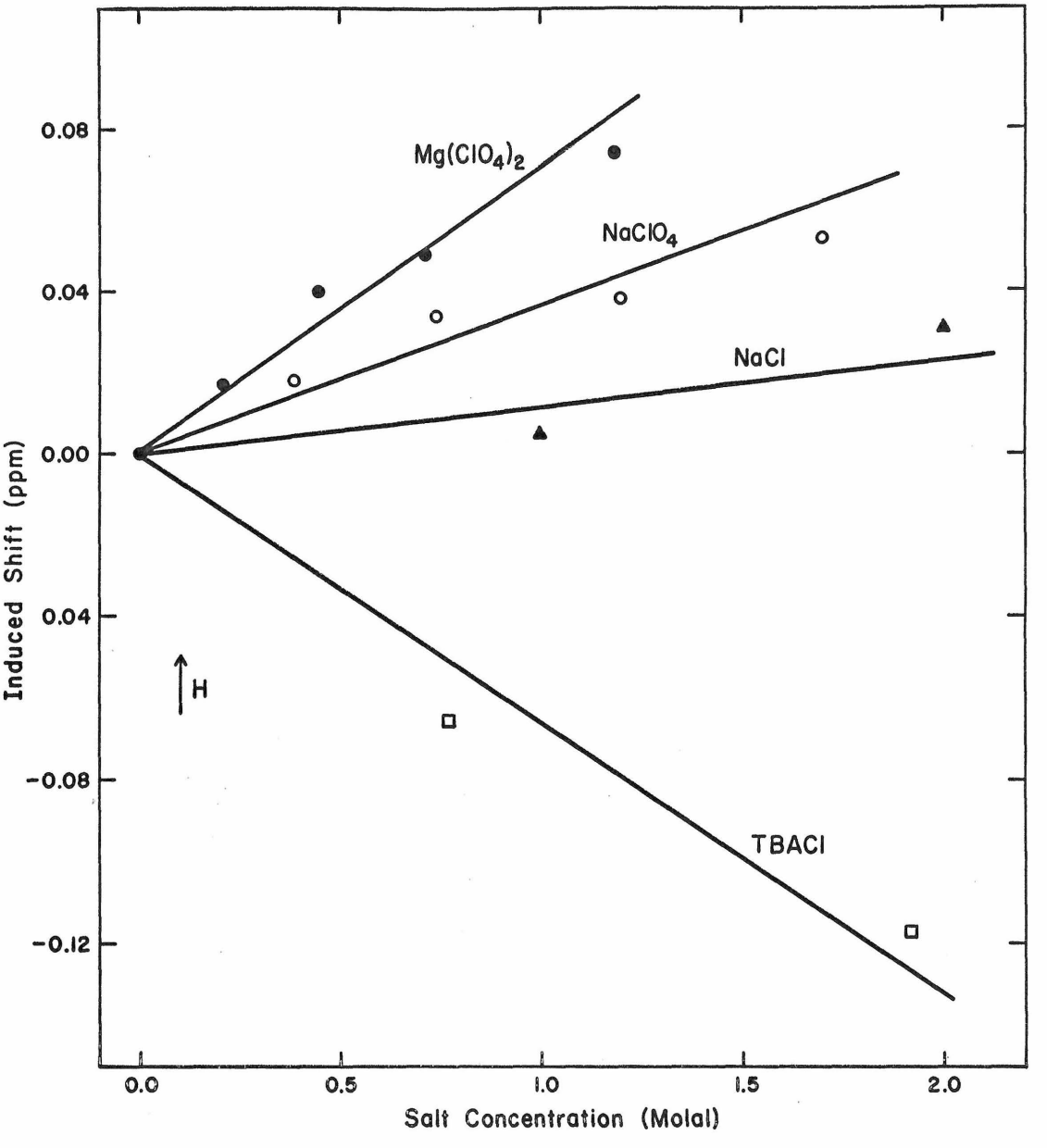


FIGURE 4

Salt-induced shifts of the $H_6$ resonance for a 0.01 m solution of uridine in $D_2O$ at pD 8.3, 30°.

shifting the $H_6$ resonance 0.07 ppm upfield over a salt concentration range of 1 m. Similarly, 2 m $NaClO_4$ and 2 m NaCl shift the $H_6$ resonance upfield by 0.07 ppm, and 0.018 ppm, respectively. However, 2 m TBACl causes a downfield shift of 0.13 ppm.

The $H_5$ and $H_1$, resonances are also shifted by the addition of these electrolytes. However, the shifts are all less than 0.03 ppm over the entire range of salt concentrations investigated.

5'-UMP. The chemical shifts of the $H_6$, $H_5$, and $H_1$, resonances of a 0.01 m solution of 5'-UMP at pD 8.4 as a function of the concentration of the various salts under study are summarized in Figures 5 and 6. These salts can be seen to produce a pronounced shift of the resonance position of the $H_6$ proton. $Mg(ClO_4)_2$ has the greatest effect, inducing an upfield shift of 0.19 ppm over a salt concentration range of 0.6 m. At salt concentrations of 2 m, the observed electrolyte shifts for NaCl, $NaClO_4$, and NaOAc are 0.124, 0.125, and 0.054 ppm upfield, respectively. Tetramethylammonium chloride has little effect on the $H_6$ chemical shift over the entire concentration range studied, while the shifts observed in tetrabutylammonium chloride are slightly downfield (-0.012 ppm at 2 m).

In contrast to the nearly linear induced shifts observed with increasing salt concentration for the $H_6$ resonance of uridine, the corresponding shifts for 5'-UMP at

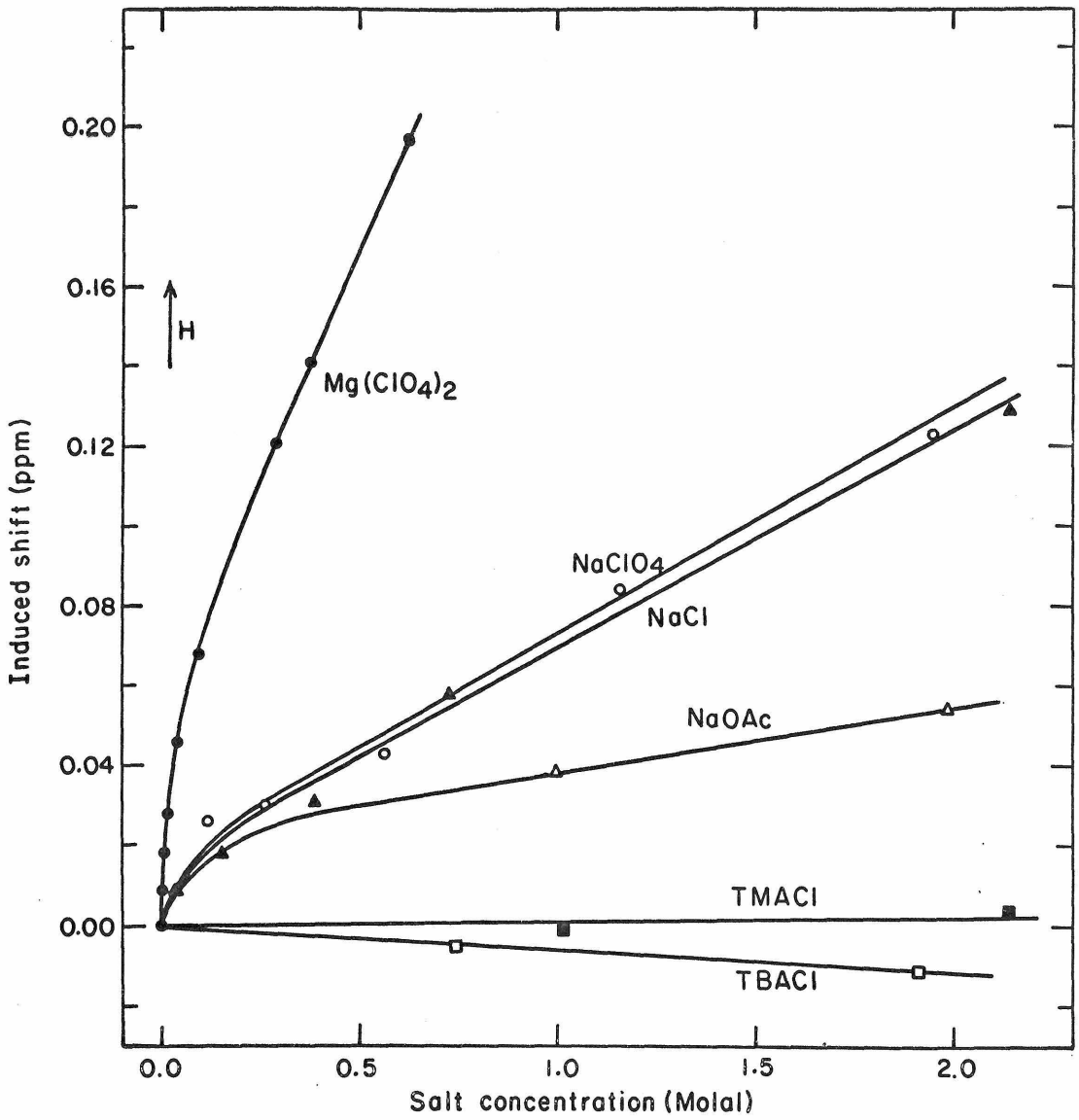


FIGURE 5

Salt-induced shifts of the $H_6$ resonance for a 0.01 m solution of 5'-UMP in $D_2O$ at pD 8.4, 30°.

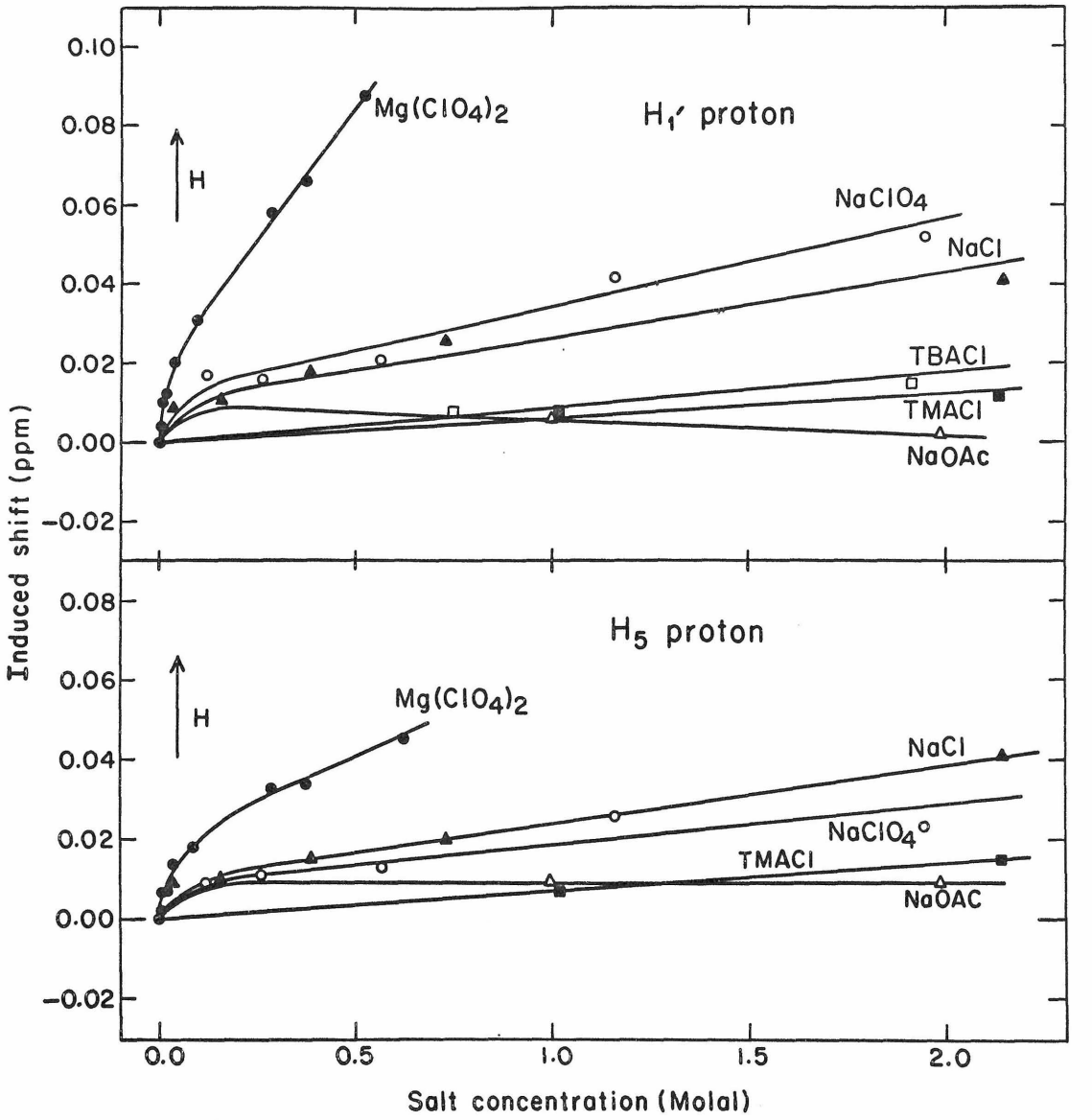


FIGURE 6

Salt-induced shifts of the $H_1$, and $H_5$ resonances for a 0.01 m solution of 5'-UMP in $D_2O$ at pD 8.4, 30°.

low salt concentrations can be seen to be abrupt. This abrupt change is most pronounced in the case of magnesium perchlorate and is also evident for the sodium salts, although to a lesser extent. At high salt concentrations, however, the $H_6$ resonance appears to vary linearly with salt concentration. As we shall show, the abrupt shifts arise from binding of the cation to the negatively charged phosphate group.

The effects of these salts on the $H_5$ and $H_1$, resonances of 5'-UMP are again small compared to effects noted for the $H_6$ resonance. However, these salt-induced $H_5$ and $H_1$, shifts are somewhat larger than those observed for uridine.

3'-UMP. In the presence of salts, similar electrolyte shifts are observed for the $H_6$(Figure 7), $H_5$, and $H_1$, resonances of 3'-UMP as in uridine. The $H_6$ resonance, however, does not exhibit the abrupt shifts depicted by 5'-UMP at low salt concentration. The magnitudes of the salt-induced shifts observed for 3'-UMP are also smaller. At 0.6 m $Mg(ClO_4)_2$, the $H_6$ resonance is shifted 0.065 ppm upfield from its value in the absence of salt, and the corresponding shifts induced by 2 m $NaClO_4$ and NaCl are 0.09 ppm and 0.05 ppm, respectively. Again these salts do not affect $H_1$, and $H_5$ chemical shifts significantly, the induced shifts being less than 0.03 ppm.

Deoxyuridine. Deoxyuridine was investigated in

FIGURE 7

Salt-induced shifts of the $H_6$ resonance for a 0.01 m solution of 3'-UMP in $D_2O$ at pD 8.1, 30°.

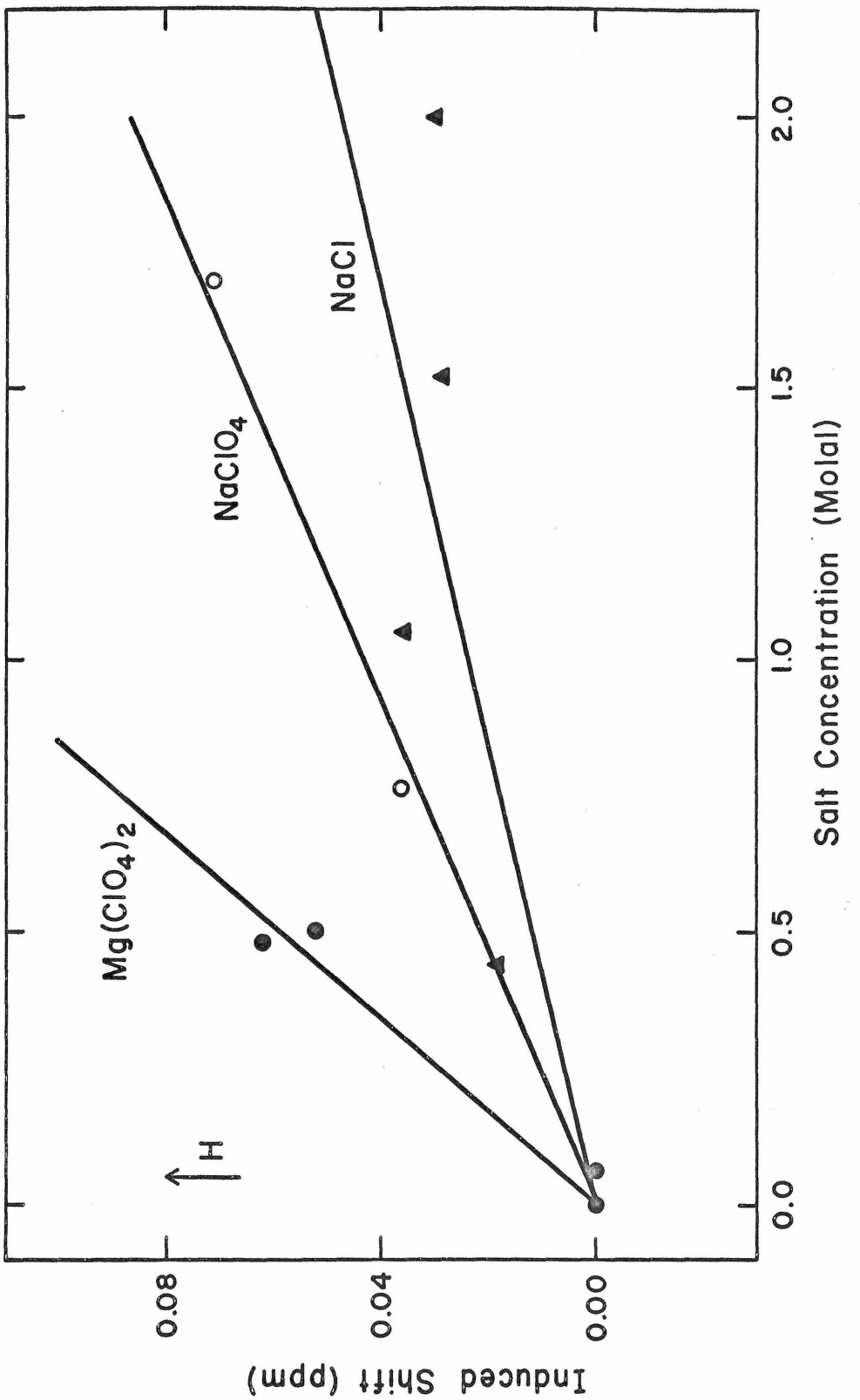
Induced Shift (ppm)
0.08
0.04
0.00
0.0
0.5
1.0
1.5
2.0
Salt Concentration (Molal)
$Mg(ClO_4)_2$
$NaClO_4$
NaCl
H

order to ascertain the possible influence of the 2'-hydroxyl group on the electrolyte shifts observed for uridine, 3'-UMP and 5'-UMP. It was found that the addition of salts again shifts the $H_6$ resonance upfield from the aqueous solution value. The shifts, however, are somewhat smaller than those observed for the ribose nucleoside and nucleotides. For 2 m $NaClO_4$, the upfield shift is 0.042 ppm, and for 1 m $Mg(ClO_4)_2$, the observed shift is 0.030 ppm. The salt-induced shifts of the $H_1$, and $H_5$ resonances are again of smaller magnitude, being 0.02 ppm or less over the salt concentration range investigated.

Uracil. A similar study was undertaken for uracil to ascertain any direct effects which the electrolytes might have on the chemical shifts of the ring protons. Both the $H_5$ and $H_6$ resonances were found to be shifted upon the addition of salt. In salt solutions of $NaClO_4$, NaCl, and $Mg(ClO_4)_2$, these resonances are shifted downfield. At 1 m salt, the electrolyte-induced shifts are 0.008, 0.028, and 0.019 ppm, respectively, for the $H_6$ resonance, and the corresponding electrolyte shifts for the $H_5$ resonance are 0.012, 0.017, and 0.028 ppm, respectively. TBACl (1 m) produces a downfield shift of 0.047 ppm for the $H_6$ resonance and an upfield shift of 0.023 ppm for the $H_5$ resonance.

## 3.3. Salt-Induced Coupling Constant Changes

Changes in the $H_6$ chemical shifts described above were in many cases accompanied by simultaneous changes in the $J_{H_1',-H_2'}$ coupling constant.

5'-UMP. For 5'-UMP, for example, the same salts which produced large $H_6$ shifts were found to have large effects on the coupling constant between the $H_1'$ and $H_2'$ protons of the ribose ring. These results are summarized in Figure 8. $|J_{H_1',-H_2'}|$ is generally reduced upon the addition of salt. For example, it is lowered from 4.8 to 3.8 cps when the $Mg(ClO_4)_2$ concentration is increased from 0.0 to 0.6 m; 2 m $NaClO_4$ causes a 1.0 cps decrease. Tetrabutylammonium chloride, however, has no effect on $J_{H_1',-H_2'}$. A near linear correlation between these induced coupling constant changes and the induced $H_6$ chemical shifts can be demonstrated for this molecule by the simple plot shown in Figure 9. For 5'-UMP the slope of the plot, $\Delta J_{H_1',-H_2'}/\Delta\delta$, is equal to 8 Hz/ppm.

Uridine. In uridine, a similar relation exists as can be seen in Figure 10. $Mg(ClO_4)_2$ again produces the greatest effect, with $|J_{H_1',-H_2'}|$ decreasing from 4.5 to 3.9 Hz at a salt concentration of 1 m. A 0.7 Hz decrease in the coupling constant was noted for 2 m $NaClO_4$, while NaCl and TBACl were found to have only a small effect. The plot of an induced coupling constant change versus an induced shift

FIGURE 8

Salt-induced change of $|J_{H_1'-H_2'}|$ for a 0.01 m solution of 5'-UMP in $D_2O$ at pD 8.4, 30°.

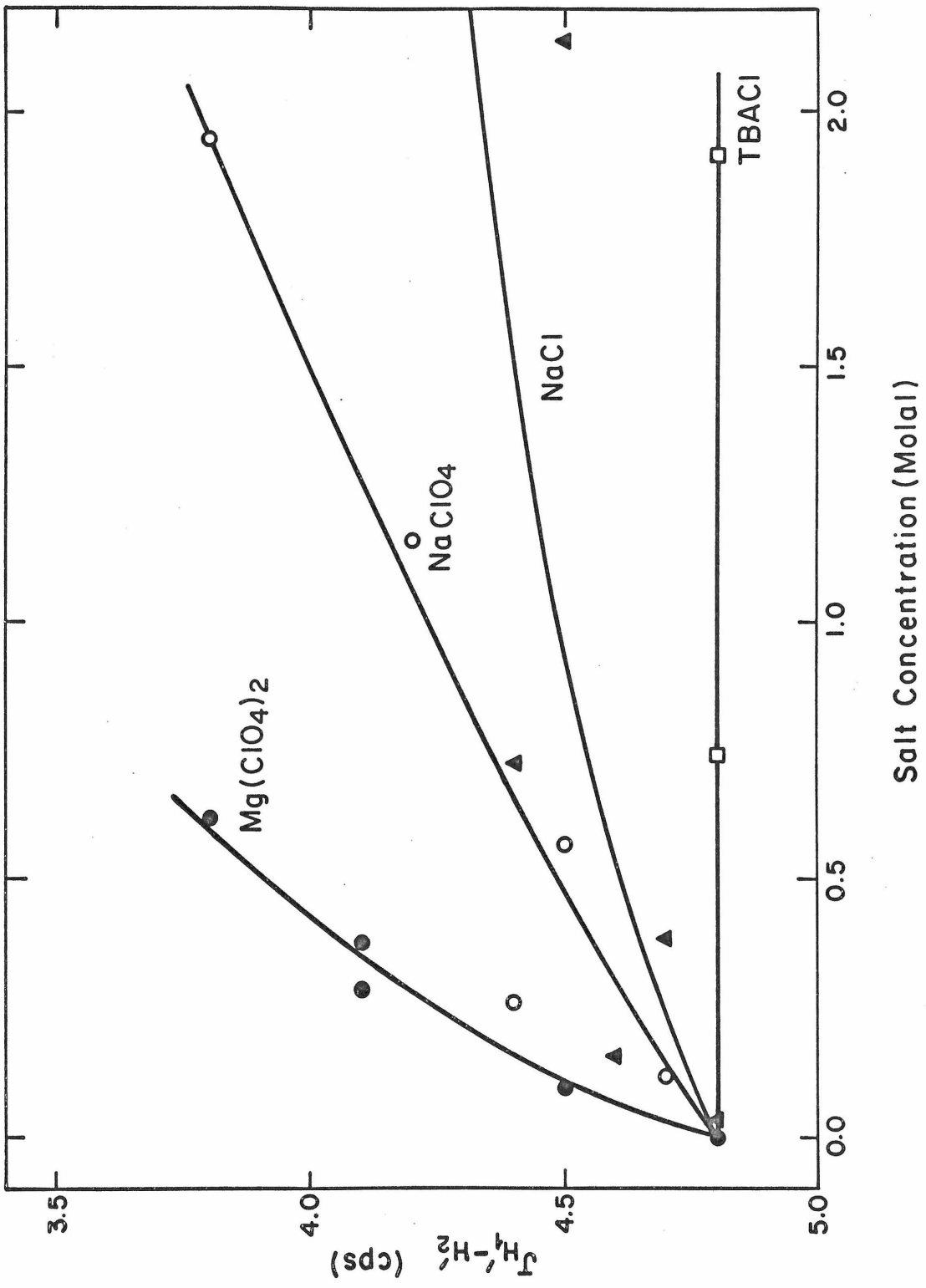
3.5
4.0
4.5
5.0
0.0
0.5
1.0
1.5
2.0
$J_{H_1'-H_2'}$ (cps)
Salt Concentration (Molal)
$Mg(ClO_4)_2$
$NaClO_4$
NaCl
TBACl

FIGURE 9

Correlation of salt-induced $H_6$ shifts with the salt-induced change of $|J_{H_1',-H_2'}|$ for various 0.01 m solutions of 5'-UMP in $D_2O$ containing different electrolytes at pD 8.4, 30°.

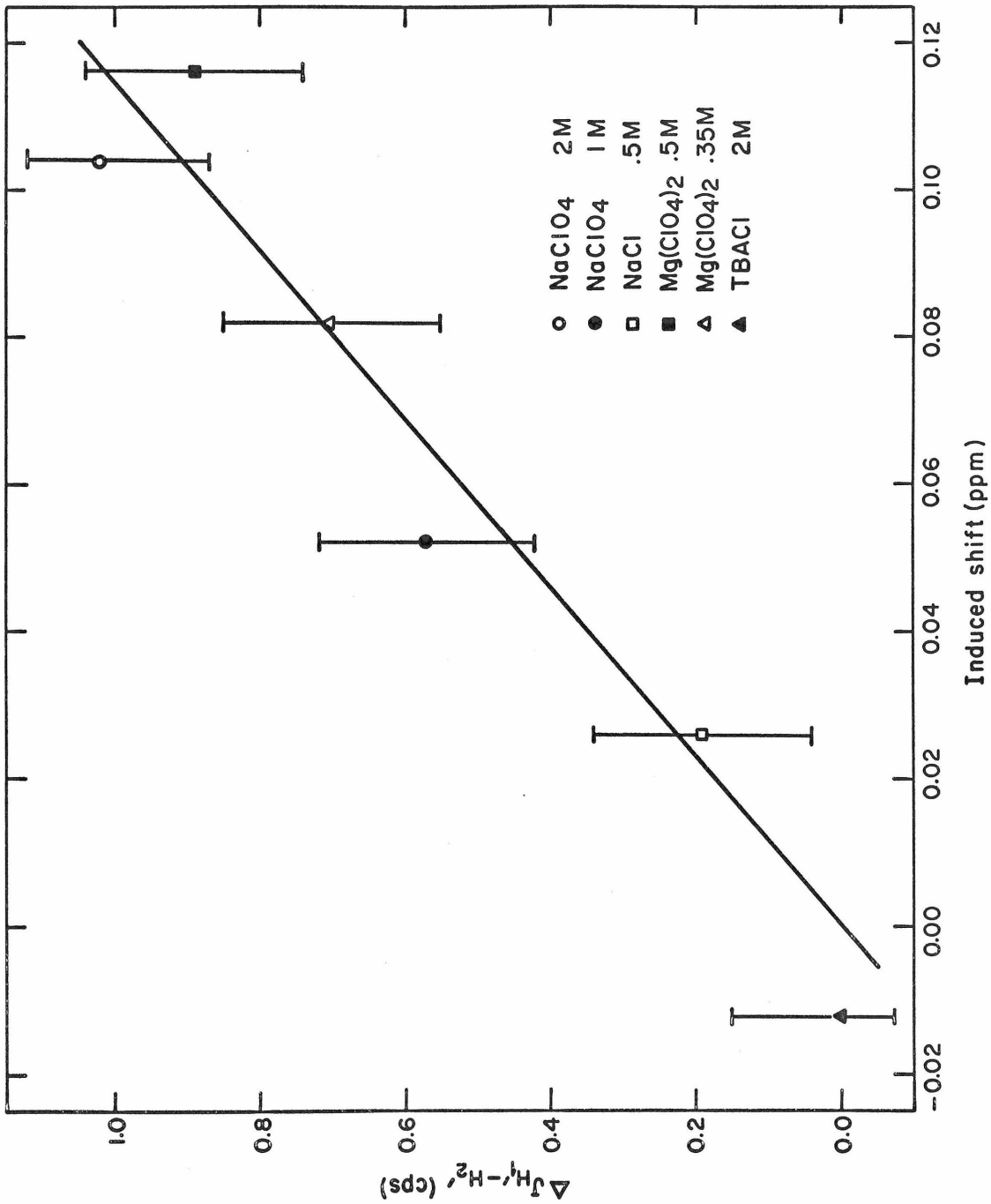
NaClO4 2M
NaClO4 1M
NaCl .5M
Mg(ClO4)2 .5M
Mg(ClO4)2 .35M
TBACl 2M
Induced shift (ppm)
-0.02
0.00
0.02
0.04
0.06
0.08
0.10
0.12
0.0
0.2
0.4
0.6
0.8
1.0
ΔJH1'-H2' (cps)

FIGURE 10

Salt-induced change of $|J_{H_1',-H_2'}|$ for a 0.01 m solution of uridine in $D_2O$ at pD 8.3, 30°.

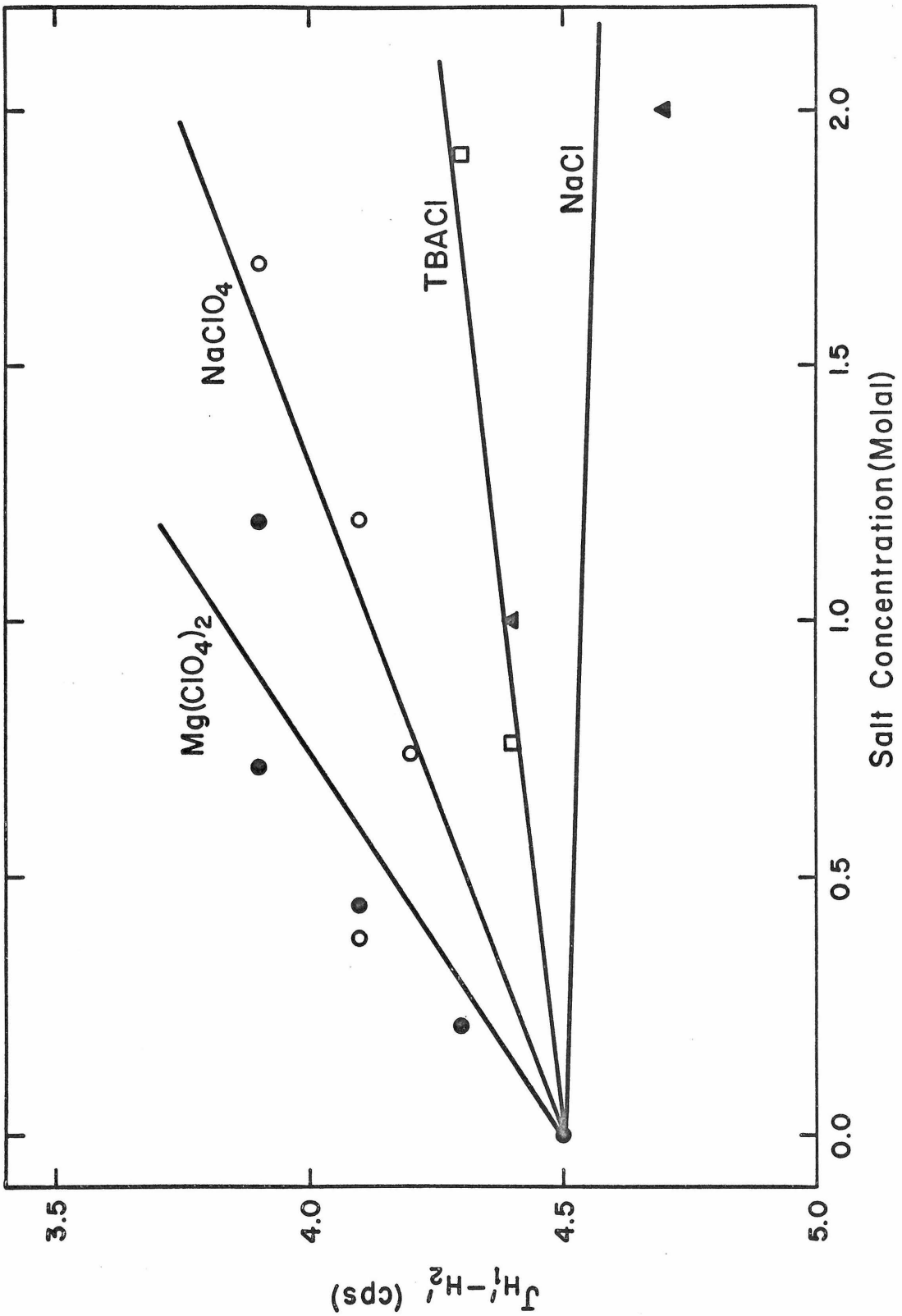
$J_{H_1'-H_2'}$ (cps)
3.5
4.0
4.5
5.0
0.0
0.5
1.0
1.5
2.0
Salt Concentration (Molal)
$Mg(ClO_4)_2$
$NaClO_4$
TBACl
NaCl

is again linear, but $\Delta J_{H_1',-H_2'} / \Delta \delta$ is 10 rather than 8 Hz.

3'-UMP. Not all nucleosides or nucleotides can, however, demonstrate such a relation between induced shift and induced coupling constant change. In contrast to the coupling constant changes observed for 5'-UMP and uridine, the $H_1',-H_2'$ coupling constant in 3'-UMP appears to be insensitive to the added electrolytes: $Mg(ClO_4)_2$, $NaClO_4$ and NaCl (Figure 11). Since some induced $H_6$ shift does exist for 3'-UMP this can be viewed as a case where the $\Delta J$ versus $\Delta \delta$ plot has a slope equal to zero.

Deoxyuridine. And finally, for deoxyuridine the average $H_1',-H_2'$ coupling constant, $\frac{1}{2}\left|J_{H_1',-H_2'} + J_{H_1',-H_2''}\right|$, also appears to be unaffected by the addition of salt to the deoxyuridine solution. However, here the small value of the induced shifts and the relative insensitivity of the average coupling constant would tend to obscure any non-zero correlation which might exist.

## 3.4. Nuclear Overhauser Effects

Nuclear Overhauser effects between nuclei of the same species are relatively small and in our experiments we wish to observe a change in this relatively small effect. Therefore, it is logical to choose the system which is apt to produce the largest effect. In view of the chemical shift and coupling constant experiments, 5'-UMP in the presence or absence of 2 m $NaClO_4$ would seem the best choice.

FIGURE 11

Salt-induced change of $|J_{H_1'-H_2'}|$ for a 0.01 m solution of 3'-UMP in $D_2O$ at pD 8.1, 30°.

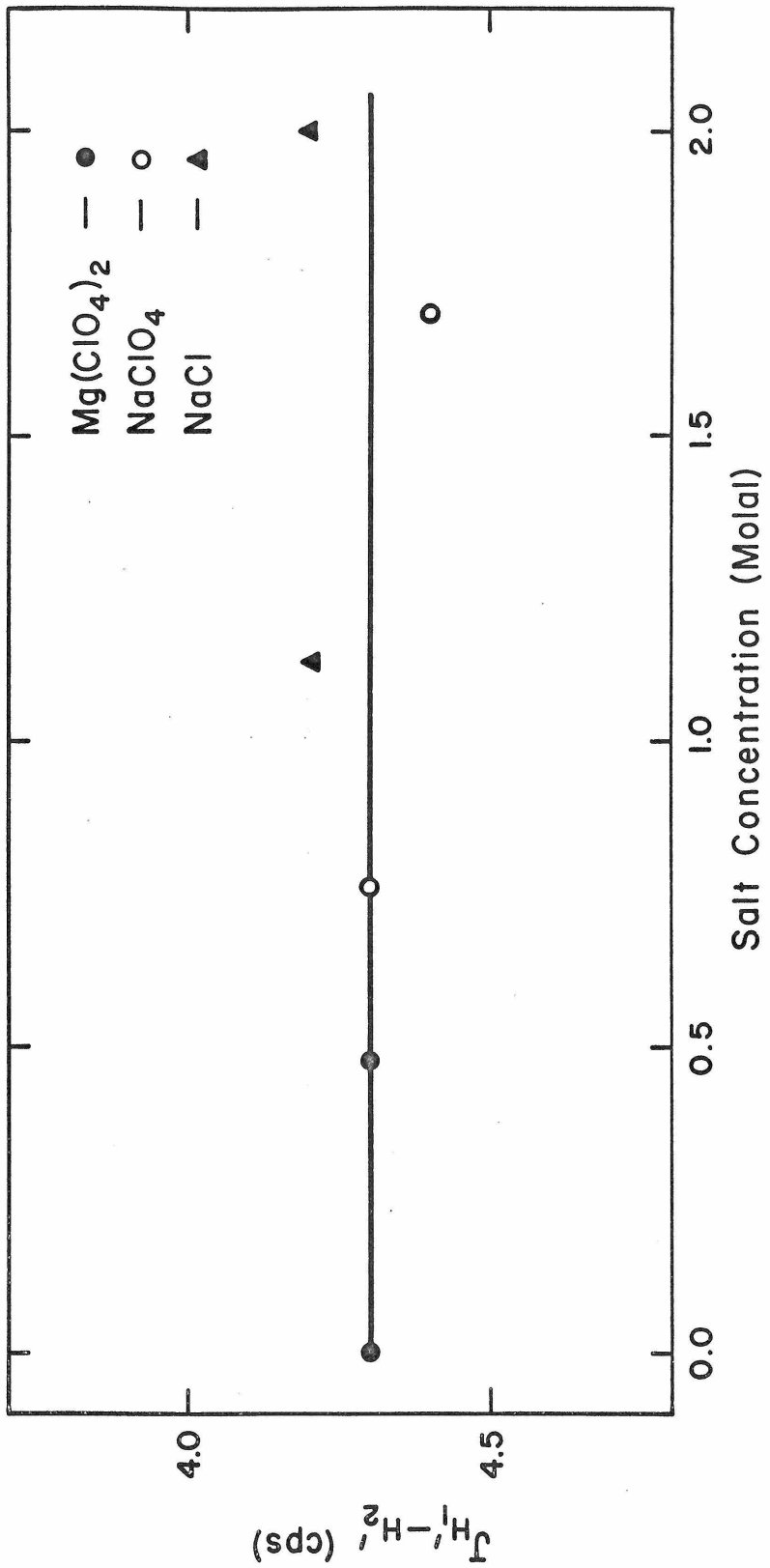
$Mg(ClO_4)_2$
$NaClO_4$
NaCl
$J_{H_1'-H_2'}$ (cps)
4.0
4.5
0.0
0.5
1.0
1.5
2.0
Salt Concentration (Molal)

The results for irradiation of the $H_2$, proton and $H_{5'}$,$_{5''}$ protons while observing $H_6$ of 0.1 M 5'-UMP solutions are presented in Table II. The optimum irradiation amplitude for each proton and each sample was determined to be 300 ± 100 mv. Experiments at this amplitude were repeated 15-30 times to determine the average effects and standard deviations presented in the table. In comparing the effects in the 2 M $NaClO_4$ solution to those in the 0 M $NaClO_4$ solutions, we note that the NOE for $H_2$, has increased slightly, 12.0 to 17.1%, and the effect for $H_{5'}$,$H_{5''}$ has decreased slightly, 12.4 to 6.8%. Unfortunately, the uncertainties are such as to place the results at the limit of statistical validity. An attempt to improve the situation by going to 0.3 M solutions was made. The results, as presented in Table II, are qualitatively the same, but the magnitude of the change seems to have decreased so as to place these results in doubt also. The experiments as a whole are included only as corroborative results consistent with the model to be derived on the basis of chemical shift and coupling constant data to be presented in the next section.

TABLE II: Nuclear Overhauser Effects Observed for the $H_6$ Proton of 5'-UMP.

| | Proton Irradiated | |
|---|---|---|
| | $H_{2'}$ | $H_{5'}$,$_{5''}$ |
| 0.1 M 5'-UMP<br>0 M $NaClO_4$ | 12.0 ± 6.0 | 12.4 ± 5.5 |
| 0.1 M 5'-UMP<br>2 M $NaClO_4$ | 17.1 ± 4.1 | 6.8 ± 2.8 |
| 0.3 M 5'-UMP<br>0 M $NaClO_4$ | 15.1 ± 1.8 | 9.2 ± 2.5 |
| 0.3 M 5'-UMP<br>2 M $NaClO_4$ | 16.4 ± 1.5 | 5.5 ± 1.9 |

# 4. DISCUSSION

The addition of salt to aqueous solutions of uracil nucleosides and nucleotides appears to affect the chemical shifts of the base protons, the value of the $H_1$,-$H_2$, ribose coupling constant, and the magnitude of the intramolecular proton-proton nuclear Overhauser effects. The chemical shifts could be modified either through direct interactions between the ions and the nucleoside or nucleotide molecule, or through indirect effects of the salt on the solvent structure. In addition to being the consequence of a conformation change in response to modification of the solvent structure by the added electrolyte, the chemical shifts could arise from specific ion-binding, both to the uracil ring and to the phosphate group of the ribose moiety, as well as from a more general change in the solvation of the uracil base. The changes in coupling constants and the changes in nuclear Overhauser effects, however, most certainly arise solely from an induced conformation change.

## 4.1. Initial Nucleotide Conformation

Interpretation of conformational changes induced by the addition of salts to aqueous solutions of the uracil nucleoside and nucleotides necessitates the assignment of some initial aqueous solution conformation to these molecules. The uracil base can assume several rotational

conformations relative to the ribose moiety about the glycosidic bond, and there are also several possible ribose conformations. The rotational conformation of the base and the conformation of the ribose ring, however, might not be totally uncorrelated, since nonbonded interactions presumably play an important role in deciding the average conformation of each moiety.[15-17] But, analysis of our nmr data, along with data already in the literature, can be used to assign an initial conformation to each.

4.1.1. Chemical Shift Implications

Considerable evidence has been accumulated in recent years, both from crystallographic studies[15-17] and from solution nmr studies,[19,22] to indicate that the rotational conformation of the pyrimidine base in the pyrimidine nucleosides and nucleotides is preferentially anti. In the case of 5'-UMP, the conformation of the uracil base in solution can be inferred from the chemical shifts of the $H_5$ and $H_6$ base protons relative to the corresponding shifts in uridine. In a situation where chemical shifts of protons with identical local molecular bonding are to be compared, chemical shift differences can be considered the result of variations in the electric polarization or magnetic anisotropy of neighboring groups. In comparing uridine and 5'-UMP, the addition of a negatively charged phosphate in 5'-UMP is particularly significant. Buckingham has proposed a method

for treating such charge effects.[45] For an atom in an S state, the presence of an external electric field will distort electron distribution in such a way as to reduce the circulation of electrons which normally gives rise to diamagnetic screening. Since the atom has spherical symmetry in this case, the effect must be insensitive to field reversal and thus proportional to the square of the field. In an axially symmetric molecule, X-H, terms which depend on E in another manner arise. A dependence on $E_z$, for example, is expected for a factor which measures the extent to which the external field reinforces or cancels the existing bond polarization. Buckingham has calculated proportionality constants for these two terms and has applied the resulting equation (1) for the induced shielding, $\Delta\delta_{elec}$, to the calculation of shifts for C-H protons in a number of molecules.

$$\Delta\delta_{elec} = -2 \times 10^{-12} E_z - 10^{-18} \times E^2 \qquad (1)$$

In this work, we will apply the equation to the induced shifts of the $H_5$ and $H_6$ protons.

In the case of 5'-UMP, $H_5$ and $H_6$ resonances appear appreciably downfield from the corresponding protons in uridine (see Table I), and it can be concluded from this observation that the uracil base assumes a rotational conformation about the glycosidic bond, such that the part of the uracil ring bearing these protons is in close proximity

to the doubly charged phosphate group (Figure 1), where both $E_z$ and $E^2$ terms are expected to produce downfield shifts. This deduction is substantiated both by protonation studies and by the diamagnetic ion-binding studies presented in this work. Protonation of the phosphate group over the pD range between 8 and 5 has been shown to result in an upfield shift of 0.15 ppm for the $H_6$ resonance (Figure 12). Qualitatively, this upfield shift can be understood in terms of the decreased electric field effect accompanying the reduction in the effective charge of the phosphate moiety upon phosphate protonation. Similar upfield shifts are observed on the binding of magnesium ions to 5'-UMP in aqueous solution.

In the case of uridine, deoxyuridine, and 3'-UMP, there is less direct pmr evidence to indicate the preferred solution conformation of the uracil base about the glycosidic bond. In these molecules, the phosphate moiety is either absent or, in the case of 3'-UMP, constrained to a position far removed from the base. Perturbations of the phosphate, therefore, have little effect on the resonance positions of the uracil base protons. There is, however, no <u>a priori</u> reason not to expect a similar <u>anti</u> conformation for the uracil base in these molecules, since the rotational conformation of the base about the glycosidic bond is largely determined by nonbonded interactions between the base and the ribose ring.[15] Esterification of the nucleoside to the phosphate group at either the 3'- or 5'-

FIGURE 12

pD-induced shift of the $H_6$ resonance for a 0.01 m solution of 5'-UMP in $D_2O$ at 30°.

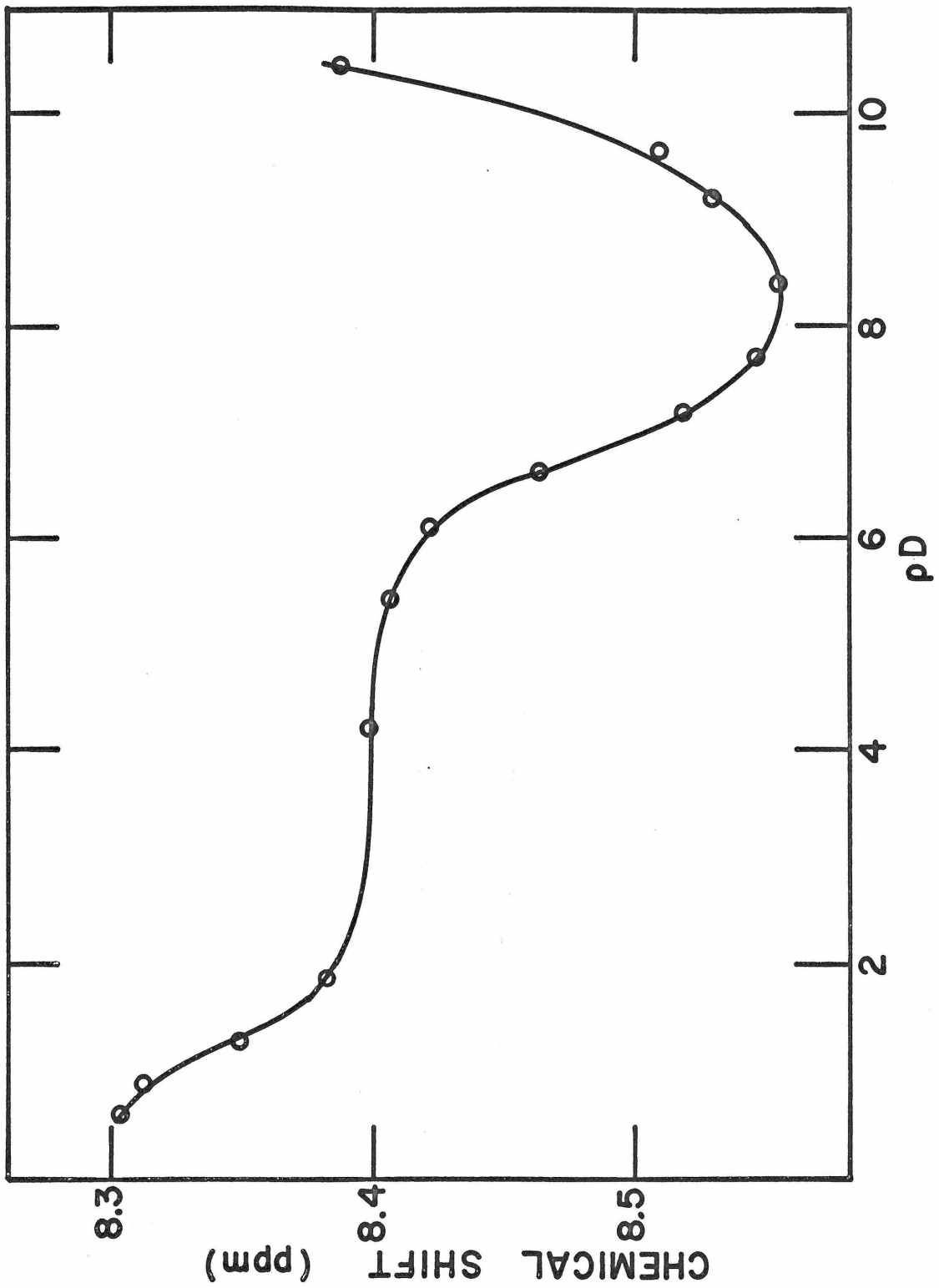
8.3
8.4
8.5
CHEMICAL SHIFT (ppm)
2
4
6
8
10
pD

position of the ribose ring is not expected to have a pronounced effect on the rotational conformation of the base, even though some perturbation undoubtedly occurs indirectly through the effect of the phosphate substitution on the conformation of the ribose ring. Beyond characterization as being within the anti range, it becomes difficult to assign an absolute value of the torsional angle, $\phi_{CN}$, for any nucleoside or nucleotide. First, the actual conformation is not likely to be fixed, but more probably represents a time-average of several rotomers within the anti range, and second, any precise estimate of $\phi_{CN}$ on the basis of nmr data requires consideration of factors far more complex than the effect of a charged phosphate group. We shall, however, attempt to employ the Donohue-Trueblood notation to designate relative differences in rotational conformation of the base about the glycosidic bond for various nucleosides or nucleotides, all of whose average glycosidic rotational conformations may be within the limits of the anti range.

In making a distinction between various conformations within the anti range, we must first consider the effects of other neighboring groups on the chemical shifts of the $H_6$ and $H_5$ protons. For example, the proximity of the $H_6$ proton to the ribose ring and the variability of this geometric relation with glycosidic bond angle may make the dipolar groups of the ribose moiety a particularly important consideration. The small differences between the chemical

shifts of the $H_6$ proton in uridine, deoxyuridine, and 3'-UMP may, in part, be due to small variations in the base orientation and base-ribose interaction in these molecules. Experimentally, the effect of the ribose ring on the resonance position of the $H_6$ proton can be ascertained by comparing the $H_6$ chemical shifts in uracil and uridine. The $H_6$ resonance of uridine is 0.34 ppm downfield from the corresponding resonance in uracil. In other words, attachment of the ribose moiety to $N_1$ of the uracil base causes an appreciable downfield shift of the $H_6$ resonance. This does not appear to be caused by an inductive effect due to an alkyl type substituent, since a nearly equal shift of 0.30 ppm[43] is observed when the methyl group in $N_1$-methylcytosine is replaced by the ribose moiety in cytidine. The 0.3 ppm downfield shift induced by the ribose ring most likely arises from an electric field effect and/or magnetic anisotropy effect due to some group in the ribose ring, and can be treated in a manner analogous to the phosphate effect. In view of the proximity of the uracil $H_6$ proton to the ether oxygen linkage, this ether group appears to be the most likely candidate. The magnetic anisotropy effect on chemical shift is expected to be small, compared to the electric dipole effect, on the basis of results obtained for other oxygen-containing functional groups.[46] The effect of the ether dipole moment can be estimated by substituting a dipolar field for the point charge field used in the

calculation of the phosphate effect. The dipole moment was assumed to be that of a tetrahydrofuran ring with the dipole centered on the ether oxygen, and the proper geometrical relationships were assessed by examination of a CPK model of 5'-UMP. For torsion angles, $\phi_{CN}$, in the vicinity of $\sim -30^{\circ}$ (the base conformation which is generally observed for the pyrimidine nucleosides in the crystalline state), the calculations indicate that the electric field effect of the ether oxygen can account for the observed ribose shift of the $H_6$ resonance. When $\phi_{CN} \approx -60^{\circ}$, this electric field effect was found to be negligible. Although such calculations have often been found to be quantitatively unreliable, it is, nevertheless, clear from these considerations that the chemical shift of the uracil $H_6$ proton would be expected to be sensitive to the conformation of the base, relative to the ribose moiety about the glycosidic bond. Specifically, the $H_6$ resonance is expected to move to higher fields when the uracil base assumes average rotational conformations corresponding to more negative torsion angles. This should prove useful in the analysis of salt effects on chemical shifts, as well as in the assignment of initial nucleoside conformations.

At first glance, one might also expect the chemical shift of the ribose or deoxyribose $H_1$, proton to give a similar indication of the rotational conformation of the base, due to the close proximity of this proton to the

2-keto group of the uracil ring when the base conformation is anti. Both the bond dipole and the magnetic anisotropy of the carbonyl group are expected to influence the chemical shift of this proton, with the dominant electric field effect being of the order of several tenths of a ppm downfield. The dependence of the carbonyl effect on the base orientation is not difficult to ascertain. Since rotation of the base towards a torsion angle, $\phi_{CN}$, of $\sim -90^{\circ}$ brings the keto oxygen in closer proximity to the $H_1$, proton, a downfield shift is to be expected when the average orientation of the base tends towards more negative torsional angles within the range of $0^{\circ}$ and $-90^{\circ}$. However, in the ribose nucleosides and nucleotides, the 2'-OH group of the ribose ring also contributes to the $H_1$, shifts, and this contribution is most likely dependent upon the conformation of the ribose ring. The 2'-OH group results in increased shielding of the $H_1$, proton, as can be ascertained by comparing the chemical shifts of the $H_1$, protons in the ribose and deoxyribose nucleosides in Table I. Conformational changes within the ribose ring, which alter the dihedral angle between the 1'-CH and 2'-CO bonds and the distance between the anomeric hydrogen and the 2'-OH group, should therefore be reflected in the chemical shift of the $H_1$, resonance. A change in the ribose ring conformation from 2'-endo to 3'-endo, the two most commonly found ribose conformations, for example, would be expected to result in an

upfield shift, since the 2'-OH group is closer to the $H_{1'}$ proton when the ribose conformation is 3'-endo. The factors which affect the $H_{1'}$ shifts are therefore quite complex, and the interpretation of these shifts is not necessarily straightforward, since the two contributions which we have considered here can add or subtract, depending on the detailed nature of the conformational changes within the nucleoside or nucleotide molecule. Moreover, there are probably other factors influencing the $H_{1'}$ shifts, such as the local solvent structure, the solvation of 2'-keto oxygen, the 2'-OH group, and the ether oxygen of the ribose ring.

4.1.2. Nuclear Overhauser Implications

The nuclear Overhauser results also give some insight into the initial conformation about the glycosidic bond. For a dilute solution of a molecule such as 5'-UMP in an aprotic solvent, in this case $D_2O$, spin relaxation of the various protons is mediated largely by intramolecular spin-spin interactions and, to a certain extent, strongly coupled transitions of the type $\alpha_N\beta_{N'} \longleftrightarrow \beta_N\alpha_{N'}$ and $\alpha_N\alpha_{N'} \longleftrightarrow \beta_N\beta_{N'}$ become important. Under these circumstances, alteration of the population levels of one nucleus, in this case through saturation of the $H_{2'}$ or $H_{5'}$ resonances, can lead to effects on the population of the coupled spin levels ($H_6$) and an observed nuclear Overhauser enhancement. The effect

can be more easily illustrated with the aid of the diagram in Figure 13.[47] $W_N$ and $W_{N'}$ correspond to the more usual single nuclear transitions, while X and Y correspond to the double nuclear transitions of interest here. The transition probabilities between various states, weighted by appropriate Boltzmann factors, are then $W_N e^{\pm q}$, $W_{N'} e^{\pm q'}$, $Xe^{\pm(q-q')}$, and $Ye^{\pm(q'-q)}$. Under steady state conditions, the sum of the transitions into any one level must equal the sum of the transitions out of that level. Expressing this fact in equation form and imposing the condition that nucleus N is saturated by applied rf power (i.e., $N_{\alpha\alpha'} = N_{\beta\alpha'} = \frac{1}{2}N^+$, and $N_{\alpha\beta'} = N_{\beta\beta'} = \frac{1}{2}N^-$) one finds the following equation for the ratios of the populations of the $\alpha'$ and $\beta'$ spin states:

$$\frac{N^+}{N^-} = e^{2q'} \left[ 1 + \frac{2q\,(Y - X)}{2W_{N'} + X + Y} \right] . \qquad (2)$$

Since the thermal equilibrium ratio of $N^+$ to $N^-$ is simply $e^{2q'}$, $\frac{(Y - X)}{2W_{N'} + X + Y}$ can be viewed as a nuclear Overhauser enhancement factor (for dipole-dipole interactions $Y > X$). In general $W_{N'}$ (the sum of the normal spin-lattice transitions) is much larger than either X or Y and the enhancement is roughly proportional to $(Y - X)$. X and Y transitions arise only from time dependent perturbations which have non-zero matrix elements between states which differ in spins of both nuclei. In other words, the perturbation must

FIGURE 13

Energy level diagram illustrating transitions in a dipole-dipole coupled two spin system.

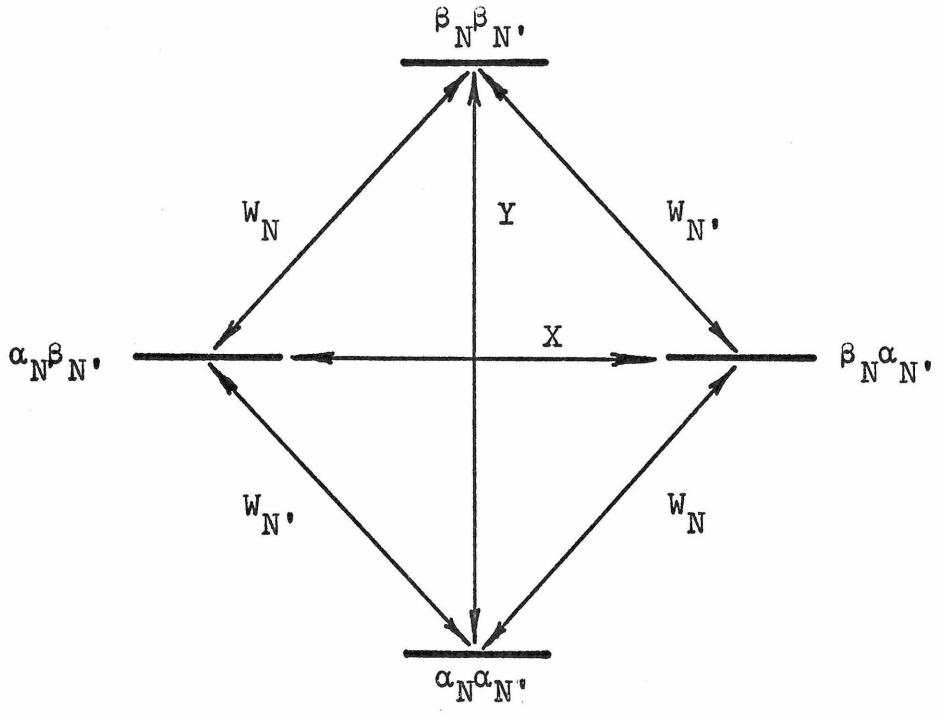

be of one of the following forms: $\langle\beta\beta|I^-I'^-|\alpha\alpha\rangle$, $\langle\alpha\alpha|I^+I'^+|\beta\beta\rangle$, $\langle\alpha\beta|I^+I'^-|\beta\alpha\rangle$, or $\langle\beta\alpha|I^-I'^+|\alpha\beta\rangle$. The direct dipole-dipole interaction (3),

$$H_D = \frac{g_N^2\beta_N^2}{r^3} \quad \vec{I} \cdot \tilde{D} \cdot \vec{I}' \qquad (3)$$

where D is a tensor containing only angular dependence, and r is the internuclear distance, can be expanded in a form which has elements of this type. Since transition probabilities are proportional to $\langle|H_D|\rangle^2$: X, Y, and, hence, the nuclear Overhauser enhancements are roughly proportional to $\frac{1}{r^6}$. Thus for a nucleotide in the <u>anti</u> conformation one would expect appreciable enhancement of the $H_6$ resonance when the neighboring protons, $H_{2'}$ or $H_{5''}$, are irradiated. This situation has been experimentally verified in the case of uridine by Hart and Davis.[34] These authors cite their results as evidence for a range of rotational isomers for uridine, <u>anti</u> presumably being dominant. Our results with 5'-UMP show a 12% enhancement through both $H_{2'}$-$H_6$ and $H_{5',5''}$-$H_6$ interactions and can be interpreted in a similar manner. We have chosen $H_{2'}$-$H_6$ and $H_{5',5''}$-$H_6$ interactions for study in our salt effect experiments simply because they reach a maximum at alternate limits of the normal <u>anti</u> conformational range ($\phi_{CN}$=-5°, and $\phi_{CN}$= -65°) and should be of use in observing small shifts in the equilibrium among <u>anti</u> rotational conformers. A shift to more negative torsional

angles decreases the $H_2$,-$H_6$ distance and increases $H_5$,-$H_6$. An increase in torsional angle on the other hand produces the opposite effect with a corresponding difference in the observed NOEs.

4.1.3. Coupling Constant Implications

Having assigned the initial base conformation about the glycosidic bond to be anti for these uracil nucleosides and nucleotides, and having established means of monitoring variations within the anti range, we must accomplish similar ends with respect to the conformation of the ribose moiety. The $H_1$,-$H_2$, coupling constant provides a means of monitoring the average conformation of the ribose ring. Vicinal proton couplings along carbon-carbon single bonds occur principally via the transfer of spin polarization through the intervening bonding electrons. The couplings then depend on the electron density at each of the coupled nuclei, as well as electron exchange integrals between orbitals centered on atoms along the coupling chain. The former is fairly independent of bond angle, but the latter is not. A calculation of these terms even on the basis of simple valence bond structures leads to a prediction of a coupling constant dependence on the dihedral angle ($\theta$) between the two planes defined by the atoms of the 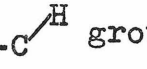 group. Karplus first expressed this relation in a simple functional form:[48]

$$J_{HH'} = \begin{cases} 8.5\cos^2\theta - 0.28 & 0^\circ \leq \theta \leq 90^\circ \\ 9.5\cos^2\theta - 0.28 & 90^\circ \leq \theta \leq 180^\circ \end{cases} \quad (4)$$

It has since been applied with only minor modification to a variety of compounds by many authors.[33,49,50] Of course, factors other than molecular geometry may influence electron densities or electron exchange in the intervening bonds and, in turn, the observed coupling constants may vary. These factors, including the effect of increased substituent electronegativity, have also been considered.[51-53] But in general effects on coupling constants are small, even when electronegativity is changed substantially. Chemical shift is a far more sensitive probe of such factors: a change of several ppm normally corresponding to a coupling constant change of a few Hz. Since variations in substituent electronegativity among the molecules considered here are small and since chemical shift variations are of the order of one or two tenths of a ppm, coupling constants would seem a rather straightforward indicator of rotational geometry of the single bond in the ribose ring. However, even with this assurance of the theory's validity, we shall stress only the qualitative aspects of its predictions.

The ribose rings of pyrimidine nucleosides and nucleotides, in crystal structures at least, are most commonly found in either the 3'-endo or 2'-endo conformations where either the 3'-carbon atom or the 2'-carbon atom is out of

the plane formed by the other four atoms of the ring and is on the same side of the plane as the base and the 5'-linkage (Figure 2).[11] Theoretical values for the $H_{1'}$-$H_{2'}$ coupling constant when the $C_{1'}$-$C_{2'}$ bond has the appropriate geometry for the 2'-endo and 3'-endo conformations are 6.9 and 1.7 Hz, respectively.[32] On the basis of these limiting values, it appears that uridine, 5'-UMP and 3'-UMP, which exhibit $H_{1'}$-$H_{2'}$ coupling constants of 4.5, 4.8 and 4.3 Hz, respectively, all have average ribose conformations intermediate between 2'-endo and 3'-endo, with the conformations in uridine and 3'-UMP pushed more toward the 3'-endo side. More recent studies of uridine which have taken all of the ribose coupling constants into account have been in general agreement with this interpretation.[30,31] In the case of deoxyuridine, the theoretical values for the average coupling constant, $\frac{1}{2}\left|J_{H_{1'}\text{-}H_{2'}} + J_{H_{1'}\text{-}H_{2''}}\right|$, in the 2'-endo and 3'-endo limits, are 6.4 and 4.8 cps, respectively. The observed coupling constant is 6.7 Hz; it thus appears that the conformation of the deoxyribose ring in deoxyuridine is centered about the 2'-endo form.

## 4.2. Salt-Induced Conformation Changes

With the above background, we can now discuss the salt-induced effects observed in this work. In view of the low nucleoside or nucleotide concentrations, we do not believe that the observed effects arise from enhanced or

reduced stacking of the uracil bases due to modification of the solvent system. Even though uracil-uracil interaction is not expected to be reflected in the chemical shifts of the uracil $H_5$ and $H_6$ resonances due to the small magnetic anisotropy of the uracil ring,[54] changes in the base-stacking interaction might be reflected in the $J_{H_1'-H_2'}$ coupling constants. We note, for example, that in 3'-UMP and 5'-UMP, where the base-stacking interaction can be monitored by the chemical shifts of the base protons, the $J_{H_1'-H_2'}$'s are also concentration dependent, these coupling constants varying about 1 to 1.5 cps over the concentration range of ~0.01 m to 0.2 m.[55] However, in the present systems, we find that both the uracil $H_5$, $H_6$ shifts, and the ribose $H_1'-H_2'$ coupling constants are independent of concentration over the concentration range of 0.01 m to 0.08 m. Thus, our results would appear to be indicative of a change resulting from a direct interaction of the solvent with the nucleotide or nucleoside.

4.2.1. Chemical Shift Implications

We consider first the interpretation of our salt-induced chemical shifts. Our results with uracil would seem to rule out the importance of any effects related to specific ion-binding to the uracil ring and to changes in the solvation of the base as a consequence of modifications in the solvent structure. With the exception of TBACl, the

salt-induced shifts of both $H_5$ and $H_6$ resonances of uracil are quite small, but more significantly, these shifts are opposite in direction (downfield instead of upfield) to those noted for the corresponding nucleosides and nucleotides. Moreover, in the uracil nucleosides and nucleotides, only the $H_6$ resonance appears to be significantly shifted upon the addition of salt to the solutions, indicating that the perturbation in the magnetic environment of the $H_6$ proton must be inherent in the close proximity of this proton to the ribose or ribose-phosphate moiety. In the case of 3'-UMP and 5'-UMP, specific cation-binding to the negatively charged phosphate group is expected with $Mg(ClO_4)_2$, and to some extent with the sodium salts. However, only in the case of 5'-UMP is the phosphate close enough for specific ion-binding to directly affect the chemical shifts of the uracil $H_6$ proton. It thus appears that the addition of salt to the nucleoside or nucleotide solutions has resulted in some perturbation of the ribose moiety and/or a change in the average conformation of the uracil base about the glycosidic bond. In the case of uridine and 5'-UMP, the observed changes in the $H_{1'}$-$H_{2'}$ coupling constant upon the addition of salt do indicate a change in the conformation of the ribose ring. However, even though a salt-induced upfield shift of the $H_6$ resonance is noted in 3'-UMP, a concomitant change in the $H_{1'}$-$H_{2'}$ coupling constant is not observed for this molecule. These observations would seem to suggest that the

salt-induced $H_6$ shifts are not the direct result of conformational changes in the ribose moiety, and, with the exception of 5'-UMP, we can also rule out contributions due to specific ion-binding. With these possibilities eliminated in the case of uridine, deoxyuridine and 3'-UMP, there remains only one other reasonable interpretation of the salt-induced upfield shifts of the uracil $H_6$ resonance. That is, the addition of salt to these nucleoside and nucleotide solutions produces a change in the average rotational conformation of the uracil base about the glycosidic bond, and the resultant variations in the position of the $H_6$ proton relative to the ribose ring oxygen give rise to the observed shifts. In accordance with our discussion of the electric field effects arising from this furanose oxygen, the upfield shifts induced by the addition of the "structure-breaking" salts would seem to indicate a redistribution among rotational conformations of the base about the glycosidic bond to emphasize those with more negative torsional angles.

The different variations in the salt-induced shifts with salt concentration among the various nucleosides and nucleotides are noteworthy and serve to distinguish 5'-UMP from uridine, deoxyuridine and 3'-UMP. Whereas the induced shifts are within experimental error, linear with respect to the salt concentration over the range of concentration investigated for uridine, deoxyuridine and 3'-UMP, the

salt-induced shifts in the case of 5'-UMP, by contrast, vary abruptly at low salt concentrations, even though the variation again becomes linear as the concentration is increased. In the case of 5'-UMP, specific cation-binding to the phosphate group leads to additional shifts of the uracil $H_6$ resonance, since the ion-binding in effect decreases the effective charge of the phosphate and its deshielding effect on the $H_6$ proton. The effect of this complex formation on the chemical shift of the $H_6$ resonance can be estimated from its pH dependence. Since the first protonation of the doubly charged phosphate in 5'-UMP over the pD range 8 to 5 shifts the $H_6$ resonance upfield 0.15 ppm, and the second protonation of phosphate at a pD of 1.2 results in an additional 0.12 ppm, one might expect, upon the formation of a 1:1 ion-nucleotide complex, an upfield shift of the $H_6$ resonance by 0.27 ppm for a divalent ion, and by 0.15 ppm for a univalent ion. However, even for a divalent cation such as $Mg^{++}$ which is expected to bind quite strongly to the negatively charged phosphate group, the complex formation is not expected to be complete when the nucleotide concentration is of the order of 0.01 m, due to the increasing importance of activity coefficients for the ionic species at the salt concentrations necessary to drive the reaction toward completion. The observed chemical shift, therefore, represents a weighted average of the shifts for the complexed and uncomplexed molecules; that is,

$$\delta_{obs} = \delta_u f_u + \delta_c f_c \ , \qquad (5)$$

where $f_c$ is the fraction of nucleotide complexed, $f_u$ is the fraction uncomplexed, and $\delta_u$ and $\delta_c$ denote the chemical shifts of the uncomplexed and complexed molecules, respectively. When the shifts are not complicated by salt-induced conformational changes, both $\delta_u$ and $\delta_c$ are independent of the salt concentration. The following expression for the salt-induced shift can then be obtained from mass-action considerations for the formation of 1:1 cation-nucleotide complexes.

$$\delta_{obs}-\delta_u = \tfrac{1}{2}(\delta_c-\delta_u)\left\{\left(1 + \frac{M}{N} + \frac{\gamma_c}{\gamma_M\gamma_N KN}\right) - \left[\left(1 + \frac{M}{N} + \frac{\gamma_c}{\gamma_M\gamma_N KN}\right)^2 - \frac{4M}{N}\right]^{\frac{1}{2}}\right\} . \qquad (6)$$

Here, M and N denote the stoichiometric concentration of the cation and the nucleotide, respectively; K is the formation constant of the complex, and $\gamma_M$, $\gamma_N$, $\gamma_c$ are the activity coefficients of the cation, nucleotide, and the complex, respectively.

We have applied equation (6) to the $H_6$ shifts of 5'-UMP induced by the addition of $Mg(ClO_4)_2$, but without success. In this treatment, we have assumed that $\gamma_c \approx 1$, and have estimated $\gamma_M\gamma_N$ from the known mean activity

coefficients ($\gamma_{\pm}$) of $ZnSO_4$ at the same ionic strength.[56] While equation (6) does predict the abrupt salt-induced shifts at low $Mg^{++}$ concentrations, it does not reproduce the linear dependence noted at salt concentrations above 0.1 m. Instead, calculations made using reasonable values of the parameters ($\delta_c - \delta_u \approx 0.27$ ppm, $K = 100$ molal$^{-1}$) indicate that if specific ion-binding were the only contribution to the observed salt-induced shifts, the induced shifts would level off at ~0.06 ppm at a $Mg^{++}$ concentration of ~0.1 m. The results of this analysis suggest that, as in the case of uridine, deoxyuridine, and 3'-UMP, the addition of salt to the 5'-UMP solution induces a change in the nucleotide conformation which affects the chemical shift of the $H_6$ resonance. If this were the case, then $\delta_c$ and $\delta_u$ would both be dependent upon the salt concentration. Under the assumption that the effects due to specific ion-binding and those related to nucleotide conformation change are independent of each other, we can write

$$\delta_{obs} = (\delta_c^o + \delta_c')f_c + (\delta_u^o + \delta_u')f_u \,, \qquad (7)$$

where $\delta_c^o$ and $\delta_u^o$ denote the chemical shifts of complexed and uncomplexed nucleotide, and $\delta_c'$ and $\delta_u'$ represent the modifications in the shifts of the complexed and uncomplexed molecules as a result of the salt-induced

conformation changes. If we now assume that the salt-induced conformation changes are quite similar for both the complexed and uncomplexed nucleotide molecule, then

$$\delta'_c f_c + \delta'_u f_u = \delta'_c = \delta'_u = \delta' \tag{8}$$

and equation (7) simplifies to

$$\delta_{obs} = \delta^o_c f_c + \delta^o_u f_u + \delta' \ . \tag{9}$$

For small conformational changes, we expect $\delta'$ to be proportional to the salt concentration; hence,

$$\delta' = kM \tag{10}$$

and we obtain the following expression for the salt-induced shifts:

$$\delta_{obs}-\delta^o_u = kM + \tfrac{1}{2}(\delta^o_c-\delta^o_u)\left\{\left(1 + \frac{M}{N} + \frac{\gamma_c}{\gamma_M\gamma_N KN}\right) - \left[\left(1 + \frac{M}{N} + \frac{\gamma_c}{\gamma_M\gamma_N KN}\right)^2 - \frac{4M}{N}\right]^{\frac{1}{2}}\right\} \tag{11}$$

It is not difficult to see that equation (11) does predict the abrupt variations in the salt-induced shifts at low salt concentration and the linear dependence observed at high

salt concentrations. We have fitted the $H_6$ shifts of 5'-UMP induced by $Mg(ClO_4)_2$ to equation (11) without difficulty. k can be determined from the linear dependence at high salt concentrations; and the non-linear part of the data, as given by the difference between the experimental points and the broken line in Figure 14, can be fitted by the second term in equation (11) using the following parameters: K = 60 molal$^{-1}$ and $\delta_c^o - \delta_u^o$ = 0.25 ppm. Both of these values are reasonable. We have indicated earlier that the binding of a divalent ion to the phosphate in 5'-UMP would reduce the deshielding effect of the phosphate on the $H_6$ proton by 0.27 ppm. The formation constant of the Mg-5'-UMP complex can be compared with the value of 90 molar$^{-1}$ previously reported for the Mg-5'-AMP complex by other workers.[57] A similar analysis of the data for the sodium salts can also be made. However, since the binding constant for the $Na^+$-nucleotide complex is much smaller, the effects of specific ion-binding are much less dramatic, and at high salt concentrations, the induced $H_6$ shifts are dominated by the linear portion of the curve. Thus in the case of 5'-UMP, the residual linear portion of the chemical shift curve for both $Mg^{++}$ and $Na^+$ salts may be attributed to a change in base orientation, just as it was in the uridine, deoxyuridine and 3'-UMP experiments.

It is interesting to compare the shifts associated with the salt-induced conformation change for the various

FIGURE 14

$Mg(ClO_4)_2$-induced shifts of the $H_6$ resonance for a 0.01 m solution of 5'-UMP in $D_2O$ at pD 8.4, 30°.

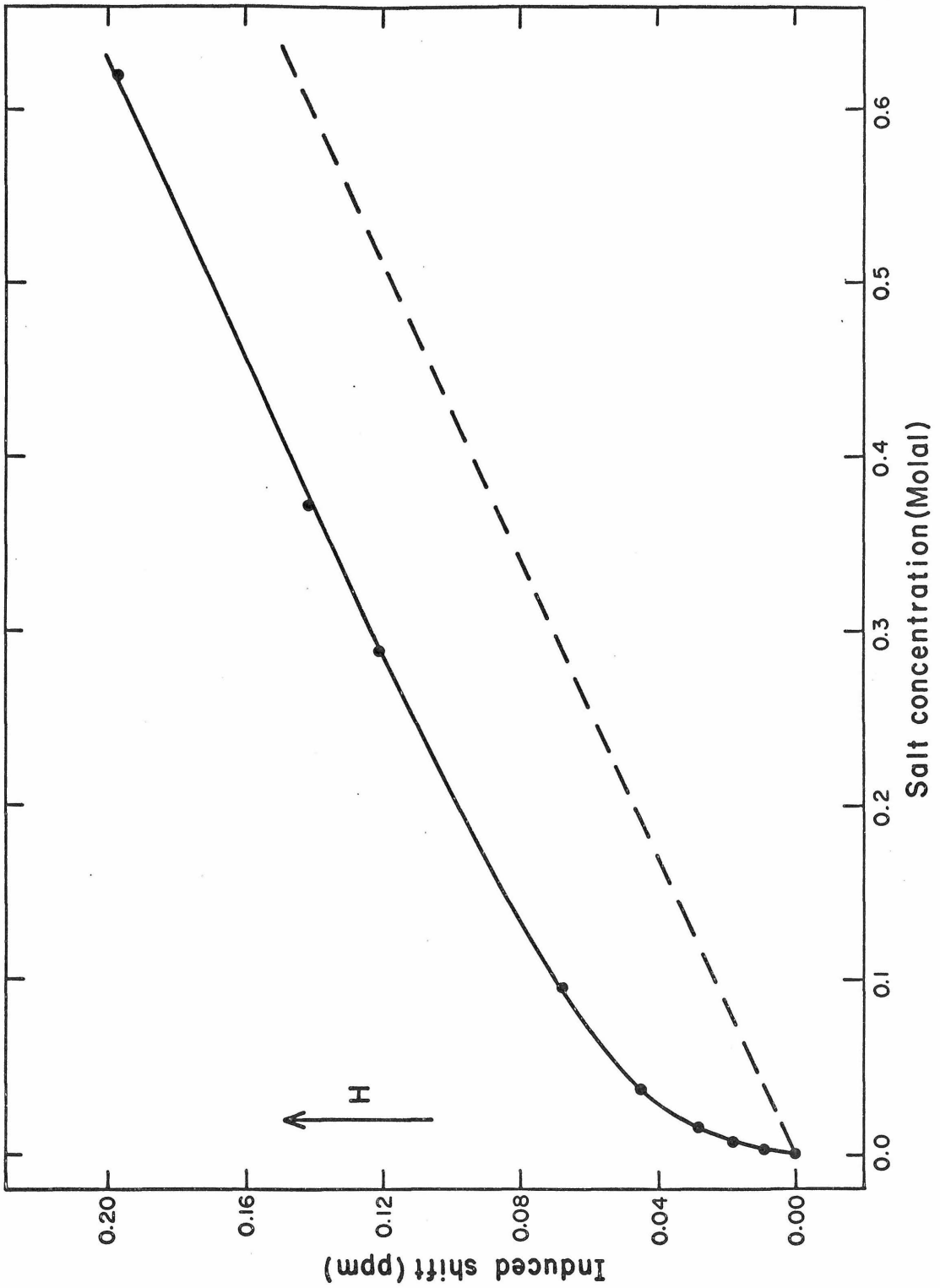
Induced shift (ppm)
0.20
0.16
0.12
0.08
0.04
0.00
H
0.0
0.1
0.2
0.3
0.4
0.5
0.6
Salt concentration (Molal)

nucleosides and nucleotides. A comparison of the $H_6$ shifts for 3'-UMP, uridine, and deoxyuridine with the results obtained for 5'-UMP in Figure 5 indicates that the effects are much more pronounced for 5'-UMP than for the other molecules. At 0.6 m $Mg(ClO_4)_2$, e.g., the shifts attributable to the salt-induced conformation change are 0.14, 0.07, 0.04, and 0.02 ppm for 5'-UMP, 3'-UMP, uridine, and deoxyuridine, respectively. This may indicate that the $H_6$ resonance in 5'-UMP is more sensitive to the orientation of the uracil base about the glycosidic bond because of the close proximity of the $H_6$ proton to the phosphate group. Or it may be that the 5'-UMP molecule is more susceptible to the salt-induced conformation change. In this connection, we note that the salt-induced shifts per unit salt concentration are in general larger for the nucleotides than for the nucleosides. If the $H_6$ shifts are indeed more sensitive to the base conformation because of the deshielding effect of the phosphate group, then we expect the shifts induced per unit conformational change to depend upon the effective charge of the phosphate group, in which case the assumption $\delta'_u = \delta'_c$ used in obtaining expression (11) may not be valid. However, since the fraction of nucleotide molecules complexed is not large, even at the highest salt concentration studied (~25% in the case of $Mg(ClO_4)_2$), any departure from the assumption given by (8) is not likely to be discernible experimentally.

Except in the case of 5'-UMP, the salt-induced shifts observed for the $H_5$ and $H_{1'}$ protons of the uracil nucleosides and nucleotides are quite small, and consequently do not deserve the same attention which we have devoted to the $H_6$ shifts. The ribose ring might be expected to exert some influence on the chemical shift of the $H_5$ proton; however, the $H_5$ proton being further removed, the effect of the ether oxygen is expected to be smaller, as can be seen by comparing the chemical shift difference between uridine and uracil for the $H_5$ and $H_6$ protons (0.11 ppm versus 0.34 ppm). Small changes in the base conformation are then not readily monitored by the position of the $H_5$ resonance. Moreover, with the exception of 5'-UMP, the salt-induced shifts of the $H_5$ proton are all downfield, as in the case of uracil, illustrating the probable importance of changes in the local solvent structure and specific solvation of the uracil base in determining the small salt-induced $H_5$ shifts. In 5'-UMP, the negatively charged phosphate also deshields the $H_5$ proton somewhat (~0.11 ppm), and part of the salt-induced upfield shifts observed, particularly in the case of $Mg^{++}$, is undoubtedly due to specific cation-binding. As mentioned earlier, the factors which contribute to the salt-induced $H_{1'}$ shifts are quite complex, the electric and magnetic properties of the uracil keto and the ribose 2'-OH groups being prominent factors in determining the $H_{1'}$ chemical shift. As we shall point out in the following section, the

salt-induced changes in glycosidic bond rotational angle in uridine and 5'-UMP are accompanied by a slight shift toward a 3'-endo ribose conformation and as a result the contributions of the 2'-keto and 2'-OH effect would be expected to partially compensate one another, so that the $H_1$, salt-induced shifts would be small. This is the generally observed case. The large salt-induced upfield shifts observed for the $Mg(ClO_4)_2$-5'-UMP system are somewhat surprising, but may reflect gross changes in the solvation of the ribose ether oxygen upon specific cation-phosphate binding in view of the close proximity of the negatively charged phosphate group to the ribose ether oxygen in this mononucleotide. In this connection, we note that the chemical shifts of the $H_1$, proton of 5'-UMP appears to be somewhat anomalous in that it is 0.08 ppm downfield from that of the $H_1$, proton of uridine (see Table I).

In summary, we may say that the only interpretable salt-induced shifts are those of the $H_6$ proton. These shifts may be divided into two parts: a part involving ion-binding to the phosphate, apparent only in 5'-UMP, and a near-linear part arising from a shift in distribution among base orientations about the glycosidic bond. In the presence of a "structure-breaking" salt, such as $NaClO_4$ or $Mg(ClO_4)_2$, the shift is toward conformations with more negative torsional angles in accordance with our original interpretation of the effect of the ribose-ring oxygen on $H_6$

chemical shift. The size of the shift varies somewhat from nucleoside to nucleotide, 5'-UMP showing the maximum response.

4.2.2. Nuclear Overhauser Implications

The results obtained by nuclear Overhauser experiments on solutions of 5'-UMP in the presence and absence of 2 M $NaClO_4$ can be shown to be consistent with the proposed shift in average glycosidic torsional angle. At 0.1 M 5'-UMP in the absence of added salt, for example, the NOEs on $H_6$ for $H_{2'}$ irradiation and $H_{5',5''}$ irradiation are 12.0 and 12.4%, respectively. This would indicate a nearly equal distribution among conformers which bring $H_6$ close to $H_{2'}$ and conformers which bring $H_6$ close to $H_{5'}$ or $H_{5''}$. Now when 2 M $NaClO_4$ is added, the NOE for $H_{5'}$ irradiation decreases to 6.8 while the NOE for $H_{2'}$ irradiation increases to 17.1%. This indicates an increased dipole-dipole interaction between the $H_6$ and $H_{2'}$ protons with a simultaneous decrease in the $H_6$-$H_{5',5''}$ interactions. There are two types of nucleotide conformation change which might bring about this effect. The first is the aforementioned shift to more negative torsional angles for the uracil base, and the second is a shift in the ribose conformational equilibrium. We tend to discount the latter possibility. Although a shift to the 2'-endo ribose conformation does tend to decrease the $H_6$-$H_{2'}$ distance, examination of a molecular model

shows this to be a minor perturbation compared to the change in base orientation. Furthermore, it is difficult to see how such a ribose conformational change could lead to a simultaneous decrease in the $H_{5',5''}$ interaction. Thus, the shift to more negative torsional angles in the presence of $NaClO_4$ seems to be the more likely implication of our nuclear Overhauser data. There are, however, several complications in the interpretation of NOE data which detract from the definity of these experiments.

First, the nature of the average conformation determined is slightly different from that determined in the chemical shift experiments. In the NOE experiment the quantity of primary importance is the expectation value of $\frac{1}{r^6}$ to which rotomers with the closest $H_2$, and $H_5$, approach contribute predominantly. This makes the meaning of an average rotational conformation somewhat tenuous, but qualitatively the increase in the population of rotomers with more negative torsional angles would seem correct. Second, NOE results depend to a certain extent on the intrinsic relaxation time for each proton ($W_{N'}$). Some effort was made to keep this invariant by excluding excess solvent protons and dissolved oxygen in both samples, but other factors vary inherently with the addition of $NaClO_4$. A change in solvent viscosity, for example, will affect natural relaxation mechanisms. This difficulty is overcome to a certain extent by our ability to monitor the NOE through two protons.

Viscosity effects, at least, should be comparable for both, and consideration of one effect relative to the other should eliminate much of the difficulty. But other factors (the residual sensitivity of $W_{N'}$ to molecular conformation changes, for example) remain a problem. And third, the results of the 0.3 M 5'-UMP seem at variance with the 0.1 M results. Although the effect of adding $NaClO_4$ again decreases the $H_{5',5''}$-$H_6$ effect and increases the $H_{2'}$-$H_6$ effect, the magnitudes are much reduced. This, however, we believe to be the result of the necessarily high 5'-UMP concentration. If one compares the 0.3 M 5'-UMP, 0 M $NaClO_4$ results to the results at 0.1 M 5'-UMP, it appears that the initial conformation at 0.3 M is at more negative torsional angles, even before the addition of salt. This is perhaps not unreasonable since at 0.3 M the 5'-UMP disodium salt could itself produce a significant salt effect. Thus, in spite of these difficulties we believe that the NOE results are valid and at least qualitatively confirm the interpretation of our chemical shift data.

### 4.2.3. Coupling Constant Implication

The changes in the $J_{H_{1'}\text{-}H_{2'}}$ coupling constant which occur concurrently with the chemical shift and NOE changes just described can be interpreted in terms of a change in average ribose conformation on the addition of salt. Most notably, the coupling constants for 5'-UMP and uridine

decrease markedly when $NaClO_4$ or $Mg(ClO_4)_2$ is added to the solution and decrease somewhat less when NaCl or TABCl is added. Following the lines of our discussion of the initial ribose conformation, these changes may be described as a shift in the equilibrium between 2'-endo and 3'-endo ribose conformations toward the 3'-endo side when in the presence of one of the perchlorate salts. The induced coupling constant changes for 3'-UMP and deoxyuridine are, however, negligible, indicating that the ribose conformations in these cases are either insensitive to the addition of salt or are rigidly held in their initial conformations.

The changes observed for 5'-UMP and uridine may not be wholly uncorrelated with the change in conformation about the glycosidic bond predicted on the basis of the chemical shift and nuclear Overhauser data. We note that the plots of change in coupling constant versus salt concentration are again linear and the relative effectiveness of each salt in producing the change, in general, follows the sequence established in the chemical shift experiments. In fact, as we pointed out in the results section, a plot of the changes in $|J_{H_{1'}-H_{2'}}|$ versus the observed salt-induced $H_6$ shifts is linear for both uridine and 5'-UMP.

As it turns out, there is some rationale for such a correlation. Examination of CPK molecular models for the pyrimidine nucleosides and nucleotides indicates that, while the base can assume a range of torsion angles near the

anti conformation, the range of torsion angles allowed depends upon the ribose conformation due to non-bonded interactions between the $H_6$ hydrogen of the base and various atoms on the ribose ring. When the ribose ring is in its 2'-endo conformation, the steric interaction between the $H_6$ and $H_{2'}$ hydrogens is particularly important, and the allowed torsion angles are limited to the range between $\sim -10^{\circ}$ and $\sim -60^{\circ}$. This non-bonded interaction is partially relieved, however, when the ribose ring is in its 3'-endo conformation, thus permitting the allowed range of torsion angles to be extended toward more negative values somewhat beyond $-90^{\circ}$. These ideas regarding the interrelationship between the allowed base conformations and the conformation of the ribose ring are in general agreement with the conclusions obtained by Haschemeyer and Rich on the basis of their analysis of hard sphere interactions in molecules having crystal structures exhibiting different ribose and glycosidic conformations.[15] They conclude that the 3'-endo ribose conformation has an allowed rare contact region for glycosidic bond rotomers of the anti range that extends to slightly more negative torsional angles. We should point out that agreement on this point is not universal. Lakshminarayanan and Sasisekharan, for example, contend that there is little difference in ribose-base interactions for 3'-endo and 2'-endo forms of the same torsional angle, $\phi_{CN}$.[58] But in view of the very high energy of steric

interaction on which all agree, we feel that the possibility of a glycosidic rotomer to ribose conformer correlation cannot be ignored, especially in view of the experimental correlations of the coupling constant and chemical shift data noted here. Thus, any perturbation which affects the average rotational conformation of the base may induce a conformational change in the ribose ring. The direction and the extent of the induced conformational changes will, of course, depend upon the nature of the non-bonded interactions and the rigidity of the furanose ring toward changes in the out-of-plane ring deformation. For example, in the case where two furanose ring conformations are in equilibrium, it is clear that changes in the non-bonded interactions between the base and the furanose residue can influence the relative stability of the two conformations, with the average ring conformation shifted toward the limit, stabilized by the non-bonded interaction. In uridine and 5'-UMP, the observed ribose conformational changes toward the 3'-<u>endo</u> direction are, therefore, not contrary to expectation, since on the basis of the salt-induced shifts of the uracil $H_6$ resonance, we have surmised that the addition of salt induces a change in the rotational conformation of the base toward more negative $\phi_{CN}$'s.

The difference in slopes for the $\Delta J$ versus $\Delta\sigma$ plots of 5'-UMP and uridine could be the result of either a change in the flexibility of the ribose ring or a change in the

sensitivity of one of the measured parameters to a conformation change. Since the ribose ring structures of 5'-UMP and uridine are identical, their rigidity is expected to be quite similar and the smaller slope for the 5'-UMP plot is probably a result of the greater sensitivity of chemical shift to rotational isomerization because of the proximate negatively charged phosphate group. In 3'-UMP, however, the situation is quite the opposite. Here no salt-induced ribose conformation change was observed, even though a sizeable salt-induced shift was observed for the uracil $H_6$ resonance of this molecule (0.065 ppm in the presence of 0.6 m $Mg(ClO_4)_2$). This result probably reflects the increased rigidity of the ribose ring when the 3'-OH group is substituted with the bulkier phosphate group. No noticeable change in the average $H_{1'}$-$H_{2'}$($H_{2''}$) coupling constant was detected in the case of deoxyuridine. However, the salt-induced shifts observed for the $H_6$ resonances are also quite small. The value of the average $H_{1'}$-$H_{2'}$($H_{2''}$) coupling constant indicates that the conformation of the deoxyribose ring is close to 2'-endo, and it may be that removal of the 2'-OH group significantly stabilizes the 2'-endo conformation in deoxyuridine.

In summary then, the addition of a salt such as $Mg(ClO_4)_2$ or $NaClO_4$ appears to induce a linear shift in average nucleotide conformation which involves a rotation of the base about the glycosidic bond to more negative

torsional angles and, in some cases, a shift in population of ribose conformers toward the 3'-endo side. The two conformation changes may be correlated, the ribose change being a result of the base conformation change, with the extent of ribose change depending on the rigidity of the ring and the initial population of the various ribose conformers.

## 4.3. A Possible Origin of the Salt Effect

Despite our ability to fairly accurately describe the nucleotide conformation changes induced by these various salts, the mechanism whereby they act remains open to conjecture. We would, however, like to explore one possible mechanism in detail: that of a salt-induced variation in hydrophobic forces. This mechanism is suggested by the fact that irrespective of the nucleoside or nucleotide molecule, the various salts investigated possess the same relative effectiveness in inducing the $H_6$ shifts ( $Mg(ClO_4)_2$ > $NaClO_4$ > NaCl > NaOAc, TMACl > TBACl). Variations in the magnitude of the effects observed for the four nucleoside and nucleotide molecules studied might be accounted for on the basis of minor differences in the local solvent structure about these molecules and/or small differences in the non-bonded interactions opposing the conformational change. The relative effectiveness of the various salts does not appear to correlate with the specific cation or anion present in the solution or with the solution ionic strength.

But there appears to be a rough correlation with the solvent "structure-breaking" and "-making" properties of the salts ( $Mg(ClO_4)_2$ > $NaClO_4$ > NaOAc > TMACl > TBACl).[35,40] These considerations suggest the possibility that the salts act indirectly through their effect on the water structure in influencing the rotational conformation of the uracil base about the glycosidic bond. In other words, hydrophobic forces may be involved.

4.3.1. Qualitative Aspects of Hydrophobic Factors

Several authors have attempted to put forth an esoteric description of the forces which underlie hydrophobic bonding. Basically they portray the hydrophobic bond as arising from a large negative entropy associated with exposing a non-polar surface area to an aqueous solvent. Water molecules at this surface self-associate extensively, forming local regions of ice-like structure which greatly reduce the entropy of the system. The minimization of exposed non-polar surface area is thus a principal criterion of a hydrophobically stable conformation. The addition of salts to an aqueous solution can influence the extent of hydrophobic bonding in such a system. They act by increasing or decreasing the extent of solvent structure in the bulk solvent relative to that near the hydrophobic surface. Since the net entropy change on exposure of the hydrophobic surface is the important thermodynamic quantity, the

addition of a "structure-breaking" salt can increase or decrease hydrophobic bonding depending on whether its effect on surface or bulk water structure is greater. If, as is usually the case, its effect on bulk water structure is greater it will increase the net entropy change on exposure of a hydrophobic surface and thus shift a thermodynamic equilibrium involving this change toward the state with small surface area.

Quantitative calculations of the contribution of hydrophobic bonding to conformational equilibria have been approached along two independent lines of reasoning. The first, exploited by Némethy and Scheraga, employs a statistical-mechanical evaluation of the aqueous states of various hydrophobically bonded moieties from which the appropriate thermodynamic quantities are derived.[59] In essence, the exposure of a non-polar surface to its local aqueous environment preferentially lowers the energy of a structured water molecule relative to that of a labile water molecule by van der Waals interactions with the solute. The result is an increase in the population of the structured state. Since the number of these interactions depends on the number of geometrically allowed water-solute interactions, the total structuring depends on the area of the hydrophobic surface. Partition functions are estimated for the water in the structured and unstructured states, as well as for the solute molecule itself. From these a free energy

change is calculated.

The alternate system for treating hydrophobic forces, and aqueous molecular associations in general, is the more empirical method proposed by Sinanoğlu.[60] He views the free energy change in bringing a hydrophobic residue from a gaseous environment to an aqueous one as arising from two terms: a cavity term expressing the energy required to open a hole of appropriate dimension to encapsulate the residue, and an interaction term arising from electrostatic and van der Waals forces between the residue and its new environment. Entropy corrections for changes in free volume are, of course, also included. Each of these terms is related to physically measurable quantities. The cavity term is related to the macroscopic surface energy or surface tension of the solvent, as well as the surface area of the cavity, and the interaction term can be expressed in terms of molecular polarizabilities, dipole moments and solvent dielectric constants.

### 4.3.2. Calculation of Hydrophobic Factors

We have chosen to apply Sinanoğlu's theory to our data simply because the effects of adding various salts to an aqueous solution are more easily expressed in terms of changes in solvent dielectric and solvent surface tension, than in terms of a change in the partition function of the system. The response to these solvent changes, a variation

in molecular surface area, could be equally well interpreted on the basis of either model.

In its final form, Sinanoğlu's equation for the free energy of solvation can be expressed as:[60]

$$-\Delta F_A^o \approx a + b\frac{\mu_A^2}{v_A} - cv_A^{2/3}\gamma_1 - RT\ln\frac{kT}{v_1} + \ldots , \qquad (12)$$

where $\gamma_1$ is the surface tension of solvent "1", $v_1$ is the molecular volume of the solvent, $\mu_A$ is the dipole moment of solute "A", and $v_A$ is its molecular volume. Sinanoğlu considers "a", "b" and "c" all to be physical "constants" for a variety of solutes and solvents, but here we shall consider each explicitly. The "a" term is a measure of the van der Waals interaction and depends on factors which should be largely independent of the solvent changes considered here. Moreover, according to equation (12), the free energies of molecular states, differing only in conformation, vary uniformly with changes in "a" and this term need not be considered in our discussion. The same can be said of the fourth term in the equation. The "b" term arises principally from an electrostatic interaction of the solute dipole with a reaction field induced in the surrounding solvent. For solute molecules of large molecular volume, proteins for example, it need not be considered, since its $\frac{1}{v_A}$ dependence is quickly overcome by the $v_A^{2/3}$ dependence of the "c" term. But for these relatively small

nucleotide and nucleoside molecules it cannot be disregarded. The following expression for the "b" coefficient can be extracted from Sinanoğlu's paper:

$$b = \frac{2}{3}\pi \frac{D_s'}{1 - D_s'\left(\frac{\alpha_A}{v_A}\right)\frac{4}{3}\pi} , \qquad (13)$$

where $D_s'$ is the reaction field in a dielectric medium, $\frac{2(\epsilon_s-1)}{(2\epsilon_s+1)}$. For an aqueous solution in the absence of any salt, $b \simeq 0.654$. Replacing the dielectric reaction field with an expression modified to take account of the presence of an electrolyte, "b'" can be calculated. For a 1 M 1:1 electrolyte solution in water $b' \simeq 0.616$.

The third term, or "c" term, is a measure of the surface free energy of a cavity of the size required to hold a nucleoside. In the case where curvature effects can be neglected, as in the comparison of two conformations of reasonably large volume, this should be simply the product of the surface area and the solvent surface tension. In equation (12) Sinanoğlu has assumed all molecules to be approximately spherical so that c becomes the proportionality constant between the area of a sphere and its volume to the 2/3 power or 4.84. This constant should be independent of our salt-induced solvent changes. The surface tension factor of the third term, however, will not necessarily be insensitive to these changes. Upon the addition of 1 M NaCl, for example, $\gamma$ changes by 1.5 gr $sec^{-2}$.(61)

We can now compare the magnitude of the change in the electrostatic and cavity terms for a molecule such as uridine on the addition of 1 M NaCl. The dipole moment of uridine is dominated by that of the uracil ring, 3.9 debeyes, and the molecular volume, $v_A$, is of the order of 500 $\mathring{A}^3$. Therefore, the electrostatic term can be calculated to be $0.1 \times 10^{-14}$ ergs. Similarly, employing our estimate of "c", the change in surface tension for a 1 M NaCl solution and $v_A^{2/3} = 63$, the cavity term, is estimated to be $4.5 \times 10^{-14}$ ergs. It is apparent that, although the energy is dominated by the cavity term, both are important factors in producing molecular conformation changes. The electrostatic term, however, depends principally on the ionic strength of the solution and should be more or less independent of type of salt for equal concentrations of 1:1 electrolyte. The cavity term, on the other hand, will vary with the nature of the salt. The effect on aqueous solution surface tension for various electrolytes follows the classical lyotropic or Hofmeister series, which is in close agreement with the relative effectiveness of the salts studied here in inducing a uridine conformation change.(61) Thus for the present study, the cavity term would seem the more important consideration. The magnitude of the free energy change on the addition of salt, $5 \times 10^{-14}$ ergs, we note, is of a magnitude comparable to kT and should be sufficient to produce a perturbation in a uridine conformational equilibrium providing

the various conformers differ in surface area by more than a few percent. We also note that, since the addition of a "structure-breaking" salt increases the surface tension, the equilibrium is expected to shift to the conformer with the smaller surface area.

It is therefore obvious that the next consideration should be that of the surface area of various uridine conformers. In Sinanoğlu's equation this surface area was correlated with a molecular volume on the assumption that all molecules are approximately spherical. Although adequate for large globular proteins, this assumption is poorly suited to the smaller uridine nucleotides and nucleosides, and we have resorted to a less restrictive evaluation. Qualitatively, an examination of a CPK molecular model reveals the fact that a change from small negative glycosidic torsional angles to large ones tends to fill a hydrophobic pocket on the surface of the ribose moiety and thus reduce the exposed non-polar surface area. For a quantitative estimate of this change, however, a more elaborate technique must be employed.

The mathematical procedure used to calculate the molecular surface area is explained in detail in Appendix I, but, briefly, it may be described as follows: the molecule in question is depicted as a set of Cartesian coordinates representing the positions of its constituent atoms. A sphere of appropriate size to represent the distance to

which a solvent molecule may approach these atomic centers is moved toward the solute molecule until it contacts the first solute atom. A point midway between the center of the test sphere and the atom is then taken as a surface point for the molecule. The locus of points determined in this manner is assumed to represent the surface of the molecule as seen by the solvent, and the area of this surface is used in conjunction with Sinanoğlu's theory to calculate solvent effects. The calculation of molecular surface area was performed for uridine in 2'-endo and 3'-endo conformations taken from typical uracil nucleosides and nucleotides of these structures.[62,63] The atomic coordinates were also manipulated mathematically to produce molecules of varying glycosidic torsional angles with the results shown in Figure 15.

There are actually two variable parameters in this treatment which warrant further discussion. First, the radius of the test sphere should represent the effective size of a water molecule at a hydrophobic surface. The sphere used (radius = 2.76 Å), although somewhat larger than the sum of the van der Waals atomic radii for uridine and water, is perhaps too small. It is rather important that the surface water molecules be hydrogen bonded to a reasonable number of its neighboring water molecules. This somewhat restricts the size of the surface cavity into which it can actually fit. Unfortunately, no rational method exists

FIGURE 15

Calculated molecular surface area as a function of nucleotide conformation.

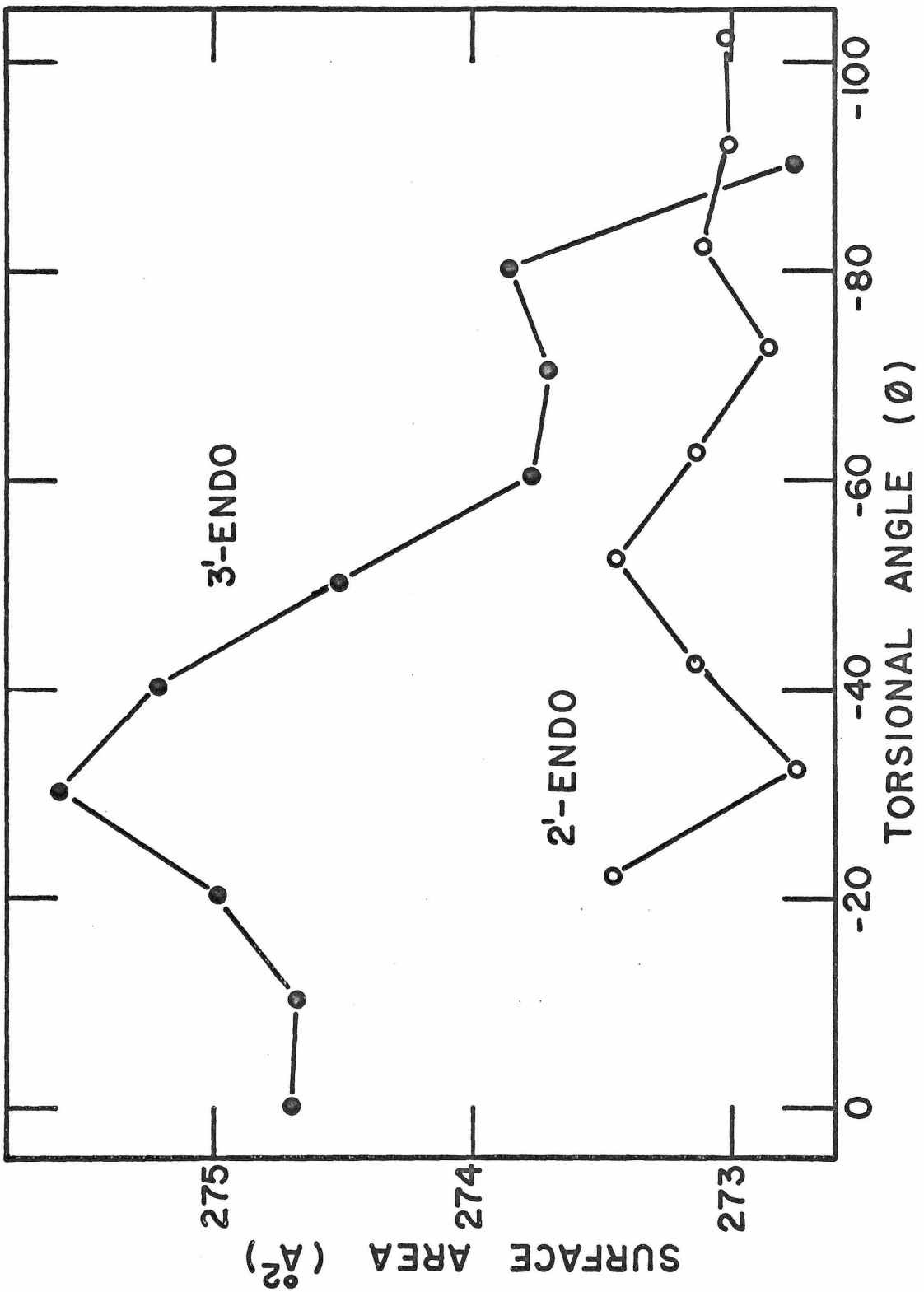
SURFACE AREA (Å²)
275
274
273
0
-20
-40
-60
-80
-100
TORSIONAL ANGLE (Ø)
3'-ENDO
2'-ENDO

for the accurate estimation of such an effective radius. Second, it is apparent that we should only consider the hydrophobic parts of uridine as contributing to the non-polar surface area, since highly polar groups may fit into the water structure rather well. This distinction between hydrophobic and hydrophilic groups is again somewhat arbitrary. In the calculations presented here, the exchangable protons, the hydroxy oxygens of the ribose and the keto oxygens of the uracil were not considered a part of the hydrophobic area.

In spite of the crudity of this calculation, the results give some qualitative insight into a possible response of the uridine molecule to the addition of structure-perturbing salts. First, over most torsional angles of the glycosidic bond the 2'-endo conformation has a lower surface area than the corresponding 3'-endo conformer. Thus, our observed 2'-endo to 3'-endo shift on the addition of a "structure-breaking" salt is contrary to what one might have predicted on the basis of a minimization of molecular surface area. The surface area dependence on glycosidic bond torsional angle, especially that of the 3'-endo conformer, is, however, more promising. This shows a substantial, although still not large, decrease in the surface area in moving to more negative torsional angles. This is consistent with our observations and our expectations on the basis of Sinanoğlu's theory. In view of the fact that only a

change in glycosidic bond angle appears to be a logical response to the addition of these salts, the calculations add credence to our suspicion that a change in average glycosidic bond angle is the primary response, while the change in ribose conformation is the result of the strong coupling between the two types of structural change by steric interaction. And, although contributions of other forces such as those of electrostatic nature cannot be ruled out, the calculations do hint at a possible role of hydrophobic bonding in determining uracil nucleoside conformation. As for the method itself, the results show promise for the calculation of hydrophobic forces in larger, less polar molecules.

# 5. CONCLUSION

In conclusion, the results of this work indicate that electrolytes can have important effects on the conformation of nucleosides and nucleotides.[64] The implications of these findings to the conformational properties of dinucleotides, oligonucleotides, and to polynucleotide structure, however, remain to be ascertained, since the vertical base-stacking interactions presumably also play an important role in stabilizing the base orientations and the conformations of each furanose residue in these molecules. Some important lessons can nevertheless be gained from the research presented here. The first is that common electrolytes are not neutral agents, and their effects, hydrophobic, as well as electrostatic, must be considered when they are employed in any study of a biological macromolecule. Recently, there has been some controversy over the nature of the intramolecular base-stacking interaction in several pyrimidine-pyrimidine dinucleotides.[1,2,41] However, in these works, the molecules were examined under quite different experimental conditions of added electrolytes and ionic strengths. The observed discrepancies are therefore probably real, rather than experimental artifacts, and may well reflect the effects of solvent structure on both the vertical stacking interaction and the conformational properties of the individual nucleotide units, as demonstrated in this work.

This is especially true since the intramolecular stacking interaction is generally considered to be weak in the pyrimidine-pyrimidine dinucleotides, and subtle differences in the conformational properties of the nucleotide units might be expected to have a very profound influence on the overall conformation of the molecule. The second point to be gained from the present study is that ribose and glycosidic bond conformation is an important aspect in the structure of a nucleotide which may change in response to its local environment, even in the absences of base-stacking forces. In this case the response to the addition of a "structure-breaking" salt has been one of an increased negative glycosidic torsional angle and a concomitant shift to a higher population of the 3'-endo ribose conformer. The exact nature of the correlation between observed changes in ribose conformation and changes in base orientation about the glycosidic bond will require further investigation. However, temperature dependence studies of dinucleotides which display a similar correlation promise to provide additional insight into the problem, and pH studies of purine mononucleotides now under way should further elucidate the nature of the base-ribose interaction.[65] The significance of these facts in relation to the conformational states of the natural polynucleotides, DNA and RNA, of course remains a point for speculation and further study.

# APPENDIX I

## Program SUF2

### General Description

It has become necessary in the course of this work to estimate the surface area of a molecule as it is seen by its surrounding solvent. Previous methods of estimating surface area have assumed a simple geometric molecular shape so that surface area could easily be related to a measured or calculated molecular volume.[60,65] The assumption, no doubt, is reasonable in the case of a globular macromolecule, but for the comparison of the surface areas of small molecules, such as mononucleotides, differing only slightly in their conformation, the imposition of a fixed molecular geometry seems an undue restraint. To lift this restriction program SUF2 was written and used in conjunction with an IBM 360/75 computer system to calculate molecular surface areas.

The program has as its basic tenet the assumption that any cavity on the surface of a molecule with dimensions large enough to accomodate a solvent molecule should be considered a part of the solute molecular surface. The various parts of the program are then designed to manipulate the molecular geometry, to establish a locus of surface points describing the surface for each conformation, and to calculate from this locus of points a molecular surface area.

In the first part of the program the Cartesian coordinates of a molecule are read into the system, and the set of points is translated so that the first point entered becomes the origin of the coordinate system. In each succeeding run the points undergo a rotational transformation which corresponds to rotating the molecule about a given single bond by a specified angular increment, producing, in effect, a molecule of a different geometry.

In the second part of the program, a sphere whose radius represents the sum of an average van der Waals radius of a solute atom and an effective radius of a solvent molecule are used as a test sphere to determine the effective surface of the molecule.[67] The van der Waals radius of the solute atom is included as a part of the test sphere, rather than as a sphere about each fixed atomic center, as a matter of convenience in calculation. This complex test sphere is moved along a radial line either toward the origin until the first atom of the solute is contacted or away from the origin until all solute atoms are outside the boundaries of the test sphere. The true surface of the solute molecule is then re-established by picking the surface point to be an appropriate fraction of the distance between the test sphere center and the point of atomic center-test sphere contact. Having established one point, the test sphere is moved a specified angular increment in either $\phi$ or $\theta$ directions, and the process repeated until a uniform distribution of surface

points has been established.

In the last part of the program, the surface points are connected to form a continuous surface of triangles whose areas can easily be calculated and summed to give as output the surface area of a molecule with variable molecular conformation.

The program, as it stands, has a few shortcomings which should be noted. First, the surface area is somewhat underestimated by the fact that the test sphere is forced to move along radial lines. In cases where the surface is convoluted inward, the program will tend to approximate the surface area of the cavities with radially directed cones. The effects of this approximation, however, can be partially eliminated by repeating the calculation with the coordinates of a number of different solute atoms chosen as origin. The second shortcoming lies in the fact that the method of establishing surface points in a few cases leads to discontinuities in the distribution of surface points, even in the limit of extremely small angular incrementation of the radial test lines. These discontinuities occur when the point of contact between solute and test sphere suddenly shifts from one atomic center to another in the course of incrementation of the radial test line. Both of these defects are unavoidable with the present scheme of calculation, but both contribute insignificantly to the error in calculated surface area for solute molecules of sufficient size.

## Listing of Program SUF2

```
FORTRAN IV G LEVEL 1, MOD 4            MAIN              DATE =     5/23/70      15:00:36

      C     PROGRAM TO ROTATE MOLECULAR COORDINATES ABOUT A GIVEN BOND
      C     NP AND NQ INDICATE THE ROTATABLE BOND AXIS
      C     N IS THE TOTAL NUMBER OF POINTS,N<40
      C     Y(I,K) ARE THE COORDINATES OF THE ATOMS, K, K<,=N
      C     RMIN AND RMAX ARE THE INITIAL AND FINAL VALUES FOR ROTATION
      C     C     M IS THE NUMBER OF ROTATION INTERVALS TO BE CONSIDERED
      C     ALL ANGLES MUST BE GIVEN IN RADIANS
0001        DIMENSION Y(3,40),X(3,40),W(3,40),V(3,40,10),RMAT(3,3),O(10),
           1Z(3,40),DIST(40),S(3),SUF(3,50,100),A(3),B(3),AA(3),BB(3),
           1AREAT(10)
0002        READ(5,5) NP,NQ,N
0003        READ(5,15) RMIN,RMAX,MI
0004        READ(5,6) L,N,JJ,DELR,ERR,START
0005        READ(5,16) RTEST,P
0006        READ(5,25) (Y(1,K),Y(2,K),Y(3,K),K=1,N)
      C     TRANSLATE ORIGIN TO POINT P
0007        DO 10 K=NP,N
0008        DO 10 I=1,3
0009     10 X(I,K)=Y(I,K)-Y(I,NP)
      C     CALCULATE SIN, COS VALUES FOR ROTATION MATRIX
0010        DISZ=SQRT(X(1,NQ)**2+X(2,NQ)**2)
0011        IF(DISZ) 9,8,9
0012     8  COSP=1.0
0013        SINP=0.0
0014        GO TO 7
0015     9  COSP=-X(2,NQ)/DISZ
0016        SINP=X(1,NQ)/DISZ
0017     7  DISX=SQRT(X(1,NQ)**2+X(2,NQ)**2+X(3,NQ)**2)
0018        COSQ=X(3,NQ)/DISX
0019        SINQ=DISZ/DISX
      C     GENERATE VALUES OF SINO, COSO
0020        O(1)=RMIN
0021        RINC=(RMAX-RMIN)/MI
0022        MM=MI+1
0023        DO 20 INC=1,MM
0024        COSO=COS(O(INC))
0025        SINO=SIN(O(INC))
      C     ASSIGN VALUES OF RMAT
0026        RMAT(1,1)=COSO*COSP**2+COSO*(COSQ**2)*SINP**2+(SINQ**2)*SINP**2
0027        RMAT(1,2)=SINO*COSQ+COSP*COSO*SINP-COSO*SINP*COSP*COSQ**2-COSP*
           1SINP*SINQ**2
0028        RMAT(1,3)=COSP*SINO*SINQ-COSQ*SINP*COSO*SINQ+SINQ*SINP*COSQ
0029        RMAT(2,1)=-SINO*COSQ+COSP*COSO*SINP*SINQ**2-COSP*SINQ*SINQ*SINP
0030        RMAT(2,2)=COSO*SINP**2+COSO*(COSQ**2)*COSP**2+SINQ*SINQ*COSP**2
0031        RMAT(2,3)=SINP*SINO*SINQ+COSO*COSQ*SINQ*COSP-COSP*COSQ*SINQ
0032        RMAT(3,1)=-SINQ*COSP*SINO-SINQ*COSO*COSQ*SINP+COSQ*SINQ*SINP
0033        RMAT(3,2)=-SINQ*SINO*SINP+SINQ*COSO*COSQ*COSP-COSQ*COSP*SINQ
0034        RMAT(3,3)=COSO*SINQ**2+COSQ**2
      C     OPERATE RMAT ON X(I,J)
0035        DO 30 K=NQ,N
0036        DO 30 I=1,3
0037     30 W(I,K)=RMAT(I,1)*X(1,K)+RMAT(I,2)*X(2,K)+RMAT(I,3)*X(3,K)
      C     TRANSLATION TO ORIGINAL COORDINATE SYSTEM
0038        DO 11 K=NQ,N
0039        DO 11 I=1,3
0040     11 V(I,K,INC)=W(I,K)+V(I,NP)
```

```
0041                DO 12 K=1,NP
0042                DO 12 I=1,3
0043                W(I,K)=Y(I,K)-Y(I,NP)
0044             12 V(I,K,INC)=Y(I,K)
                 C  PROGRAM TO CALCULATE THE SURFACE AREA OF A MOLECULE
                 C  A TEST SPHERE OF RADIUS RTEST IS MOVED RADIALLY IN INCREMENTS OF
                 C    DELR FROM START UNTIL IT IS WITHIN ERR OF THE NEAREST ATOM
                 C  JJ*JJ/2 SUCH POINTS ARE FOUND
                 C  P IS THE FRACTION OF RTEST WHICH APPROXIMATES THE VAN DER WAALS
                 C    RADIUS OF THE SOLVENT - THE SURFACE POINTS ARE PLACED AT THIS
                 C    DISTANCE
                 C  THESE POINTS FORM A CONTINUUM OF TRIANGLES WHICH ARE USED TO
                 C    CALCULATE THE SURFACE AREA
                 C  DELR MUST BE LESS THAN ERR
                 C  DETERMINATION OF SURFACE POINTS
0045                DO 19 M=1,3
0046                DO 19 K=1,N
0047             19 Z(M,K)=W(M,K)
0048                DELA = 2*3.1416/JJ
0049                II=(JJ/2)+1
0050                DT=1000.0
0051                D=START
0052                DO 61 I=1,II
0053                DO 71 J=1,JJ
0054                FJ=J-1
0055                FI=I-1
0056                S(1)=D*SIN(FI*DELA)*COS(FJ*DELA)
0057                S(2)=D*SIN(FI*DELA)*SIN(FJ*DELA)
0058                S(3)=D*COS(FI*DELA)
0059             74 CONTINUE
0060                DO 13 K=1,N
0061             13 DIST(K)=SQRT((Z(1,K)-S(1))**2+(Z(2,K)-S(2))**2+(Z(3,K)-S(3))**2)
0062                CALL MAXMIN (DIST, N, DMX, DMN)
0063                DO 60 K=1,N
0064                IF(DIST(K)-DMN) 60,70,60
0065             70 KK=K
0066             60 CONTINUE
0067             80 CONTINUE
0068                IF(ABS(DMN-RTEST)-ERR) 23,23,29
0069             29 IF(DMN-RTEST) 40,40,50
0070             50 D=SQRT(S(1)**2+S(2)**2+S(3)**2)
0071                S(1)=S(1)-DELR*S(1)/D
0072                S(2)=S(2)-DELR*S(2)/D
0073                S(3)=S(3)-DELR*S(3)/D
0074                DMN=SQRT((S(1)-Z(1,KK))**2+(S(2)-Z(2,KK))**2+(S(3)-Z(3,KK))**2)
0075                IF(DMN-DT) 72,72,73
0076             72 DT=DMN
0077                GO TO 80
0078             73 DT=DMN
0079                GO TO 74
0080             23 CONTINUE
0081                DO 90 K=1,N
0082             90 DIST(K)=SQRT((Z(1,K)-S(1))**2+(Z(2,K)-S(2))**2+(Z(3,K)-S(3))**2)
0083                CALL MAXMIN (DIST,N,DMX,DMN)
0084                DO 21 K=1,N
0085                IF(DIST(K)-DMN) 21,31,21
```

```
0086          31 KK=K
0087          21 CONTINUE
0088             IF(ABS(DMN-RTEST)-ERR) 41,41,40
0089          40 D=SQRT(S(1)**2+S(2)**2+S(3)**2)
0090             S(1)=S(1)+DELR*S(1)/D
0091             S(2)=S(2)+DELR*S(2)/D
0092             S(3)=S(3)+DELR*S(3)/D
0093             DMN=SQRT((S(1)-Z(1,KK))**2+(S(2)-Z(2,KK))**2+(S(3)-Z(3,KK))**2)
0094             IF(ABS(DMN-RTEST)-ERR) 23,23,40
0095          41 SUF(1,I,J)=((1-P)*S(1)+P*Z(1,KK))
0096             SUF(2,I,J)=((1-P)*S(2)+P*Z(2,KK))
0097             SUF(3,I,J)=((1-P)*S(3)+P*Z(3,KK))
0098          71 D=SQRT(S(1)**2+S(2)**2+S(3)**2)
0099          61 CONTINUE
            C    CALCULATION OF SURFACE AREA
0100             DO 14 I=1,II
0101             DO 14 M=1,3
0102          14 SUF(M,I,JJ+1)=SUF(M,I,1)
0103             III=II-1
0104             AREAT(INC)=0.0
0105             DO 22 I=1,III
0106             DO 22 J=1,JJ
0107             DO 32 M=1,3
0108             A(M)=SUF(M,I+1,J)-SUF(M,I,J)
0109             B(M)=SUF(M,I,J+1)-SUF(M,I,J)
0110             AA(M)=SUF(M,I+1,J+1)-SUF(M,I,J+1)
0111          32 BB(M)=SUF(M,I+1,J+1)-SUF(M,I+1,J)
0112             AREAA=SQRT((A(2)*B(3)-A(3)*B(2))**2+(A(3)*B(1)-A(1)*B(3))**2+
                1(A(1)*B(2)-A(2)*B(1))**2)
0113             AREAB=SQRT((AA(2)*BB(3)-AA(3)*BB(2))**2+(AA(3)*BB(1)-AA(1)*BB(3))
                1**2+(AA(1)*BB(2)-AA(2)*BB(1))**2)
0114             AREA=(AREAA+AREAB)/2
0115          22 AREAT(INC)=AREAT(INC)+AREA
0116          20 O(INC+1)=O(INC)+RINC
            C    OUTPUT
0117             WRITE(6,86) RTEST
0118             WRITE(6,95) P
0119             WRITE(6,96) ERR
0120          93 DO 91 INC=1,MM
0121             WRITE(6,75) O(INC)
0122             WRITE(6,76) AREAT(INC)
0123             WRITE(6,45)
0124          91 WRITE (6,85)(K,V(1,K,INC),V(2,K,INC),V(3,K,INC),K=1,N)
0125           5 FORMAT(3I5)
0126          15 FORMAT(2F5.3,I5)
0127          25 FORMAT(3F10.5)
0128          35 FORMAT(3I5)
0129          45 FORMAT(49H FOR  K =     Z(1)=          Z(2)=          Z(3)=)
0130          55 FORMAT(37HTHE DISTANCE FROM    I   TO    J    =)
0131          65 FORMAT(19X15,5X15,5XF10.5)
0132          75 FORMAT(/18HFOR O IN RADIANS =F6.3)
0133          85 FORMAT(9X15,5XF10.5,5XF10.5,5XF10.5)
0134          96 FORMAT(22H   THE ERROR LIMIT IS F10.5)
0135          95 FORMAT(43H   THE FRACTION DUE TO THE ATOMIC RADII IS F10.5)
0136          86 FORMAT(/30H   THE TEST SPHERE HAS RADIUS F10.5)
0137          76 FORMAT(/24H   THE SURFACE AREA IS  F10.5)
0138          16 FORMAT(2F10.5)
0139           6 FORMAT(3I5,3F10.5)
0140             STOP
0141             END
```

REFERENCES

1. J. Brahms, J. C. Maurizot, A. M. Michelson, J. Mol. Biol., 25, 481 (1967).

2. M. M. Warshaw, I. Tinoco, Jr., J. Mol. Biol., 20, 29 (1966).

3. R. C. Davis, I. Tinoco, Jr., Biopolymers, 6, 223 (1968).

4. R. M. Epand, H. A. Scheraga, J. Am. Chem. Soc., 89, 3888 (1967).

5. F. E. Hruska, S. S. Danyluk, Biochim. Biophys. Acta, 157, 238 (1968).

6. S. I. Chan, J. H. Nelson, J. Am. Chem. Soc., 91, 168 (1969).

7. B. W. Bangerter, S. I. Chan, J. Am. Chem. Soc., 91, 3910 (1969).

8. P. O. P. Ts'o, N. S. Kondo, M. P. Schweizer, D. P. Hollis, Biochemistry, 8, 997 (1969).

9. P. A. Hart, J. P. Davis, J. Am. Chem. Soc., 91, 512 (1969).

10. C-Y. Lee, private communication.

11. F. E. Hruska, S. S. Danyluk, J. Am. Chem. Soc., 90, 3266 (1968).

12. J. T. Yang, T. Samejima, in "Progress in Nucleic Acid Research and Molecular Biology," J. N. Davidson and W. E. Cohn, eds., Academic Press, New York, 1969, p273.

13. S. Arnott, W. Fuller, A. Hodgson, I. Prutton, Nature, 220, 561 (1968).

14. F. H. C. Crick, J. Mol. Biol., 19, 548 (1966).

15. A. E. V. Haschemeyer, A. Rich, J. Mol. Biol., 27, 369 (1967).

16. M. Sundaralingam, Biopolymers, 7, 821 (1969).

17. A. V. Lakshminarayanan, V. Sasisekharan, Biopolymers, 8, 475 (1969).

18. D. W. Miles, M. J. Robins, R. K. Robins, M. W. Winkley, H. Eyring, J. Am. Chem. Soc., 91, 831 (1969).

19. M. P. Schweizer, A. D. Broom, P. O. P. Ts'o, D. P. Hollis, J. Am. Chem. Soc., 90, 1042 (1968).

20. J. Brahms, J. C. Maurizot, A. M. Michelson, J. Mol. Biol., 25, 465 (1967).

21. A. J. Adler, L. Grossman, G. P. Fasman, Biochemistry, 7, 3836 (1968).

22. S. S. Danyluk, F. E. Hruska, Biochemistry, 7, 1038 (1968).

23. A. J. Adler, L. Grossman, G. P. Fasman, Biochemistry, 8, 3846 (1969).

24. B. Zmudzka, C. Janion, D. Shugar, Biochem. Biophys. Res. Commun., 37, 895 (1969).

25. A. M. Bobst, F. Rottman, P. A. Cerutti, J. Am. Chem. Soc., 91, 4603 (1969).

26. W. F. Dove, N. Davidson, J. Mol. Biol., 5, 467 (1962).

27. K. Hamaguchi, E. P. Geiduschek, J. Am. Chem. Soc., 84, 1329 (1962).

28. D. W. Gruenwedel, Chi-Hsia Hso, Biopolymers, 7, 557 (1969).

29. J. Donohue, K. N. Trueblood, J. Mol. Biol., 2, 363 (1960).

30. F. E. Hruska, A. A. Grey, I. C. P. Smith, J. Am. Chem. Soc., 92, 214 (1970).

31. B. J. Blackburn, A. A. Grey, I. C. P. Smith, F. E. Hruska, Can. J. Chem., in press.

32. C. D. Jardetzky, J. Am. Chem. Soc., 82, 229 (1960).

33. M. Smith, C. D. Jardetzky, J. Mol. Spectry., 28, 70 (1968).

34. P. A. Hart, J. P. Davis, Biochem. Biophys. Res. Commun., 34, 733 (1969).

35. P. H. von Hippel, K.-Y. Wong, J. Biol. Chem., 240, 3909 (1965).

36. H. Inoue, S. N. Timasheff, J. Am. Chem. Soc., 90, 1890 (1968).

37. J. F. Brandts, L. Hunt, J. Am. Chem. Soc., 89, 4826 (1967).

38. G. G. Hammes, J. C. Swann, Biochemistry, 6, 1591 (1967).

39. T. T. Herskovits, H. Jaillet, Science, 163, 283 (1969).

40. J. D. Worley, I. M. Klotz, J. Chem. Phys., 45, 2868 (1966).

41. H. Simpkins, E. G. Richards, J. Mol. Biol., 29, 349 (1967).

42. R. Lumry, E. L. Smith, R. R. Glantz, J. Am. Chem. Soc., 73, 4335 (1951).

43. C. D. Jardetzky, O. Jardetzky, J. Am. Chem. Soc., 82, 222 (1960).

44. C. D. Jardetzky, J. Am. Chem. Soc., 83, 2919 (1961).

45. A. D. Buckingham, Can. J. Chem., 38, 300 (1960).

46. R. F. Zürcher, in "Progress in Nuclear Magnetic Resonance Spectroscopy," Vol. 2, J. W. Emsley, J. Feeney, L. H. Sutcliffe, eds., Pergamon Press, Oxford, 1967, p. 205.

47. A. Carrington, A. D. McLachlan, in "Introduction to Magnetic Resonance," Harper and Row, New York, 1967, p. 232.

48. M. Karplus, J. Chem. Phys., 30, 11 (1959).

49. R. J. Abraham, L. D. Hall, L. Hough, K. A. McLauchlan, J. Chem. Soc., 3699 (1962).

50. V. F. Bystrov, S. L. Portnova, V. I. Tsetlin, V. T. Ivanov, Y. A. Ovchinnikov, Tetrahedron, 25, 493 (1969).

51. M. Karplus, J. Am. Chem. Soc., 85, 2870 (1963).

52. K. L. Williamson, J. Am. Chem. Soc., 85, 516 (1963).

53. P. Laszlo, P. von R. Schleyer, J. Am. Chem. Soc., 85, 2709 (1963).

54. M. P. Schweizer, S. I. Chan, P. O. P. Ts'o, J. Am. Chem. Soc., 87, 5241 (1965).

55. J. H. Nelson, Ph.D. Thesis, California Institute of Technology, Pasadena, Calif., 1969, p. 79.

56. H. S. Harned, B. B. Owen, in "The Physical Chemistry of Electrolyte Solutions," 3rd ed., Reinhold Publishing Corp., New York, 1958, p. 564.

57. M. M. Taqui Khan, A. E. Martell, J. Am. Chem. Soc., 89, 5585 (1967).

58. A. V. Lakshminarayanan, V. Sasisekharan, Biochim. Biophys. Acta, 204, 49 (1970).

59. G. Némethy, H. A. Scheraga, J. Phys. Chem., 66, 1773 (1962).

60. O. Sinanoğlu, in "Molecular Associations in Biology," B. Pullman, ed., Academic Press, New York, 1968, p. 427.

61. J. J. Bikerman, in "Surface Chemistry," Academic Press, New York, 1958, p. 76.

62. A. E. V. Haschemeyer, H. M. Sobell, Acta Cryst., 18, 527 (1956).

63. E. Shefter, K. N. Trueblood, Acta Cryst., 18, 1069 (1965).

64. These findings have been published in part: J. H. Prestegard, S. I. Chan, J. Am. Chem. Soc., 91, 2843 (1969).

65. C.-Y. Lee, private communication.

66. O. Sinanoğlu, S. Abdulnur, Fed. Proc., 24, S-12 (1965).

67. We acknowledge J. W. Meyer for this suggestion.

# PROPOSITION I

## Investigation of the Influence of Nonpolar Groups on Water Structure by Attenuated Total Reflectance Spectroscopy

The postulated existence of regions of highly ordered water structure within normal aqueous solutions has been with us for some time. Frank and Evans were perhaps the first to introduce the concept when they proposed the formation of miniature "icebergs" about nonpolar groups to explain an apparent anomaly in the entropy change which occurs on dissolving a hydrocarbon in an aqueous phase.[1] The concept has, however, become a topic of much current interest with the assignment of "special" properties to regions of water near various surfaces,[2,3] and with the implication of "hydrophobic bonding" as an important force in maintaining the tertiary structure of numerous biological macromolecules.[4,5]

A number of recent studies have appeared which claim to demonstrate an increase in the "structuring" of an aqueous solution in the presence of hydrophobic solutes. These have included investigations by nmr,[6] ultrasonic[7] and infrared methods.[8,9] The bulk of the evidence appears to lie on the side of the "iceberg" model, but agreement is by no means unanimous. And since most of the studies are sensitive only to the bulk properties of the solution, estimates of the extent of structuring about specifically

hydrophobic regions vary greatly. Estimates of the depth to which order extends range from a few molecular diameters on one hand,[10] to a few hundred or even thousand[2] on the other hand. Thus, the physical existence of local regions of water structure, or at least the dimensions of these regions, requires further study.

The study of water structure at hydrophobic surfaces by attenuated total reflectance spectroscopy proposed here, I believe, will further define both the nature and the extent of these local regions of order. The infrared region of the spectrum has been shown to be sensitive to the hydrogen bonding properties of the water molecule.[8,9] In fact, Worley and Klotz have interpreted changes in the overtone region of the HDO infrared spectrum on the addition of polyvinylpyrrolidone to be the results of increased hydrogen bonding among water molecules in structured regions. Attenuated total reflectance spectroscopy, on the other hand, has proven useful in the investigation of surface phenomena. Specifically, it has been used to monitor reactions at electrode interfaces[11] and to follow adsorption at various surfaces.[12] We therefore propose to combine the two techniques in the application of ATR spectroscopy in the IR region to the study of water structure near nonpolar surface groups. A polymer containing nonpolar groups could be plated onto an ATR cell and water placed over it, much as depicted in Figure 1. The ATR spectrum of the HDO (HDO,

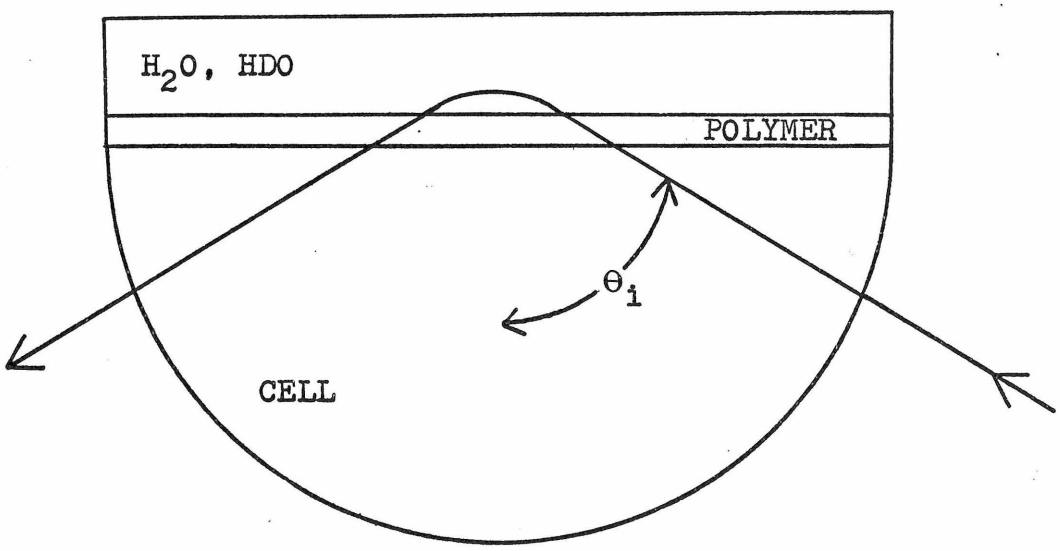


FIGURE 1

Attenuated total reflectance cell.

rather than $H_2O$, is used because of its simpler IR spectrum) could be studied as a function of polarity of the polymer and as a function of distance from the surface. The experiment should be similar to an infrared absorption study in results, except for the following. First, the method is only sensitive to a thin layer of water over the polymer, so that surface effects masked out in a solution study should become more apparent. Second, one can vary the number of nonpolar groups at the surface without having the solubility problems inherent in a solution study. And third, structure can be studied as a function of distance from the surface to determine the depth of structuring.

In theory, attenuated total reflectance spectroscopy depends on the total reflection of radiation from the interface between media of different indices of refraction when the angle of incidence is greater than the critical angle. This is true only for nonabsorbing regions. In absorbing regions radiation is absorbed and the reflected intensity is attenuated. Thus for the IR region, a spectrum of reflected intensity versus frequency has the same general features as does an IR absorption spectrum. As stated previously, the major differences arise from the fact that only a thin layer at the interface absorbs. The depth of penetration of radiation into the rarer (absorbing) medium can be given by

$$d_{\frac{1}{2}} = \frac{0.693\,\lambda}{2\pi(\sin^2\theta_i - n^2)^{\frac{1}{2}}} \quad , \qquad (1)$$

where $d_{\frac{1}{2}}$ is the depth at which the intensity has decreased to one-half its initial value, $\lambda$ is the wave length of radiation in the denser medium, $\theta_i$ is the angle of incidence, and n is the relative index of refraction.[13] For an AgCl-water interface in the region of the HDO asymmetric stretch, the depth of penetration is calculated to be in the range of 5000 Å. Use of the absorptions in the overtone region should give a correspondingly smaller depth of penetration. Either depth should be suitable for the study of water structuring proposed here and as indicated in equation (1), the effective depth of penetration, depending on the angle of incident radiation, can be easily varied throughout the study. The addition of a sufficiently thin polymer film between the cell and water phase is not expected to affect these reflectance properties greatly.

The ATR spectral observations upon increased structuring of the water near the polymer film should be similar to the effects noted for the IR absorption study on dissolving hydrophobic solutes. Namely, an increase in hydrogen bonding in structured regions should shift absorption to lower frequencies. For the HDO bond at 3400 $cm^{-1}$ the shift is 60 $cm^{-1}$ to higher frequency on heating from 0 to 100°C.[14] A redistribution of intensities toward lower frequencies

among overtone bands upon addition of structure-making agents has also been observed and may actually be more definitive in the case of a structure study such as this.[8,9]

The exact nature of the polymer film to be applied to the cell is highly variable, the main requirements being that the polymer can be applied to the cell in a thin coat, that the coat be stable to water, but wettable to a certain extent, and that the polymer's IR spectrum be transparent in the region of HDO absorption. Polymethyl-polyethylacrylate copolymers fill these criteria. They also offer the possibility of varying the methyl-ethyl ratio and thus the nonpolar character of the surface.

The experiment proposed then is to plate a thin film of copolymer on an ATR cell and observe a 6M HDO, $D_2O$ solution at this interface. The ATR spectrum will be monitored in the 3000-4000 $cm^{-1}$ region as a function of copolymer ethyl content and as a function of the angle of incident radiation. The resultant frequency shifts should give direct evidence of the effect of a nonpolar group on water structure and of the depth to which structuring might extend. Of course, it would also be useful to study HDO over a polyvinylpyrrolidone film by ATR for the purpose of comparison to the solution study by Worley and Klotz.

# REFERENCES


1. H. S. Frank, M. W. Evans, J. Chem. Phys., 13, 507 (1945).
2. W. Drost-Hansen, Ind. Eng. Chem., 61, #11, 10 (1969).
3. B. V. Derjaguin, Discussions Faraday Soc., 42, 109 (1966).
4. J. E. Brandts, L. Hunt, J. Am. Chem. Soc., 89, 4826 (1967).
5. G. Némethy, H. A. Scheraga, J. Phys. Chem., 66, 1773 (1962).
6. G. A. Johnson, S. M. A. Lecchini, E. G. Smith, J. Clifford, B. A. Pethica, Discussions Faraday Soc., 42, 120 (1966).
7. G. G. Hammes, P. R. Schimmel, J. Am. Chem. Soc., 89, 442 (1967).
8. O. D. Bonner, G. B. Woolsey, J. Phys. Chem., 72, 899 (1968).
9. J. D. Worley, I. M. Klotz, J. Chem. Phys., 45, 2869 (1966).
10. J. Clifford, B. A. Pethica, in "Hydrogen-Bonded Solvent Systems; Proceedings of a Symposium," A. K. Covington, P. Jones, eds., A. K. Taylor and Francis, Ltd., London, 1968, p. 169.
11. W. N. Hansen, R. A. Osteryoung, T. Kuwana, J. Am. Chem. Soc., 88, 1062 (1966).

12. G. Kortüm, in "Reflectance Spectroscopy," Springer-Verlag, New York, 1969, p. 331.

13. W. W. Wendlandt, H. G. Hecht, in "Reflectance Spectroscopy," Interscience, New York, 1966, p. 23.

14. M. Falk, T. A. Ford, Can. J. Chem., 44, 1699 (1966).

# PROPOSITION II

## Study of the Guanine Tautomeric Equilibrium by $^{17}O$ NMR

Guanine, as found in nucleosides, nucleotides and polynucleotides, can exist in several tautomeric forms, as indicated below:

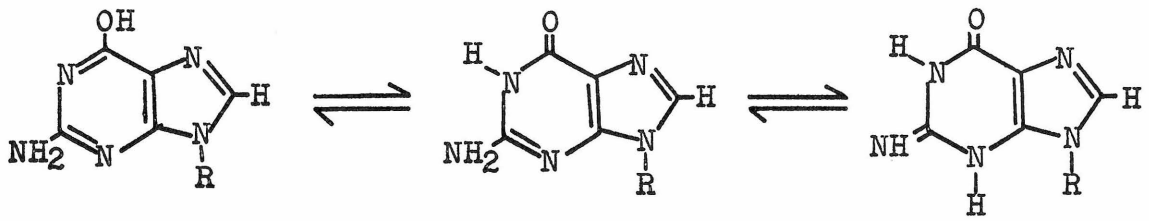

1 2 3

For years it was assumed, by analogy to cytosine, that the ketone form (2) dominated this equilibrium with a small contribution from the enol tautomer (1).[7] Despite the presumed low percentage of the enol form it is by no means unimportant. Even in the original papers postulating the Watson-Crick base-pairing scheme, the existence of minor tautomers was cited as the primary source of mutation and transcription error.[2] With this added motivation, several estimates of the percentages of minor nucleotide tautomers have appeared. Analysis of uv spectra and pK shifts has given rise to estimates ranging from less than a tenth of a percent in adenine to nearly 50% in inosine.[3] In the case

of guanine, alone, a wide range of estimates have appeared. In 1963 Miles et al. concluded that the keto form (2) was by far the major species by comparing the IR spectrum of guanosine in $D_2O$ to that of 1,9-dimethyl guanine, which can exist only in the keto form, and to that of 2-amino-6-methoxy-9-d-ribofuranosyl purine, which can exist only in the enol form.[4] The keto form is characterized by a band at 1665 $cm^{-1}$ found in both guanosine and 1,9-dimethyl guanine, but because of the lack of a band definitely characterizing the enol form, no precise limit on the minor tautomer percentage was set. Subsequent theoretical calculations have been slightly more definitive, but they range from $10^{-24}$ mole fraction minor tautomer in the G-C base pair[5] to $\sim 10^{-7}$ mole fraction in a free G molecule.[6] The calculations also suffer from the neglect of any contribution from solvent hydrogen bond formation. Recently a proton magnetic resonance study of the guanine equilibrium has led to a much higher estimate (approximately 10%) for the contribution of the enol tautomer.[7] This estimate is, however, an indirect one, based on a complex analysis of kinetic data.

In view of the discrepancy in these estimates and in view of the doubt shed on these methods, it would seem wise to seek a more definitive method for the detection and characterization of the guanine minor tautomers. We propose here an alternate approach, again based on a nuclear

magnetic resonance (nmr) technique, but employing the $^{17}O$ resonance of $C_6$-substituted guanine derivatives. In nmr experiments, detection of the minor tautomer is based on the fact that the chemical shift of a given nucleus will be slightly different for each of the tautomers. In the case where the rate of tautomerization is slow compared to the difference in chemical shifts of the species expressed in frequency units, a distinct resonance can be observed for each species and the analysis of percentage tautomer and tautomer characteristics is straightforward. In the case where the exchange rate is fast compared to this frequency separation, a single resonance is observed whose chemical shift is the weighted average of all species, and analysis in terms of both percentage and identification of the tautomer is often impossible. The existing proton experiments lie close to the second case. The frequency separation of chemical shifts for the tautomeric species is small (~0.15 ppm), not only because of the inherently narrow range of proton chemical shifts, but also because of the remote position of the $H_8$ proton of the guanine base. As a result of this small chemical shift difference, a true slow exchange limit could not be reached and the evaluation of the tautomeric equilibrium had to rely on a complex analysis of line widths in the intermediate exchange region.(7)

Although $^{17}O$ nmr relies on the same principals, observation of the $^{17}O_6$ resonance can overcome many of the

difficulties experienced in the proton work. First, $^{17}O$ chemical shifts are very large. On the basis of shifts observed in previous studies of keto-enol tautomerization we might expect a chemical shift difference between tautomers (1) and (2) of the order of 300 ppm.[8] For comparable magnetic fields, this pushes the slow exchange limit to a time scale a factor of a hundred faster than that of the pmr experiment. Thus it is likely that the minor tautomer can be observed in the slow exchange limit where its percentage can be determined by integration and where it can be identified by direct observation of its $^{17}O$ chemical shift. $^{17}O$ nmr also offers an advantage in that the direct involvement of the $^{17}O$ at the $C_6$ carbon in the tautomeric equilibrium facilitates the identification of contributing tautomers. Assignment might be based on comparison of guanine $^{17}O$ shifts to those of the 1-methyl and 6-methoxy derivatives in analogy to the IR study by Miles et al.[4]

There are a few possible disadvantages to working with $^{17}O$. First, $^{17}O$, spin 5/2, has a quadrupole moment, and the lines may be unusually broad due to quadrupole relaxation. However, in a study of proton exchange in water as a function of pH by $^{17}O$ nmr, the maximum observed line width was 10 ppm, or ~3% of the expected shift in the guanine keto-enol equilibrium.[9]

A second disadvantage in $^{17}O$ nmr is the low natural abundance of this isotope (0.037%). A solution study, such

as that proposed here, necessitates the synthesis of $^{17}O$-enriched compounds. $^{17}O$ guanine can be easily synthesized from commercially available 2,6-dichloro purine by modification of a synthesis described by Reist[10] (Figure 1). The 6-methoxy derivative can be made by addition of $Me^{17}OH$ instead of $H_2{}^{17}O$ in step 3. The 1-methyl derivative can be prepared by treatment of $^{17}O$ guanine with MeI.[11] Thus, the $^{17}O$ nmr studies proposed here should be feasible and should yield added information about the tautomeric equilibrium of the guanine base.

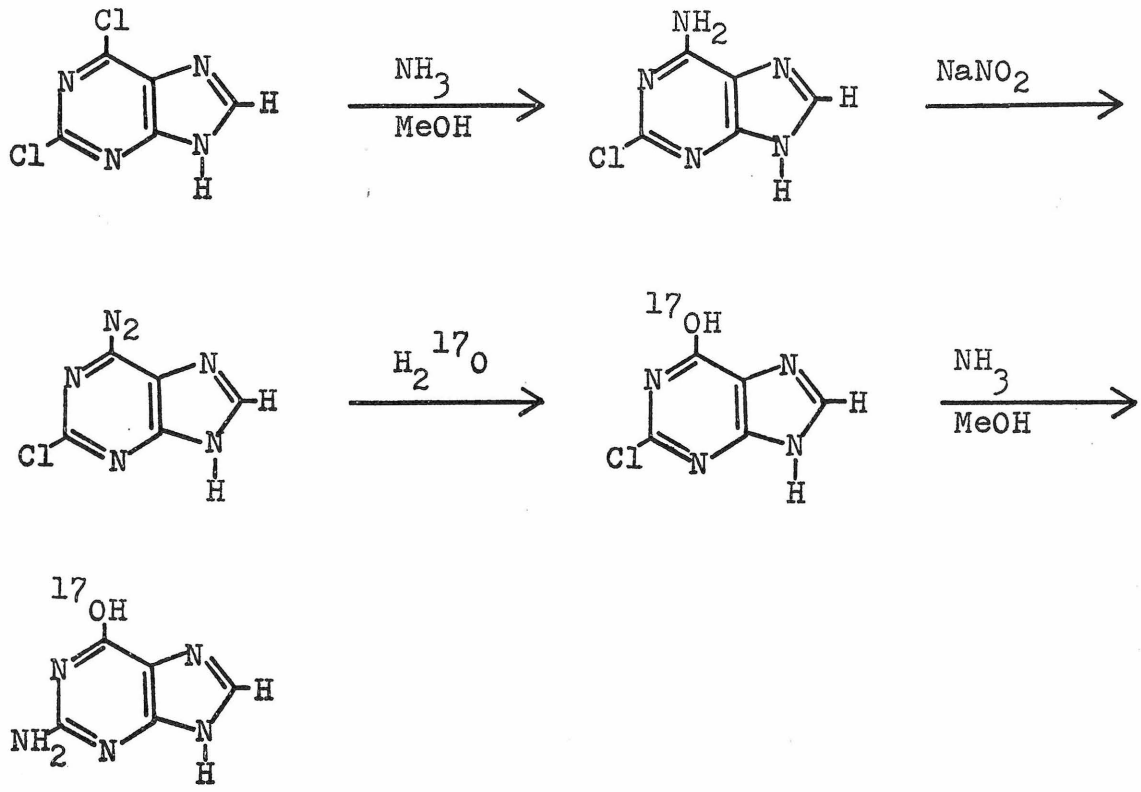


FIGURE 1

Synthesis of $^{17}O$-labeled guanine.

REFERENCES

1. R. F. Steiner, R. F. Beers, in "Polynucleotides," Elsevier, New York, 1961, p. 31.
2. J. D. Watson, F. H. C. Crick, Nature, 171, 964 (1953).
3. R. V. Wolfender, J. Mol. Biol., 40, 307 (1969).
4. H. T. Miles, F. B. Howard, J. Frazier, Science, 142, 1463 (1963).
5. D. K. Rai, J. Ladik, J. Mol. Spectry., 27, 79 (1968).
6. N. Bodor, M. J. S. Dewar, A. J. Harget, J. Am. Chem. Soc., 92, 2929 (1970).
7. C.-Y. Lee, private communication.
8. B. L. Silver, Z. Luz, Quart. Rev., 21, 458 (1967).
9. S. W. Rabideau, H. G. Hecht, J. Chem. Phys., 47, 544 (1967).
10. E. J. Reist, L. Goodman, Biochemistry, 3, 15 (1964).
11. A. D. Broom, L. B. Townsend, J. W. Jones, R. K. Robins, Biochemistry, 3, 494 (1964).

# PROPOSITION III

## A Study of Micelle Structure by Fluorine Spin Relaxation Measurements

A great variety of long chain hydrocarbons having both a hydrophobic and hydrophilic end exist in aqueous solutions as high molecular weight aggregates called micelles. These structures have long been of importance because of their detergent properties, but more recently they have become important as simple systems for the study of hydrophobic bonding[1] and as simple systems for the study of properties common to both synthetic micelles and lipid aggregates found in biological membranes. In view of these new interests it has become increasingly important to understand the structural and dynamic nature of a micelle's interior, especially as it may affect permeation of the micelle by various foreign substances.

It is generally accepted that a micelle of a molecule such as sodium dodecyl sulfate or dodecyltrimethylammonium bromide is a roughly spherical aggregate of 10 to 100 molecules with polar groups directed outward and nonpolar hydrocarbon chains directed inward. The hydrocarbon interior is known to be a highly fluid hydrophobic phase, but the way in which mobility varies as a function of distance from the surface has not been fully investigated. It is the purpose of this proposal to elucidate this characteristic of the

micelle interior.

Fluorine-19 spin relaxation times are possible indicators of molecular mobility at labeled sites. Both spin-spin and spin-lattice relaxation are induced by fluctuations in local magnetic fields. The spin-lattice relaxation time, $T_1$, for example, can, under certain simplifying assumptions, be expressed as:

$$T_1 = \frac{2\gamma^2\overline{(H')^2}\tau_c}{1 + 4\pi^2 \upsilon_o^2 \tau_c^2} \quad ,$$

where $\gamma$ is the nuclear magnetogyric ratio, $\overline{(H')^2}$ is the mean square value of the fluctuating magnetic interaction, $\upsilon_o$ is the Larmor frequency, and $\tau_c$ is a correlation time characteristic of molecular motion.[2] Under conditions where $\overline{(H')^2}$ is expected to be quite similar for different sites, $T_1$ should give a direct indication of relative mobilities at the points of interest, since neither the Larmor frequency, nor the magnetogyric ratio is variable. If $\overline{(H')^2}$ is dominated by intramolecular interactions with its nearest-neighbor atoms or functional groups and if substitution sites differ only in position along a long hydrocarbon chain, the required condition is fulfilled. We therefore propose to synthesize, according to the scheme outlined in Appendix I, a series of gemdifluoro-substituted surfactants with substitution at various well-defined sites along the chain. $^{19}F$ relaxation times, both $T_1$ and $T_2$, would be

measured by pulsed nmr techniques for micelles formed from these molecules. The relaxation times measured should be characteristic of chain mobilities at various depths into the micelle structure and should greatly clarify the structure of the micelle's hydrocarbon interior. The results should be directly applicable to other micellar systems since Muller has shown that fluorine substitution, at least at the terminal methyl group, produces a negligible effect on micelle properties.(3)

Extension of the experiments or results to the lamellar phases important in biological membranes, without actually incorporating the substituted hydrocarbon in one of the lipid molecules normally exhibiting this structure, is open to criticism. But by studying a mixed lamellar system or by arguing from analogy, the proposed experiment may also be useful in this area. As an example, the results may help to resolve a current controversy concerning the interpretation of pmr line shapes observed in phospholipid systems. In the lamellar phase the broad, non-Lorentzian lines observed have been attributed both to molecular diffusion within field gradients(4) and to the existence of of magnetically anisotropic regions within the sample.(5) Both mechanisms seem unlikely in view of the extent of inhomogeniety required to produce the observed line widths. Arguments in favor of these mechanisms are currently based on proton relaxation measurements which arise from the

average behavior of a multitude of unresolved hydrocarbon methylene protons. Measurement of relaxation times at specific sites should prove to be a better test for these explanations. Specifically, anisotropic properties of the lamellar phase should affect the $T_2$'s of all sites along a given hydrocarbon chain similarly; whereas a mechanism involving spin diffusion or incomplete averaging of dipole interactions[6] should lead to a distribution of $T_2$ values.

It should also be noted that existing pmr studies of both micelle[7] and lamellar[4] systems show a single $T_1$ decay for all methylene protons. This is seemingly inconsistent with some esr spin label studies recently completed which show a sharp drop in correlation time as the label is moved toward the end of the chain.[8] The study proposed here should nicely complement the esr results in that the gemdifluoro substituent provides a much different perturbation to the hydrocarbon chain, both sterically and functionally, than does the nitroxide derivative used in the esr study.

# APPENDIX I

The following is the proposed synthesis for a series of gemdifluorododecyltriethylammonium bromides.

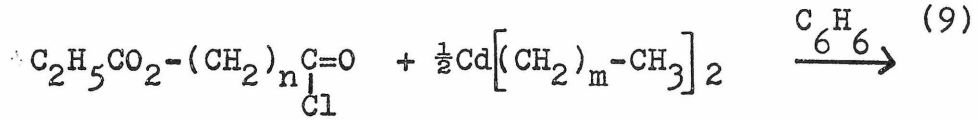

(9)

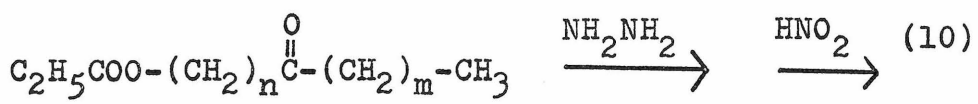

(10)

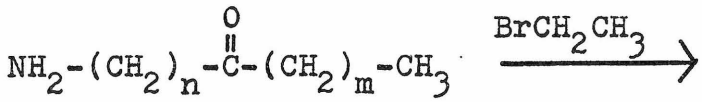

(11)

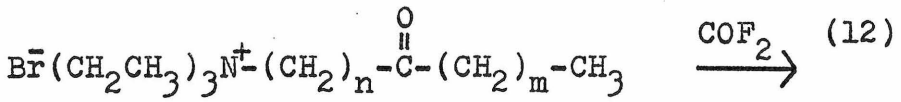

(12)

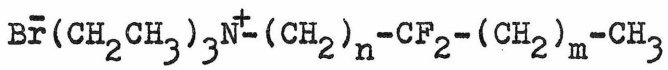

REFERENCES


1. M. F. Emerson, A. Holtzer, J. Phys. Chem., 71, 3320 (1967).
2. J. A. Pople, W. G. Schneider, H. T. Bernstein, in "High-Resolution Nuclear Magnetic Resonance," McGraw-Hill, New York, 1959, p. 201.
3. N. Muller, T. W. Johnson, J. Phys. Chem., 73, 2042 (1969).
4. J. R. Hansen, K. D. Lawson, Nature, 225, 542 (1970).
5. S. Kaufman, J. M. Stein, J. H. Gibbs, Nature, 225, 744 (1970).
6. S. A. Penkett, A. G. Flook, D. Chapman, Chem. Phys. Lipids, 2, 273 (1968).
7. J. Clifford, Trans. Faraday Soc., 61, 1276 (1965).
8. W. L. Hubbell, private communication.
9. J. Cason, F. S. Prout, in "Organic Synthesis," Vol. III, E. C. Horning, ed., Wiley, London, 1955, p. 601.
10. P. A. S. Smith, in "Organic Reactions," Vol. III, R. Adams, ed., Wiley, New York, 1946, p. 352.
11. D. J. Cram, G. S. Hammond, in "Organic Chemistry," McGraw-Hill, New York, 1964, p. 255.
12. F. S. Fawcett, C. W. Tullock, D. D. Coffman, J. Am. Chem. Soc., 84, 4275 (1962).

# PROPOSITION IV

## The Application of a New Chemical Method to the Investigation of tRNA Tertiary Structures

One of the most active areas of research in molecular biology today is the study of the secondary and tertiary structures of transfer RNA molecules. The primary structures of these relatively small polynucleotides, so necessary to the in vivo synthesis of proteins, are now known in a number of cases, and the recent development of improved purification and crystallization techniques promises to lead shortly to the solution of the complete crystal structure for one or more of them.[1,2] But before this step is taken, much can be gained through chemical studies which illuminate the structures of these molecules and, even after the crystal structures are known, chemical studies may be necessary to relate the crystal structure to the solution tertiary structures, a number of which are known to exist, even under physiological conditions.

The currently accepted secondary structure proposed for the tRNA molecule is that of the cloverleaf model depicted in Figure 1.[3] Its existance is postulated largely on the basis of maximization of intramolecular base pairing. But it gains credence from the fact that most tRNAs now characterized can be put into this general form. However, complete confirmation of this structure and the

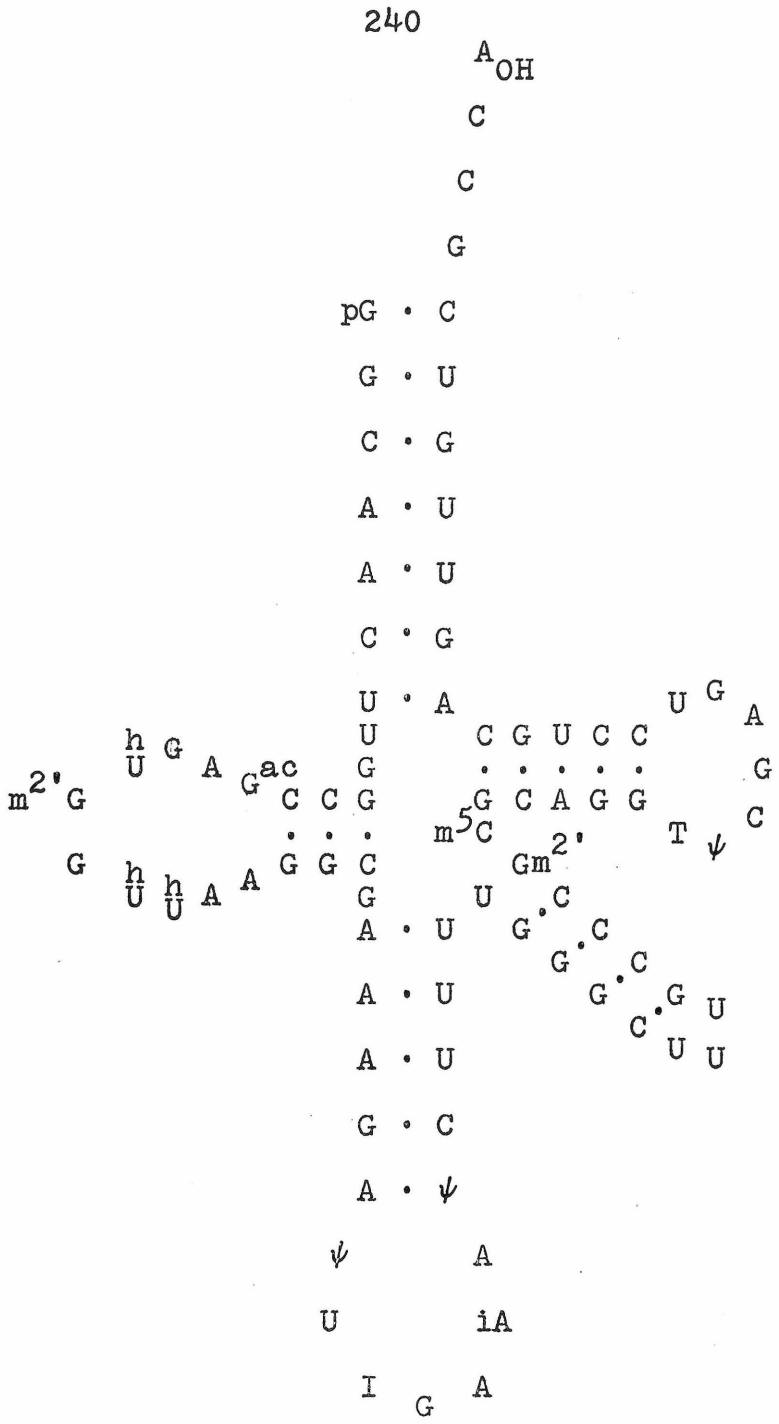


FIGURE 1

Depiction of the $tRNA^{Ser}_{Yeast}$ II molecule.

characterization of a tertiary structure awaits further chemical and physical evidence.

Chemical evidence for this cloverleaf structure relies on the proposition that the bases of the "looped" regions are more susceptible to chemical modification than the "paired" regions. Thus, by sequencing chemically treated and modified tRNAs and comparing the results to the unmodified primary structure, the bases participating in the "loops" can be assigned. A number of studies based on this principal have already provided information about the secondary and tertiary structure of tRNA[4,5] and the new chemical studies which are proposed here will add to this store of evidence.

At present available chemical methods of nucleotide modification are quite diverse and one might well question the necessity of proposing yet another technique. Upon closer examination of existing methods, however, it is apparent that improvements can be made. Bromination and alkylation were among the first reactions used, but they have been largely abandoned because they rapidly destroy the RNA molecule with little consequent structural information.[3] Many of the reactions which took their place are little better. Semicarbazide, nitrous acid, and acrylonitrile treatment have all been used, but modification here too proceeds under conditions which eventually totally denature the RNA molecule.[4] The use of formaldehyde has been

attempted, but the reaction is reversible and complicated by secondary reaction products.[6] The hydroxylamine reaction is widely used due to the extensive characterization of its rates and optimum reaction conditions.[6] Unfortunately, it too leads to multiple products and can eventually degrade the polynucleotide chain. The two reactions of most promise are the perphthalic acid reaction and the carbodiimide reaction.[6] The latter, which is specific for cytosine, proceeds under very mild conditions, but suffers from the fact that the added substituent is not only very bulky, but carries a positive charge. There are, in fact, a number of instances where this and related reactions have led to large structural changes in the region of modification and resultant secondary attack sites.[5,7,8] The perphthalic acid reaction adds a less bulky group, producing an oxide at the $N_1$ position of a number of bases. It can be run under conditions specific for adenine and as such is a useful reaction.[9] It is apparent, however, that a reaction producing a less drastic base perturbation and preferably at a base other than adenine would be of much use.

The method we propose here fills these requirements. It stems from the recent discovery that sodium bisulfite reacts preferentially with cytosine to produce uracil, according to the following mechanism.[10,11]

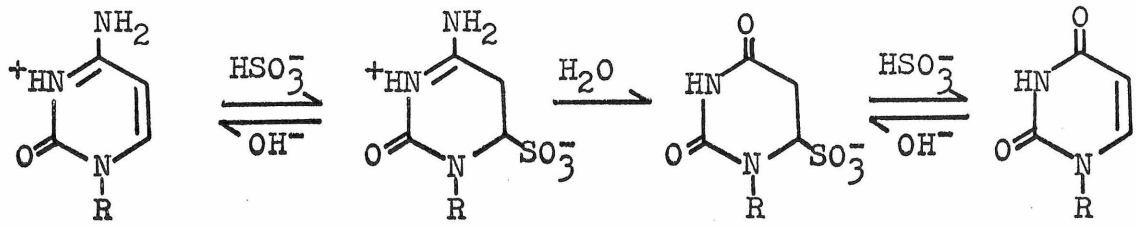

1 2 3 4

The reaction seems particularly suitable for labeling exposed regions of the tRNA structure for the following reasons. First, the reaction is specific for cytosine and thus nicely complements the perphthalic acid reaction. Second, the reaction involves a group normally protected by a Watson-Crick hydrogen-bond, so that it should be highly specific for unpaired regions. Third, the reaction conditions (1 M $NaHSO_3$, pH 5.2, 37°C) are mild enough not to cause denaturation. In fact, *in vivo* mutations have been observed with no simultaneous loss of cell function.[12] Fourth, the modification of the polynucleotide chain C→U should cause a minimum of structural perturbation. Also, the C→U conversion will not alter the points of chain incision in the normal sequence analysis procedure, and thus comparison of modified and unmodified oligonucleotide fragments should be expedited. And fifth, the reaction offers a number of possibilities for isotopically labeling modified nucleotides. To the extent that the dihydrouracil derivative (intermediate 3) is stable, tritium can be incorporated

by running the reaction in tritiated water and identification of modified oligonucleotides can be expedited by radioautographic techniques.(13) Also, the reaction might be run in $^{18}O$ enriched water. Incorporation of $^{18}O$ would be permanent and specific for cytosine. Labeled oligonucleotide might be identified by activation analysis or related methods.(14) With these advantages, the bisulfite reaction seems both useful and complementary to modification reactions already in existence.

A specific example of a case where the reaction can complement existing studies involves the characterization of the tertiary structure of the TψC loop. It has been proposed that this loop is folded against the main body of the tRNA molecule and held there by hydrogen bonds involving the ψ and C residues.(9) This conformation is believed essential to proper interaction with the appropriate aminoacyl synthase. A study of $tRNA_F^{Met}$ involving modification of ψ with acrylonitrile is known to destroy this important part of tertiary structure.(8) But because of the bulky cyanoethyl substituent, it is difficult to assess to what extent the structure change is the result of a loss of hydrogen-bonding capability and to what extent it results from steric interference. Since a C-G pair is also postulated to be involved in this hydrogen-bonded region, modification of C by the bisulfite reaction may give more definitive results. $tRNA_{Yeast}^{Ser}$ should be a suitable molecule for study. The

only exposed C's, other than that in the TψC group, are in the 3' terminal end which may be repaired after modification.[3] $tRNA^{Ser}$ also exhibits a low temperature melting of tertiary structure which may be useful in exposing the TψC region for modification. Thus, the sodium bisulfite reaction should be applicable here and in other studies of tRNA tertiary structure as well.

## REFERENCES


1. S. Nishimura, H. I. Y. Yamada, U. L. RajBhandary, M. Labanauskas, P. G. Connors, Science, 166, 1527 (1969).
2. R. D. Blake, J. R. Fresco, R. Langridge, Nature, 225, 32 (1970).
3. H. G. Zachau, Angew. Chem. Intern. Ed. Engl., 8, 712 (1969).
4. K.-I. Miura, in "Progress in Nucleic Acid Research and Molecular Biology," J. N. Davidson, W. E. Cohn, eds., Academic Press, New York, 1967, Vol. 6, p. 39.
5. J. B. Lewis, P. Doty, Nature, 225, 510 (1970).
6. N. K. Kochelkov, E. I. Budowsky, in "Progress in Nucleic Acid Research and Molecular Biology," Vol. 9, J. N. Davidson, W. E. Cohn, eds., Academic Press, New York, 1969, p. 403.
7. J. C. Lee, V. M. Ingram, J. Mol. Biol., 41, 431 (1969).
8. M. A. Q. Siddiqui, M. Krauskopf, J. Ofengand, Biochem. Biophys. Res. Commun., 38, 156 (1970).
9. F. Cramer, H. Doepner, F. v.p. Haar, E. Schlimme, H. Seidel, Proc. Natl. Acad. Sci., U.S., 61, 1385 (1968).
10. R. Shapiro, R. E. Servis, M. Welcher, J. Am. Chem. Soc., 92, 422 (1970).
11. H. Hayatsu, Y. Wataya, K. Kai, J. Am. Chem. Soc., 92, 724 (1970).

12. F. Mukai, I. Hawryluk, R. Shapiro, Biochem. Biophys. Res. Commun., 39, 983 (1970).

13. F. Sanger, G. G. Brownlee, B. G. Barrell, J. Mol. Biol., 13, 373 (1965).

14. G. Amsel, D. Samuel, Anal. Chem., 39, 1689 (1967).

# PROPOSITION V

## X-ray Photoelectron Spectroscopy of Lunar Surface Samples

The return of lunar surface samples to earth by Apollo missions 11 and 12 has opened a whole new area of research in analytical, physical, and inorganic chemistry. One of the more interesting problems uncovered in the recent studies of these samples is the discrepancy in bulk compositions of lunar rock and lunar fine samples. Foremost among the differences noted is the increased concentration of metallic iron in the dust samples. This increase has been detected by several methods including bulk chemical analysis[1] and electron spin resonance experiments.[2]

There are several possible explanations for the origin of this metallic iron. The first is that the iron centers imbedded in lunar dust particles are in a large part of foreign origin, being remnants of micro-meteorites thought to be of high metallic iron content. A second possibility is that the lunar dust is largely the product of eroded local materials, but that its composition has been modified somewhat by impact heating or other thermal events in the history of the moon. There is actually sufficient evidence to support either of these explanations. Age dating, which indicates that lunar dust may be significantly older than the native rock formations,[3] and the presence

of Ni-Fe regions on some dust particles indicates a meteoritic origin.[4] Measurement of $^{16}O/^{18}O$ isotopic ratios, on the other hand, show an increased proportion of $^{18}O$ in glass spherules found in lunar soil. This can be interpreted as the result of high temperature fusion.[5] In addition, metallic regions have been found within crystalline samples at the borders of troilite phases which are known to form metallic residues under conditions of high temperature and a reducing atmosphere.[6] Thus the origin of metallic iron centers remains a question for further study.

An analytical technique sensitive only to the first few hundred Ångstroms of the particle surface would seem to be of use in resolving this question. If the metallic centers are the result of surface deposits of meteoritic origin, a comparison of the surface analysis results to bulk analysis results should reveal a large discrepancy. If, on the other hand, the metallic centers are formed through some thermal conversion of lunar rock as the result of impact heating or other process, the iron centers may be more uniformly distributed and the results of the two analyses should not differ greatly.

Extensive bulk analysis results of lunar fines have already been obtained, but to a large extent surface analyses are lacking. Some electron microprobe studies have been conducted,[4] but they seem to have been confined to sectioned and polished crystals and selected glass

spherules. Nevertheless, in the case of the glass spherules, some surface iron particles have been noted;[7] unfortunately, most of the iron exists in centers of 100 Å or less, well below the level of detection by this technique.[8] We therefore propose to supplement these studies with an analysis of iron by X-ray photoelectron spectroscopy which will be sensitive to an average surface area of an untreated sample and will penetrate to a depth of the order of 100 Å.

Photoelectron spectroscopy by X-ray is based on the absorption of X-rays and simultaneous emission of electrons from inner atomic shells.[9,10] As a result, the energies of the emitted electrons are reasonably independent of atomic environment and quite characteristic of any given atom. Examination of binding energies for electrons in the major elemental constituents of lunar soil shows that lines arising from electrons emitted from iron $L_{II}$ and $L_{III}$ orbitals should lie in a relatively well resolved region of the spectrum,[11] and observation of electrons at these energies should provide a convenient monitor of iron content. The sensitivity of photoelectron spectroscopy only to irons in a surface layer arises largely from absorption of an electron's energy as it emerges from the sample. This absorption occurs in discrete amounts so the electron line is not broadened, but its intensity does decrease as the emitting atom is moved further beneath the surface. Absorption depends largely on the electron energy and the density of the

material, so for moon rock and a 600 eV electron, atoms much below 300 Å should not contribute to the spectrum.[12] These facts make the method ideal for the proposed study.

There are, however, several problems which must be overcome before attempting quantitative analysis of an inhomogeneous lunar dust sample. The first is the poor quantitative aspects of an irregular surface area. This can be overcome by determining a ratio of two different constituents rather than an absolute value. For the present problem, free iron and iron oxide seem promising. Despite the fact that we are observing an inner electron binding energy, metal and metal oxide lines are often resolved and their intensities can be compared directly.[13] However, should resolution of $Fe^{O}$ and $Fe^{II}$ lines fail to occur, measurement of total Fe relative to total O near the surface can be measured without question. A second factor to take into consideration in a quantitative electron spectroscopy experiment is the variation of photoelectron cross section with atomic number. If two Fe lines are compared this is of no consequence, but if Fe and O lines are compared an allowance must be made. Fortunately, well tested empirical formulas already exist[14] and confirmatory experiments on iron oxides of known composition could be carried out. A third factor involves differences in absorption of energy from electrons of differing velocity as they emerge from the solid. This factor is again insignificant if two lines of

nearly equal energy are compared, $Fe^{o}_{L_{II,III}}$ and $Fe^{II}_{L_{II,III}}$, for example. For the comparison of Fe and O lines, an empirical correction could be formulated from measurements on a laboratory sample of known composition and density approaching that of lunar material. With these factors taken into consideration, a quantitative determination of the $Fe^{o}/Fe^{II}$ ratio should be possible and should add significantly to our understanding of the history of lunar dust samples.

REFERENCES


1. J. A. Maxwell, S. Abbey, W. H. Champ, Science, 167, 530 (1970).
2. S. L. Manatt, et al., Science, 167, 710 (1970).
3. M. Tatsumoto, J. N. Rosholt, Science, 167, 461 (1970).
4. K. Keil, M. Prinz, T. E. Bunch, Science, 167, 597 (1970).
5. N. Onuma, R. N. Clayton, T. K. Mayeda, Science, 167, 536 (1970).
6. R. R. Simpson, S. H. U. Bowie, Science, 167, 619 (1970).
7. I. Adler, et al., Science, 167, 590 (1970).
8. T. Nagata, et al., Science, 167, 703 (1970).
9. J. M. Hollander, W. L. Jolly, Accounts Chem. Res., 3, 193 (1970).
10. K. Siegbahn, et al., in "ESCA; Atomic, Molecular and Solid State Structure Studied by Means of Electron Spectroscopy," Almqvist and Wiksells, Uppsala, 1967, p. 32.
11. Ibid., p. 225.
12. Ibid., p. 139.
13. Ibid., p. 224.
14. Ibid., p. 142.